STUDIA

UNIVERSITATIS BABEŞ-BOLYAI

CHEMIA

1-2

1992

CLUJ-NAPOCA

ANUL XXXVII 1992

STUDIA

UNIVERSITATIS BABEŞ-BOLYAI

CHEMIA

1-2

Redacţia: 3400 CLUJ-NAPOCA, str. M. Kogălniceanu, 1 ● Telefon 11 61 01

SUMAR — CONTENTS — SOMMAIRE — INHALT

STUDIA UNIV. BABEŞ-BOLYAI, CHEMIA, XXXVII, 1—2, 1992

FRAGMENTATION OF DIPHENYLANTIMONY (III) DIPHENYLDITHIOARSINATE $Ph_2SbS_2AsPh_2$ UNDER ELECTRON IMPACT

L. SILAGHI-DUMITRESCU, I. HAIDUC

Recieved: 01.03.1992

The electron impact fragmentation scheme of $Ph_2SbS_2AsPh_2$ is discussed on the base of the mass spectrum recorded at 70 *eV*. The loss of a sulfur is followed by the cleavage of the $Ph_2SbSAsPh_2$ in similar antimony and arsenic containing fragments. The conversion of $[Ph_2E]^+$ (E = As, Sb) into the corresponding dibenzoheterocyclic ions is observed.

Introduction. The diorganodithioarsinic anions, R_2AsS_2 are very good ligands towards both transition and main group metals. Few crystal and molecular structures are reported [1—6], most of the papers describing the spectroscopic behavior of the metallic and organometallic diorganodithioarsinates [3—13]. Data concerning the mass spectra are reported only for $Me_2As—S—As(S)Me_2$ [1], $(CO)_4ReS_2AsMe_2$ [7] and FAB spectra are discussed for $Sb(S_2AsMe_2)_3$, $PhSb(S_2AsMe_2)_2$ and $Ph_2SbS_2AsPh_2$ [6].

After the synthesis and the molecular structure [4] we report now the fragmentation of diphenylantimony (III) diphenyldithioarsinate, $Ph_2SbS_2AsPh_2$, under electron impact.

Results and Discussion. The mass spectrum of $Ph_2SbS_2AsPh_2$ recorded at 70 *eV* is presented in Fig. 1. Table 1 contains the monoisotopic *m/e* values for both, arsenic and antimony containing peaks.

Diphenylantimony (III) diphenyldithioarsinate is a dimer in solid state, as shown by the *x*-ray crystal structure determination [4]. However, as it can be seen from the spectrum and the Table 1, even the monomeric the molecular ion peak is missing. The base peak is $m/e = 154$ $[Ph_2]^+$.

The highest molecular weight fragment, $[Ph_2SbSAsPh_2]^+$, $m/e = 536$ is formed by the cleavage of a sulfur from the parent monomeric molecule. No loss of phenyl groups is observed at this stage. The next smaller fragments are formed by the cleavage of either the arsenic-sulfur bond or antimony-sulfur bond. The relative intensities of the arsenic-containing and antimony-containing fragments formed from $[Ph_2Sb—S—AsPh_2]^+$, support the preferential cleavage of the As—S bond, rather than antimony-sulfur bond. This is not a surprising behavior for the softer, compared to arsenic, antimony in relation to sulfur. The fragments are of quite similar composition: $[Ph_2ES]^+$ and/or $[Ph_2E]^+$ (E = As, Sb) and follow two alternative routes (Scheme 1).

Babeş-Bolyai University, Chemistry Department, RO—3400 Cluj-Napoca.

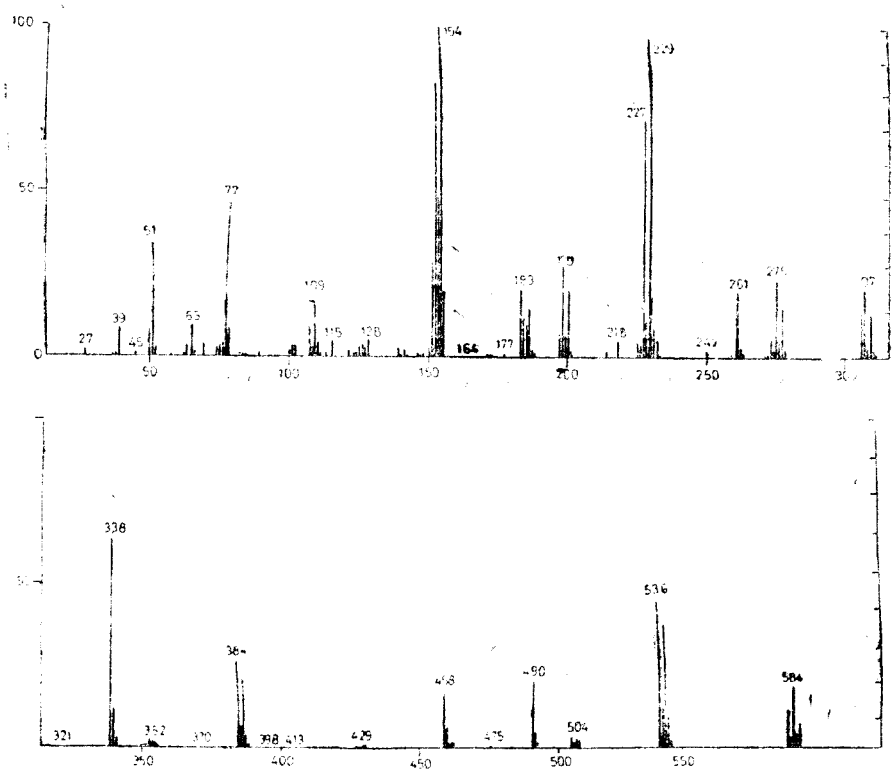

Fig. 1. Mass spectrum of $Ph_2SbS_2AsPh_2$

Table 1

Monoisotopic *m/e* values and the relative intensities of the peaks in the mass spectrum of Ph SbS AsPh

m/e	Relative intensities	Fragment
77	35.47	$[Ph]^+$
107	9.88	$[AsS]^+$
152	84.88	$[PhAs]^+$
153	50.00	$[SbS]^+$
154	100.00	$[Ph_2]^+$
183	20.93	$[PhAsS]^+$
198	35.75	$[PhSb]^+$
227	72.09	$[C_{12}H\ As]^+$
229	93.31	$[Ph_2As]^+$
261	16.28	$[Ph_2AsS]^+$
273	4.00	$[C_{12}H\ Sb]^+$
275	16.00	$[Ph_2Sb]^+$
306	14.95	$[Ph_3As]^+$
307	27.01	$[Ph_2SbS]^+$
338	10.90	$[Ph_3AsS]^+$
384	8.45	$[Ph_3SbS]^+$
536	14.29	$[Ph_2SbSAsPh_2]^+$

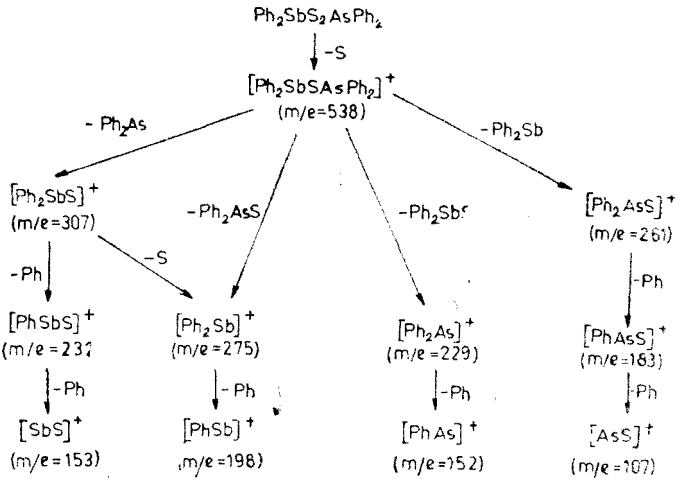

Scheme 1. The fragmentation of $Ph_2SbS_2AsPh_2$ under electron impact.

The $m/e = 229$ peak, assigned to $[Ph_2As]^+$, is accompanied by another one at $m/e = 227$, which can be the result of a cyclization process by the loss of two hydrogen atoms, with the

I E = As; II E = Sb

formation of the same dibenzoheterocyclic compounds (I) found in the mass spectra of triphenylarsine and other diphenylsubstituted arsines [14].

The identification of antimony containing peaks is facilitated by the fact that they are all doublets, in accordance with the existence of the two natural isotopes ^{121}Sb and ^{123}Sb. The ratio of the relative intensities of each pair of peaks in the mass spectrum reflects the natural abundance ratio (ca.1.33). There was only an exception from this behavior, for the $[Ph_2Sb]^+$ fragment, the ratio of the two isotopes peaks being 1.6. If the formation of the dibenzoheterocyclic ion (II) is taken into account the relative intensity of the $m/e = 275$ peak is shared between the two species $[Ph_2Sb]^+$ and the heterocycle (II), as follows:

$[Ph_2Sb]^+$	4 ($m/e = 273$)	3 ($m/e = 275$)	ratio = 1.33
II	16 ($m/e = 275$)	12 ($m/e = 277$)	ratio = 1.33.

A higher rate of cyclization is assumed from the corresponding relative intensities for the diphenylarsenic ion than for diphenylantimony ion.

Loss of phenyl groups is important in subsequent stages and the major low mass fragments are $[Ph_2]^+$, $[Ph]^+$. The smallest arsenic- or antimony-containing fragments of some significant abundance are $[ES]^+$ (E = As, Sb).

The mass spectrum contains also fragments formed as a result of collision processes. The most important collision ions are $[Ph_3ES]^+$ (E = AS, Sb), but also fragments containing two heavy atoms are formed: $[Ph_4As_2]^+$ ($m/e = 458$), $[(Ph_4As_2)S]^+$ ($m/e = 490$), $[Ph_2SbAsPh_2]^+$ ($m/e = 504$) and $[(Ph_4Sb_2)S]^+$ ($m/e = 584$).

Experimental part The diphenylantimony(III) diphenyldithioarsinate was prepared according to our previous work [4]. The mass spectrum was recorded on a Hewlett Packard 5985 A instrument, at 70 *eV*.

Aknowledgement. The authors thank Prof. dr. M. Gielen (Vrije Universiteit Brussel) for recording the spectrum.

REFERENCES

1. N. Camerman and J. Trotter, *J. Chem. Soc.*, (1964), 219.
2. D. Johnstone, J. E. Ferguson and W. T. Robinson, *Bull. Soc. Chem. Japan*, **45**, 3721 (1972).
3. L. Silaghi—Dumitrescu, I. Haiduc and J. Weiss, *J. Organomet. Chem.*, 263, 159 (1984).
4. C. Silvestru, L. Silaghi—Dumitrescu, I. Haiduc, M. Begley, M. Nunn and D. B. Sowerby, *J. Chem., Soc., Dalton, Trans.*, 1986, 1031.
5. E. W. Abel, M. A. Beckett, P. A. Bates and M. B. Hursthouse, *Polyhedron*, 1855 (1988).
6. L. Silaghi—Dumitrescu, I. Silaghi—Dumitrescu, I. Haiduc, M. M. Begley and D. B. Sowerby, *J. Chem. Soc., Dalton Trans.*, submitted for publication.
7. E. Lindner and H. M. Ebinger, *J. Organomet. Chem.*, **66**, 103 (1974).
8. A. T. Casey, and J. R. Thackeray, *Austral. J. Chem.*, **28**, 471 (1975).
9. W. Kuchen, M. Forster and H. Hertel, *Chem. Ber.*, **105**, 3310 (1972).
10. I. Haiduc and L. Silaghi—Dumitrescu, *J. Organometal. Chem.*, **225**, 225 (1982).
11. L. Silaghi—Dumitrescu and I. Haiduc, *J. Organomet. Chem.*, **259**, **65**, (1983).
12. I. Silaghi—Dumitrescu, L. Silaghi—Dumitrescu and I. Haiduc, *Rev. Roumaine Chim.*, **27**, 911(1982).
13. L. Silaghi—Dumitrescu, I. Silaghi—Dumitrescu and I. Haiduc, *Rev. Roumaine Chim.*, **34**, 305 (1989).
14. D. E. Bublitz and A. W. Baker, *J. Organomet. Chem.*, **9**, 383 (1967).

STUDIA UNIV. BABEŞ-BOLYAI, CHEMIA, XXXVII, 1—2, 1992

STEREOCHEMISTRY AND ^1H—NMR SPECTRA OF SOME NEW 2,2,5,5—TETRASUBSTITUTED 1, 3—DIOXANES

ION GROSU, MIHAI HORN, DALILA KOVACS, SORIN MAGER*

Received: 15 1 1992

ABSTRACT. New tetrasubtituted derivates of 1,3-dioxane were synthetized by means of the katalisation reaction between methyl and ethyl esters of the acetylacetic acid and bis-(hydroximethyl) malonic ester.

The stereochemical investigations by means of the ^1H—NMR spectroscopy show mobile structures proving small differences between the conformational free enthalpy of the two substituents located in the 2-position of the 1,3-dioxanic ring. The influence of the solvent (ASIS effect) on the chemical shift was also reported.

Earlier stereochemical studies [1—6] in the field of substituted 1,3—dioxanes were continued with the synthesis of new 2,2,5,5-tetrasubstituted 1,3-dioxanes (I—VI), using the ketalisation reaction of the methyl and ethylesters of the acetylacetic acid with bis-(hydroxymethyl)malonic ester (1):

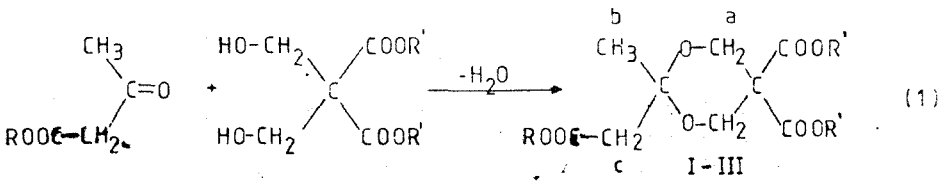

(1)

Scheme 1

$$\text{I} \quad R = R' = \overset{d}{-CH_2}\overset{e}{CH_3}$$

$$\text{II} \quad R = \overset{f}{-CH_3},\ R' = -CH_2CH_3$$

$$\text{III} \quad R = -CH_2CH_3,\ R' = \overset{g}{-CH_3}$$

The hydrolysis of *I* gave the potassium salt *IV* which with HCl in alcoolic solution delivered the acid *V*. With diazomethane it gave the trimethylester *VI* (2):

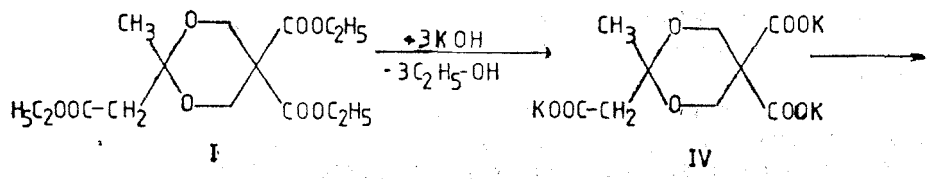

* *Babeş-Bolyai University, Chemistry Department, R—3400 Cluj-Napoca, Arany János 11, ROMANIA*

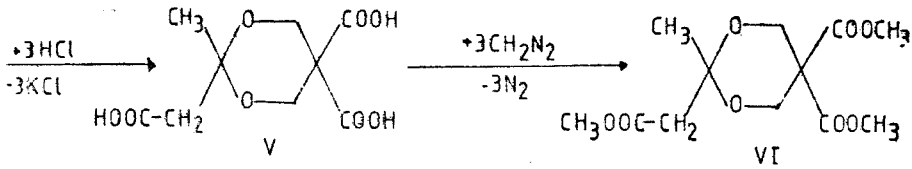

(2)

Scheme 2

The hygroscopic acid V was not isolated as a pure compound; it was treated as a raw product with diazomethane.

The conformational study of these new compounds undertaken by means of the ^1H—NMR spectroscopy, proves the existance of a mobile structure represented (Fig. 1) by the equilibrium $A \rightleftarrows B$ (3).

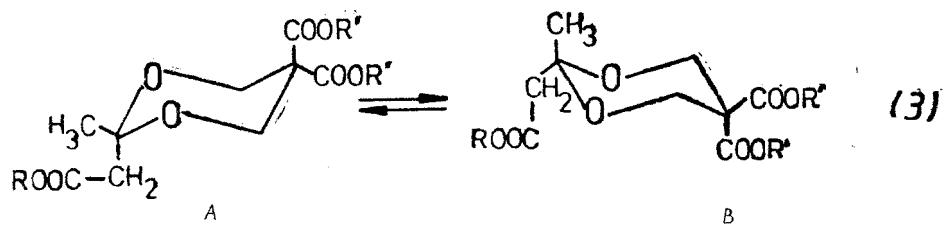

(3)

Fig. 1

The difference between the $\Delta G°$ values for a CH_3 or a $-CH_2-COOR$ group is too small for obtaining anancomeric structures. This situation was also found for other compounds which have a CH_3 and a CH_2-X group at the C_2 [7].

The mobile structures are easily proved by means of the ^1H—NMR spectra which show unique signals for the axial and equatorial protons of the dioxanic ring and for the substituents located in the 2 and 5 positions.

A representative spectrum for dioxanes *I*—*VI* is shown in Fig. 2a for compound II (R = CH_3, R' = Et). Only one peak ($\delta = 4.20$ ppm) may be observed as a mean value for the ecuatorial and axial protons of the C(4) and C(6) atoms, one quartet (mean value $\delta = 4{,}15$ ppm and one triplet (mean value $\delta = 1{,}17$ *ppm*) for the protons of the ethyloxycarbonyl groups.

In a field 1,3-dioxanic structure bearing an anancomeric isopropyl group in position 2 [4] the distinct values for the equatorial and axial protons of C4(6) atoms are 4.52 *ppm* respectively 3.77 *ppm* with the mean value 4.16 *ppm* in good concordance with the mean value for the mobile compound II ($\delta =$ = 4.20 *ppm*).

The same good concordance was found for the mean position of the equatorial and axial quartet of the $CH_3-CH_2-O-CO-$group in compound II ($\delta = 4.15$ *ppm*) as compared with the mean value ($\delta = 4.115$ *ppm*) of the $-CH_2-$ protons in the equatorial ($\delta = 4.06$ *ppm*) and axial ($\delta = 4.17$ *ppm*)

position of the anancomeric compound in which the axial one feels the deshielding influence of the two oxygen atoms belonging to the 1,3-dioxanic ring.

The overlap of the signals corresponding to the equatorial and axial protons of C(4) a C(6) with the signals corresponding to the methylene protons of the ethyloxycarbonyl groups attached to the C(5) atom, is a general feature of all spectra.

It was possible to separate the overlaped signals using as solvent C_6D_6 instead of $CDCl_3$. The ASIS effect is very easy to observe in Fig. 2b which presents the part of the spectrum of compound II involved.

The singlet and the quartet are very well separated having the values: $\delta = 4.17$ *ppm*; $\delta = 3.65$ *ppm*. The same separation of the signales was observed for compound *I*.

Table 1 — shows the difference of the chemical shifts caused by the ASIS effect for all the signals of compounds *I* and *II*.

Table 1

Compound	Solvent	δ *ppm*					
		a	b	c	d	e	f
I	$CDCl_3$	4,22	1,45	2,70	4,17	1,17	—
	C_6D_6	4,18	1,31	3,45	3,68	0,62	—
	$\Delta\delta$	0,04	0,14	0,25	0,49	0,54	—
II	$CDCl_3$	4,20	1,45	2,70	4,15	1,17	3,57
	C_6D_6	4,17	1,27	2,42	3,65	0,62	3,05
	$\Delta\delta$	0,03	0,15	0,28	0,5	0,55	0,52

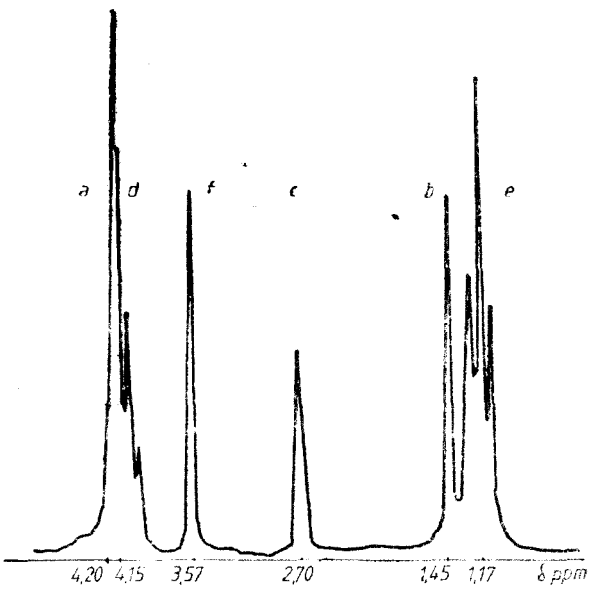

Fig. 2a. ^{1}H — NMR-Spectrum of Compound II in $CDCl_3$ solution

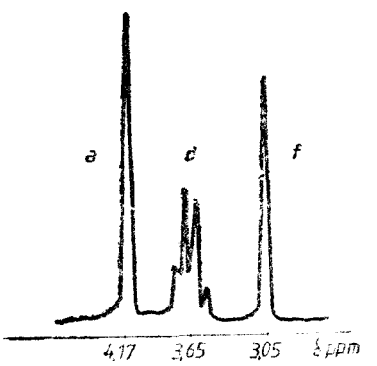

Fig. 2b. ^{1}H — NMR-Spectrum of compound II in C_6D_6 solution

The spectrum of the ester *VI* (R = R' = $-CH_3$) obtained by the esterification of the triacid *V* with CH_2N_2, is a very simple one, showing one peak for the methyl groups of C(5) atom (medium value $\delta = 3.67$ *ppm*), one peak for the methyl of the esteric group belonging at C(2) atom (medium value $\delta = 3.57$ *ppm*) and one peak for the protons of C(4) and C(6) atoms (medium value $\delta = 4.22$ *ppm*) beeing alike the spectra of compounds *IV* and *V*.

Experimental part. Compounds I—III were obtained by the following general procedure: equimolecular amounts of diol bis-(hydroxymethyl)malonic ester and acetylacetic ester were refluxed in benzene, under stirring, in the presence of catalytical amounts of *p*-toluenesulfonic acid. The reaction flask is provided with a trap for the separation of the water resulted from the reaction After the whole reaction water has been separated, the reaction product was neutralized with natrium acetate, then whashed with water. After distillation of the benzene, the pure product was obtained by vacuum distillation.

The ^1H—NMR spectra were recorded using a TESLA-BS487C 80 *MHz* spectrometer in $CDCl_3$ or C_6D_6 solutions, with HDMSO as standard.

2-Methyl,2-(methylenethyloxycarbonyl-)-5,5-bis(ethyloxycarbonyl)-1,3-dioxane (I)

Liquid (b.p. 160—2°/1 *mm Hg*). ^1H—NMR ($CDCl_3$): $\delta = 4.22$ *ppm*; $\delta = 1.45$ *ppm*; $\delta = 2.70$ *ppm*; $\delta = 4.17$ *ppm*; $\delta = 1.17$ *ppm*.

$C_{15}H_{24}O$ (332.34): %C 53,88 (calcd. 54.21), %H 7,07 (calcd. 7.27).

2-Methyl,2-(methylenemethyloxycarbonyl)-5,5-bis(ethyloxycarbonyl)-1,3-dioxane (II)

Liquid (b.p. 154—6°/1 *mm Hg*). ^1H—NMR ($CDCl_3$): $\delta = 4.24$ *ppm*; $\delta = 1.45$ *ppm*; $\delta = 2.70$ *ppm*; $\delta = 4.15$ *ppm*; $\delta = 1.15$ *ppm*; $\delta = 3.58$ *ppm*.

$C_{14}H_{22}O_8$ (318.32): %C 52,11 (calcd. 52.82), %H 6.37 (calcd. 6.96).

2-Methyl,2-(methylenethyloxycarbonyl)-5,5-bis(methyloxycarbonyl)-1,3-dioxane (III)

Liquid (b.p. 150—2°/1 *mm Hg*). ^1H—NMR ($CDCl_3$): $\delta = 4.27$ *ppm*; $\delta = 1.47$ *ppm*; $\delta = 2.72$ *ppm*; $\delta = 4.10$ *ppm*; $\delta = 1.15$ *ppm*; $\delta = 3.72$ *ppm*.

$C_{13}H_{20}O$ (314.20); %C 49,30 (calcd. 49.69), %H 6.11 (calcd. 6.41).

2-Methyl,2-(methylenoxycarbonyl)-5,5-bis(oxycarbonyl)-1,3-dioxane tripotasium salt. (V)

Solid (m.p. > 350°) ^1H—NMR (D_2O): $\delta = 4,45$ *ppm*, $\delta = 1,72$ *ppm*, $\delta = 2,92$ *ppm*.

$C_9H_9O_8K_3$(362,15) %C 29,60 (calcd. 2984) %H 2.25 (calcd. 2,50) %K 31,80 (calcd. 32.30%)

2-Methyl, 2-(methylenemethyloxycarbonyl)-5,5-bis(methyloxycarbonyl)-1,3 dioxane (VI)

Liquid (b.p. 144—6°/1 *mm Hg*). ^1H—NMR ($CDCl_3$): $\delta = 4.22$ *ppm*; $\delta = 1.45$ *ppm*; $\delta = 2.70$ *ppm*; $\delta = 3.57$ *ppm*; $\delta = 3.67$ *ppm*.

$C_{12}H_1O$ (290.26): %C 49.22 (calcd. 49.65), %H 5.95 (calcd. 6.25).

REFERENCES

1. S. Mager, E. Eliel, *Rev. Roumaine Chim.*, **18,** 1379 (1973).
2. S. Mager, E. Eliel, *Rev. Roumaine Chim.*, **18,** 2097 (1973).
3. G. Binsch, E. Eliel, S. Mager, *J. Org. Chem.*, **38,** 4079 (1973).
4. S. Mager, I. Hopârtean, M. Horn, I. Grosu, *Stud. Univ. Babeş—Bolyai Chem.* **24,** (1), 32 (1979).
5. S. Mager, I. Grosu, *Stud. Univ. Babeş—Bolyai, Chem.*, **33** (1), **47** (1988).
6. S. Mager, M. Horn, I. Grosu, M. Bogdan, *Monatsh.*, **120,** 735 (1989).
7. W. F. Bailey, E. Eliel, *J. Amer. Chem. Soc.*, **96,** 1798, 1974.

STUDIA UNIV. BABEŞ-BOLYAI, CHEMIA, XXXVII, 1—2, 1992

A COMPARATIVE STUDY OF ANALYSIS OF VARIANCE

C. SÂRBU*, V. LITEANU*, DORINA POP**

Received: 21.09.1992

ABSTRACT. The fundamentals of informational statistics are explained in their importance for analytical chemistry. Informational statistics like robust statistical techniques are resistant against uncertainties concerning the data, like outliers or divergencies from the normal distribution. Using a new informational function, namely informational energy, we tested the null hypothesis to decide whether a certain factor has a significant effect on the results.

Introduction. In any experiment two or more methods (laboratories) yield generally more or less different results, because analytical determinations may be influenced by basic factors (qualitative or quantitative) that control conditions of experiment and also by random factors.

It is the objective of the analysis of variance (ANOVA) to investigate the several kinds of factors, operating simultaneously and to decide which are important and to estimate their effects. ANOVA assumes the additivity of variances of random variable due to effect of independent factors. It is used to breakdown the total variance into its components, i.e. into a sum of several distinct components, each corresponding to a source of variance.

The F-tests that are subsequently made are determined from the ratios of these respective components. The F ratio can then be compared with tabulated F-values using the degrees of freedom corresponding to the numerator and denominator for each F ratio. If the observed F ratio exceeds the tabulated value at the chosen confidence level, then we would conclude statical significance at this level of confidence. If, on the other hand, the calculated value of F ratio is smaller than that given in tables, the factor in question doesn't affect the mean value.

When applying ANOVA one assumes that: (1) the overall errors are normally distributed; (2) the errors are statistically independent and (3) the errors have the same variance. Very often the homogeneity of variance is not respected. In these cases ANOVA could lead to erroneous conclusions, if methods with widely differing precisions are compared.

The analysis of variance can be applied in several distinct forms, according to the structure of the process being investigated. An excellent discussion of this topic has been presented by Hirsch [1] and by Massart and al. [2, 3].

In the present paper using a new informational function, namely informational energy, we tested the null hypothesis to decide whether a certain factor has a significant effect on the results.

* *Babeş-Bolyai University, Department of Analityeal and Inorganic Chemistry, 3400 Cluj-Napoca, Romania.*
** *„Phoenix" S.A. Plant, Baia-Mare, Romania*

Theory. The informational energy *(IE)* concept and its detailed theoretical study as well as its implications in the field of mathematics called „informational statistics" was introduced by Onicescu [4, 5].

IE describes with the same success as Shannon's entropy the uniformity or diversity of a system, process or phenomenon. IE is more sensitive in a certain way than the entropy to the modification of the system. Moreover this informational function permits the calculation of the informational correlation *(IC)* and the informational correlation coefficient (ICC), parameters of interest in analytical chemistry.

Informational energy and correlation. The *IE* of a finite set of events or states $A_1, A_2, \ldots, A_n$ each having a associated probability $p_1, p_2, \ldots, p_n$ with $p_i \geq 0$ and $\sum_{i=1}^{n} p_i = 1$ is given by

$$E_{(p_1, p_2, \ldots, p_n)} = \sum_{i=1}^{n} p_i^2 \tag{1}$$

The equation (1) gives information concerning the degree of organisation of a system or the mode of partition of its elements. Defined in this way, *IE* reveals some remarkable properties. First it reaches its minimum value when all the probabilities are equal ($p_1 = p_2 = \ldots = p_n$), i.e. the case of total unorganised systems:

$$E_{(p_1, p_2, \ldots, p_n)} = \frac{1}{n} \tag{2}$$

If $p_k = 1$ and $p_{i \neq k} = 0$, i.e. the case of well organised systems, then *IE* is

$$E_{(p_1, p_2, \ldots, p_n)} = 1 \tag{3}$$

Thus, it results that the possible values for *IE* are between $\frac{1}{n}$ and 1.

In the particular case of a set of two finite systems of events $A_1, A_2, \ldots, A_n$ and $B_1, B_2, \ldots, B_m$ each with probability $p_1, p_2, \ldots, p_n$ and $q_{i1}, q_{i2}, \ldots q_{im}$ respectively, the q_{ij} is the conditional probability of the event B given event A, i.e.

$$q_{ij} = p(B_j/A_i) \tag{4}$$

The *IE* of the system of events $B_1, B_2, \ldots, B_m$ conditioned by occuring of the integral system of events $A_1, A_2, \ldots, A_n$, the so called "conditional informational energy" *(CIE)* is defined by

$$E_{(B_1, B_2, \ldots, B_m \mid A_1, A_2 \ldots A_n)} = \sum_{i=1}^{n} \sum_{j=1}^{m} p_i^2 q_{ij}^2 \tag{5}$$

When the two systems are independent, *IE* of the system of events (A_i, B_j) will be

$$E_{(A_i, A_j)} = E_{(A_1, A_2, \ldots, A_n)} \times E_{(B_1, B_2, \ldots, B_m)} \tag{6}$$

This means that *IE* is multiplicative and not additive as Shannon's entropy.

The informational correlation (IC) between two systems (probabilistic partitions) has the following equation

$$IC_{(p_1, p_2, \ldots, p_n; q_1, q_2, \ldots, q_n)} = \sum_{i=1}^{n} p_i q_i \tag{7}$$

The IC is always positive, but lower than one, being zero if and only if all $p_i q_i$ are null, i.e. the two systems are "indifferent".

By the normation of correlation, similar to the statistical correlation coefficient, an informational correlation coefficient *(ICC)* may be obtained:

$$r_{(p_1, p_2, \ldots, p_n; q_1, q_2, \ldots q_m)} = \frac{C_{(p_1 p_2, \ldots, p_n; q_1, q_2, \ldots, q_n)}}{E_{(p_1, p_2, \ldots, p_n)} \times E_{(q_1, q_2, \ldots, q_n)}} = \frac{\sum_{i=1}^{n} p_i q_i}{\sum_{i=1}^{n} p_i^2 \sum_{i=1}^{n} q_i^2} \tag{8}$$

It is obvious that the possible values for ICC are between 0 and 1, being unity if and only if the probability distribution of the two partitions are the same.

Informational analysis of variance. The majority of ANOVA methods refer to the testing of the null hypothesis H_0: $\mu_1 = \mu_2 = \ldots = \mu_q$ where $\mu_i > 0$ $(0 \leqslant i \leqslant q)$ are means of q statistical populations. If the null hypothesis is true it results that the q populations have the same mean. This homogeneity concerning the means may be tested also using the informational energy concept [6, 8].

The one-way layout. Suppose some factor A which we consider as having some effect on a response variable of interest y has q levels. We set up an experiment in which n measurements are made of the response y at all levels. The levels q are called treatments of controlled factors, there being q controlled factors in the experimental design. Each y_{ij} result can be written as a sum of a constant μ (the general mean), α_i a term which measures the effect of the factor A at its level and a error term e_{ij} called the residual error or rezidual. The linear (or additive) model

$$y_{ij} = \mu + \alpha_i + e_{ij} \tag{9}$$

can be written for the one-way layout. It is necessary now to test the null hypothesis H_0: $\mu_1 = \mu_2 = \ldots = \mu_q$.

Let be ξ a new random variable with q values each having an associated probability p_i

$$p_i = \frac{\mu_i}{\sum_{i=1}^{q} \mu_i}, \quad i = 1, 2, \ldots, q \tag{10}$$

Now, it is possible to observe that the null hypothesis H_0 is equivalent with the hypothesis H^*: $p_1 = p_2 = \ldots = p_q = \frac{1}{q}$.

H^* hypothesis is true when $E_{(\xi)} = \frac{1}{q}$ i.e. when the informational energy of the random variable ξ is minimal:

$$\tilde{E}_{(\xi)} = \sum_{i=1}^{q} p_i^2 = \frac{\sum_{i=1}^{q} y_{i\cdot}^2}{\left(\sum_{i=1}^{q} y_{i\cdot}\right)^2}. \tag{11}$$

If $E_{(\xi)} = \tilde{E}_{(\xi)}$ the null hypothesis is accepted and by the other hand if $E_{(\xi)} \neq \tilde{E}_{(\xi)}$ the null hypothesis is rejected, hence the effect of factor A is taken as significant.

The two-way layout. Let us consider the case in which must set up an experiment to study the effects of two factors A and B on a response variable y. Factor A has q levels whereas factor B has m levels. For each combination of levels, we measure the response y_{ij} by carrying out n observations. In cases with no replications and if we assume that there is no interaction between the two factors, one may adopt a linear model

$$y_{ij} = \mu + \alpha_i + \beta_j + \varepsilon_{ij} \tag{12}$$

The hypothesis H_0 ($\alpha_i = 0$), i.e. the factor A has no significant effect is equivalent to the hypothesis

$$H^*: p_1 = p_2 = \ldots = p_q$$

This is equivalent to H_1^* : $E_{(\xi)} = \frac{1}{q}$

The estimated informational energy, $\tilde{E}_{(\xi)}$ concerning the probabilities p_i is given by equation (11). The null hypothesis is then accepted when $E_{(\xi)} = \tilde{E}_{(\xi)}$, hence all α_i values are equal to zero; the effect of factor A is not significant.

The hypothesis $\beta_j = 0 (j = 1, 2, \ldots, m)$, i.e. the factor has no significant effect, is equivalent to the hypothesis

$$H^*: p_1' = p_2' = \ldots = p_m'$$

where

$$p_j' = \frac{y_{\cdot j}}{\sum_{=1}^{m} y_{\cdot j}} \tag{13}$$

and which is equivalent to the hypothesis

$$H_1^*: E_{(\xi')} = \frac{1}{m}$$

The estimated informational energy concerning the probabilities p'_j is given by

$$\tilde{E}_{(\xi')} = \sum_{j=1}^{m} p_j'^2 = \frac{\sum_{j=1}^{m} y_{\cdot j}^2}{\left(\sum_{j=1}^{m} y_{\cdot j}\right)^2} \tag{14}$$

If $E_{(\xi')} \neq \tilde{E}_{(\xi)}$ the null hypothesis is rejected, hence the effect of factor B is significant.

Results and discussion. Two relevant cases discussed by Liteanu in his books [9, 10] using classical ANOVA methods are considered for comparing the advantages of informational analysis of variance.

The one way-layout. Seven steel samples containing Mn at the same concentration level and different matrix were analysed using emission spectrography [9, 10]. For each sample were performed 6 independent determinations. The aim of the study is to investigate if there is an effect of the matrix (Fe, Cr, Ni) on the difference of the line intensity of Mn ($\lambda = 2576{,}1$ Å) and the line intensity of Co ($\lambda = 2583{,}1$ Å) the last being used as a reference standard. The results obtained are given in Table 1.

Tabel 1

The determination of manganese in different matrix
(from ref. 9)

Observation No.	Different matrix					
	1	2	3	4	5	6
1	13	17	13	15	15	17
2	14	13	14	16	17	15
3	15	13	13	19	18	14
4	17	17	15	15	17	14
5	17	17	15	16	16	17
6	17	17	17	14	17	16

The null hypothesis $\alpha_i = 0$ ($i = 1, 2, \ldots, 6$) is equivalent with hypothesis

$$H^*: p_1 = p_2 = \ldots = p_6$$

The probabilities p_i are calculated with equation (10). This is equivalent to hypothesis H^*: $E_{(\xi)} = \frac{1}{q}$ or $E_{(\xi)} = \frac{1}{6} = 0.1667$. Empirical informational energy associated with the probabilities p_i is given by

$$\tilde{E}_{(\xi)} = \sum_{i=1}^{6} p_i^2 = \frac{\sum_{i=1}^{6} y_{i\cdot}^2}{\left(\sum_{i=1}^{6} y_{i\cdot}\right)^2} = \frac{52915}{316969} = 0.1669$$

Since $E_{(\xi)} = \tilde{E}_{(\xi)}$, the difference between samples is not significant, and is concluded that the matrix effect should be taken as insignificant.

By applying classical ANOVA at the 5% confidence level one obtained the same results because the calculated F value (1.1) is smaller than tabulated value $F^{.05}_{5,30}$ (2.53). The same result is obtained also, using the Abbe test. In this case one calculates

$$A = \frac{1}{2} \frac{\sum_{i=1}^{k-1} (\bar{x}_{i+1} - \bar{x}_i)^2}{\sum_{i=1}^{k} (\bar{x}_i - \bar{x})^2} = \frac{5.149}{4.78076} = 1.077$$

where $\bar{x}_i$ and $\bar{x}$ are the means and the great mean, respectively. Thus, the calculated A value (1.077) is higher than tabulated value $A_6^{0.05}$ (0.4454). As a consequence, the hypothesis that the matrix effect is null is not rejected.

The two-way layout. An experiment was conducted to evaluate the effect of two factors on spectrographically determination of molybdenum, namely aluminium content at three levels and manganese at two levels. Five replicate measurements were made for each combination of aluminium and manganese content. The response variable y was the blackening difference of molybdenum ($\lambda = 2816{,}1\ \AA$) and iron ($\lambda = 2813{,}6\ \AA$), the last was used as a reference standard. The results obtained are given in Table 2.

Table 2

The determination of molybdenum in presence of aluminium and manganese (from ref. 9)

Mn \ Al	1					2					3				
1	43	41	42	40	43	40	42	41	43	43	37	36	34	36	38
2	44	43	43	41	44	42	43	38	40	40	38	35	35	39	36

Using ANOVA at the 5% confidence level [9, 10], the first null hypothesis is rejected because the calculated F value (47.40) is higher that the tabulated value $F^{0.05}_{2,24}$ (3.40), which means that is a significant contribution to the total variance due to the aluminium content. The second hypothesis is accepted because the calculated F value (0.23) is smaller than the tabulated value $F^{0.05}_{,24}$ (4.25), which means that there is no significant contribution to the total variance due to the manganese content. In other words, the determination of manganese in different samples depends in a significant manner on the aluminium content and it is indifferent on the manganese content.

Considering the informational analysis of variance the hypothesis $\alpha_i = 0$ ($i = 1, 2, 3$) is equivalent to the hypothesis

$$H^*: p_1 = p_2 = p_3$$

This is equivalent to $H_1^*: E_{(\xi)} = \frac{1}{3} = 0.3333$

Empirical informational energy associated with the probabilities p_i is given by

$$\tilde{E}_{(\xi)} = \sum_{i=1}^{3} p_i^2 = \frac{\sum_{i=1}^{3} y_{i\cdot}^2}{\left(\sum_{i=1}^{3} y_{i\cdot}\right)^2} = \frac{19280.64}{57600} = 0.3347$$

As $E_{(\xi)} \neq \tilde{E}_{(\xi)}$, the effect of aluminium content is significant.

The hypothesis $\beta_j = 0$ $(j = 1, 2)$ is equivalent to the hypothesis

$$H^* : p_1' = p_2'$$

This is equivalent to H_1^*: $E_{(\xi')} = \frac{1}{2} = 0.5000$

The estimated informational energy concerning the probabilities p_j is given by

$$\tilde{E}_{(\xi')} = \sum_{j=1}^{2} p_j'^2 = \frac{\sum_{j=1}^{2} y_{\cdot j}^2}{\left(\sum_{j=1}^{2} y_{\cdot j}\right)^2} = \frac{28\,800.08}{57600} = 0.5000$$

As $\tilde{E}_{(\xi)} = E_{(\xi')}$ there is not a significant effect due to the manganese content.

Conclusions. The problem of analysis of variance has been dealt with in a mathematically simpler way using the informational energy concept. The informational analysis of variance (IANOVA) can be more efficient than the usual ANOVA methods because, like robust statistical techniques, it is resistant against uncertainties concerning the data, such as outliers or divergences from the normal distribution. An additional advantage of this method is that it is simple to carry out.

REFERENCES

1. R. F. Hirch, Anal. Chem., **49**, 691A (1977).
2. D. L. Massart, A. Dijkstra and L. Kaufman, *Evaluation and Optimization of Laboratory Methods and Analytical Procedures*, Elsevier, Amsterdam, 1978.
3. D. L. Massart, B. G. M. Vandeginste, S. N. Deming, Y. Michotte and L. Kaufman, *Chemometrics: a textbook*, Elsevier, Amsterdam, 1988.
4. O. Onicescu, C. R. Acad. Sci. Série A, 263, 841 (1966).
5. O. Onicescu and V. Ştefănescu, *Statistică Informațională*, Ed. Tehnică, Bucureşti, 1979.
6. C. Sârbu and H. Naşcu, Rev. Chim. (Bucureşti), **41**, 276 (1990).
7. I. Văduva, *Analiza Dispersională*, Ed. Tehnică, Bucureşti, 1970.
8. C. Sârbu, Anal. Chim. Acta, 271, 269 (1993).
9. C. Liteanu and I. Rică, *Teoria şi metodologia statistică a analizei urmelor*, Ed. Scrisul Românesc, Craiova, 1979.
10. C. Liteanu and I. Rică, *Optimizarea proceselor analitice*, Ed. Academiei, Bucureşti, 1985

STUDIA UNIV. BABEŞ-BOLYAI, CHEMIA, XXXVII, 1—2, 1992

L'ÉLECTRODÉPOSITION DU MANGANÈSE DE SOLUTIONS AQUEUSES DE $MnSO_4$. I. ÉTUDE COMPARATIF.

LIVIU ONICIU, PETRU ILEA, IONEL CĂTĂLIN POPESCU, MELANIA URDĂ et CSABA BOLLA

Received 21.09.1992

ABSTRACT. The electrodeposition of manganese from aqueous solutions of $MnSO_4$. I. Comparative study. In this paper the principal methods for the electrochemical preparation of managnese found in the literature are reviewed. A special attention is paid to the electrolysis of the $MnSO_4$ aqueous solution, the most important industrial application. The specific parameters of the process (the electrolyte composition, *pH*, temperature, current density) as well as the performances of the process (the deposit quality, the current yield and the specific energy consumption) are analyzed here. The parallel electrodeposition of Mn and the oxidation to, MnO_2 in the same electrochemical reactor, is also presented.

Introduction. Le manganèse est un métal ayant une importance stratégique et technique notable. Son importance vient du fait qu'il est employé à l'élaboration d'alliages, surtout d'aciers et des fontes, auxquel il confère une meilleure résistance à la rompre, usure et corrosion. La consommation moyenne de Mn par tone d'acier est estimée à 6,4 kg [1].

Il est difficile d'estimer la production mondiale de Mn métallique par manque de données et pour cela, nous contenterons par l'indication de la production de minerai de Mn [2—5]. Il faut noter que celle-ci montre seulement, indirectement, le développement de la production de Mn, parce que, à partir de la même matière première, on prépare du MnO_2 et des permanganates.

Les données du Tableau 1 attestent une augmentation continue de la production de minerai de Mn; jusqu'à l'année 2000 il y a prevue d'une augmentation annuelle de 2,5% [4]. Il faut mentionner aussi que des réserves pas négligeables de Mn, se trouvent dans les nodules marins de l'Océan Atlantique et Pacifique [6, 7].

L'obtention électrochimique est possible par electrolyse en solution aqueuse et par électrolyse ignée (8—11]; le Mn d'haute pureté est obtenu par électrolyse en solutions aqueuses de $MnCl_2$ ou $MnSO_4$

Les conditions d'électrolyse des solutions aqueuses de $MnCl_2$ sont présentées dans le Tableau 2 [12—15]. Il faut remarquer que, généralement, les rendements de courant se situent entre 78 et 81%. L'électrolyse des solutions de $MnCl_2$ est recommendée pour obtenir du Mn plastique d'haute pureté, ayant des destinations diverses, même pour des matrices cathodiques utilisées à électrodéposition du Mn.

Une variante ingenieuse propose une cellule équipée d'une cathode de Hg, sur laquelle le décharge d'hydrogène est inhibé et l'amalgame de Mn ne se forme pas [6].

L'électrolyse des solutions aqueuses de $MnSO_4$. L'électrodéposition du Mn^{2+} à partir des solutions aqueuses de $MnSO_4$ est l'alternative la plus répandue

Tableau 1

La production de minerai de Mn dans le monde (milles tonnes)

Anné/Reference Pays	1941—1945/ [2]	1946—1950/ [2]	1951—1955/ [2]	1956—1960/ [2]	1961/ [2]	1982/ [3]	1984/ [4]	1985/ [4]	1986/ [5]	1987/ [5]
Union Sovietique	1584	1814	4498	5352	5986	2957	9980	9980	9705	9705
Brésil	282	186	212	786	998	1268	2200	2180	2699	2721
Afrique du Sud	256	449	750	884	1418	2175	3050	3450	3719	3175
Inde	552	560	1555	1412	1214	555	1300	1300	1300	1270
Gabon	—	—	—	—	—	771	2120	2090	2510	2268
Australie	—	—	—	—	—	588	1630	1900	1649	1633
Chine	7	—	170	848	998	479	1600	1630	1596	1596
Maroc	44	183	409	455	571	—	—	—	—	—
Mexic	—	—	—	—	—	183	518	454	459	476
Roumanie	—	—	—	—	—	55	—	—	—	—
Ghana	588	698	680	392	77	—	—	—	—	—
Japon	256	73	190	308	297	—	—	—	—	—
Cuba	254	71	237	105	42	—	—	—	—	—
Autres	531	500	1400	1937	1634	—	—	—	599	608
Production mondiale	4354	4534	10101	12667	13550	—	—	24236	24236	23452

Tableau 2

Les conditions d'électrolyse de solutions aqueuse de $MnCl_2$.

No.	Composition d'électrolyte g/l				Électrodes		Séparateur interpolaire	Densité de courant A/cm²	Rendement de courant %		Ref.
	Catholyte		Anolyte		Cathode	Anode			cathodique	anodique	
	$MnCl_2$	NH_4Cl	$MnCl_2$	HCl							
1	299	98	291	22,5	Cu	Pt	asbeste	10—11	81	90	[12]
2	151—315	182—198	189—403	7,3—36,5	Fe	Ti platiné, graphite imprégné avec AgCl	céramique, polyester tresagé	10,7	78	94	[13]
3	190	200	—	—	Fe	Ti + Pt	céramique	10,7	78	94	[14]
4	110—195	150—200	—	—	—	Fe—Mn	polychlorure de vynil	5—25	81	—	[15]

dans le monde. Les conditions optimum d'électrolyse envisage à la fois la composition de l'électrolyte et les conditions d'électrolyse : la densité de courant, la nature des électrodes, la température et le séparateur interpolaire.

À cause du potentiel d'électrode fort négatif ($\epsilon^0_{Mn^{2+}/0} = -1{,}18$ *V/EHN*), le Mn^{2+} est dévancé dans la réductions électrochimique par les ions H_3O^+ ainsi que par les ions des tous les métaux plus nobles que Mn. Pour cela, de la solution de $MnSO_4$ il faut éliminer tous ces ions ou, au moins, diminuer au minimum leur concentration.

La purification des solutions de $MnSO_4$ d'ions de métaux lourds (Ni, Co, Cu, Fe) s'effectue par précipitation avec H_2S, Na_2S, $(NH_4)_2S$ ou même MnS, par retention sur une résine échangeuse d'ions, par complexation, etc..

Les solutions aqueuses d'électrolyte utilisées contient deux catégories de constituents : les constituents de base et les additifs. De la première catégorie font parti les $MnSO_4$, $(NH_4)_2SO_4$ et un agent réducteur, d'habitude Na_2SO_3. De la deuxième, font parti des composés du Se et d'agents de nivelement.

Poursuivant l'influence de la concentration des ions Mn^{2+} sur le rendement de courant, on a constaté que l'optimum est situé dans l'interval 40—60 *g/l* Mn^{2+} [17]. Des tel contenus de Mn^{2+} sont généralement réalisés dans les études consacrées à l'élucidation de l'influence des differents facteurs sur l'électrodéposition du Mn^{2+} [18—23]. Parfois, on est obligé d'utiliser, même des concentrations plus faibles [24—31], mais il est toujours préférable de travailler avec des concentrations élevées, chaque fois quand cela est possible. Dans ces solutions concentrées, l'électrodéposition du Mn^{2+} peut s'effectuer à des densités de courant plus grandes, obtenant une bonne productivité, sans affecter la qualité du dépôt cathodique par la décharge simultanée de l'hydrogène.

À coté du Mn^{2+} il est présent aussi l'ion NH_4^+, fourni par le $(NH_4)_2SO_4$, en concentration d'environ 130—150 *g/l* [1, 17]. Le $(NH_4)_2SO_4$ a le rol de tampon acido-basique (le couple NH_4^+/NH_3 à la cathode et le couple HSO_4^-/SO_4^{2-} à l'anode) et peut-être de générateur des complexes Mn^{2+}—NH_3 [32].

Pour stabiliser le Mn métallique et, à la fois, pour éviter l'oxidation du Mn^{2+} [33] à cause de la présence de l'oxygène, l'électrolyte doit être additionée d'un agent réducteur. Par exemple, en présence de Na_2SO_3 [33], en milleux alcalin :

$$SO_3^{2-} + 2HO^- \rightleftharpoons SO_4^{2-} + 2e^- + H_2O, \quad \epsilon^0_{pH=14} = -0{,}93\ V/EHN;$$

la concentration optimum de SO_2 est d'environ 0,1 *g/l* [26, 30, 34, 35], des quantités plus importantes étant résponsable de l'impurification du dépôt de Mn avec du soufre [34]. En ce qui conserne les additifs, leur efficacité se manifeste à des concentrations de l'ordre du *g/l*.

La présence des composés du Se dans l'électrolyte [36, 37] a une influence positive sur le rendement de courant, sur la pureté du dépôt cathodique, sur la résistance à la corrosion du Mn déposé et, à la fois, permet l'opération à des températures plus élevées. Ainsi, la présence du $(NH_4)_2SeO_4$ 0,1—0,2 *g/l*, à 50°C augmente le rendement de courant, jusqu'à 84% [37]. Le même additif assure des rendements de courant >70% même en milieux acid ($pH \approx 2{,}5$). L'électrolyse dans les solutions contenant d'impurétes comme

Cu et Ag, découle dans bonnes conditions en présence de 0,14 g/l $(NH_4)_2SO_4$ à $pH \approx 7$ et à des densités de courant de 500 A/m^2 [21]. Également, l'effet négatif des substances organiques accidentellement présentes dans l'électrolyte est beaucoup diminué en présence des composés du Se [34]. La stabilité du dépôt de Mn est beaucoup augmentée par la présence de l'ion SeO_3^{2-}, qui inhibe la dissolution du Mn [35]. La présence simultanée des composes de Se et d'agents de nivellement determinent l'apparition d'un éffet sinergétique sur le rendement de courant [36].

La manière d'action des composés du Se n'est pas encore entièrement connue, mais on suppose que le Se et l'ion Se^{2-} peuvent être déterminantes. Ces composés du Se augmentent le surpotentiel de décharge d'hydrogène [23, 24].

Les agents de nivellement sont des substances tensioactives qui assurent l'obtention des dépôts de Mn plus lisses [17]; pour ce but ont été utilisées: méthylorange, sulfamide [38], silicate de sodium, gélatine, dextrine, colle forte [39], phénol [40], thiourée [41], des composés du type éthyléne-diamine [42] pyridine [35], polyacrylamide [35], acide oxalyque [27], diéthylamine, sulfure de carbone [19], hexaméthylène tetraminne, urée [43], extrait de saponaria officinalis [17, 44].

Parmi les composés employés il faut remarquer la KF et les ions Zn^{2+}. La KF $\approx 0,1$ g/l augmente le rendement de courant et diminue la surtension dans la cellule d'électrolyse [28]. À coté des composés du Se, les traces de Zn^{2+} exercent un effet sinergetique sur le rendement de courant [45].

Le coût du processus et la qualité du Mn obtenu par l'électrolyse des solutions aqueuses de $MnSO_4$, dépendent, en même temps, de la nature de l'électrode, du separateur interpolaire, du pH, de la densité de courant et de la température.

Les cathodes d'acier inoxydable donnent des bons résultats jusqu'à 50°C. Pour des températures plus élevées il est recommandé le Ti. L'alimentation du Se peut se faire en utilisant une cathode d'acier inoxydable, contenant 0,1–0,7% Se [30], quand le rendement de courant est supérieur à celui enregistré avec des cathodes d'acier inoxydable sans Se et à celui avec une électrolyte contenant des composés de Se.

D'habitude, les anodes sont en plomb allié avec l'argent (1%). L'utilisation des anodes ayant qualitées électrocatalytiques pour la décharge d'oxygène conduit à la réduction de l'énergie consommée grace à la diminution du surpotentiel anodyque [46] et à la formation de MnO_2 [47].

Le séparateur interpolaire microporeux peut-être réaliser en polychlorure de vinyle [48], en polyesters ou en cotton.

Le contrôle et le réglage du pH représentent des aspects decisifs pour atteindre des rendements de courant élevés. Pratiquement il est très important le contrôle du pH de l'électrolyte. Le pH de l'électrolyte, ayant la composition 15–30 g/l Mn^{2+}, 130–150 g/l $(NH_4)_2SO_4$, 0,1–0,3 g/l SO_2 et des composés de Se, peut varier entre 2 et 9,5 [49]; par contre le pH du catholyte peut rester dans le domaine 7–8 par la suite de la difusion d'ions H_3O^+ provenant de l'anode [50]. Dans ces conditions l'augmentation du surpotentiel de déchar-

ge de l'hydrogène est nécessaire (par exemple en additionant des composés de Se et de soufre).

La majorité des études récommande des densités du courant cathodique comprises entre 400 et 500 A/m^2 ; à des valeurs supérieures, le rendement de courant et la qualité du dépôt diminuent. En présence des ions Ag^+ (≈ 25 mg/l) on obtient des rendements de courant acceptables aux densités de courant d'environ 2 500 —5 000 A/m^2 [51]. De l'étude des voltammogrames on a constaté qu'en présence de Zn^{2+}, la séparation du Mn commence aux densités de courant moins élevées [52], ce qui correspond, à des consommations d'energie plus faible [26].

En conclusion, on peut affirmer qu'au dessus de 500 A/m^2 on travaille uniquement en solution concentrées de Mn^{2+}, à des températures qui dépassent la valeur ambiante, en présence des additifs qui empêchent la décharge simultanée de l'hydrogène et, en même temps, ont des effets de nivellement.

En général, on travaille entre 15 —30 °C ; à des températures plus élevées, dans l'éspace anodique augmentent les quantités de MnO_2 [53]. Dans les solutions contenant des composés de soufre, l'élevation de la température conduit à l'impurification du dépôt cathodique avec du soufre [34]. Contrairement à l'opinion génerale pour l'influence négative des températures élevées sur la déposition cathodique de Mn, on a constaté [22] que l'on peut obtenir aussi jusqu'à 80 °C, à la condition que l'électrolyte soit ultrapur. Le rendement de courant reste bon si aux températures plus élevées on opère avec densités de courant plus grandes : par exemple, à 50 °C et à 2 000 A/m^2 le rendement de courant dépasse 80%.

Pour accroître l'efficience énergetique de l'électrolyse, en 1973, commencent les recherches pour l'obtention simultané de Mn et MnO_2 [54 —57]. Il est à souligner que 1 kWh donne 113 —127 g Mn (en parallèle avec la décharge anodique de l'oxygène) et 455 g MnO_2 (avec la décharge cathodique de l'hydrogène) [58].

Dans l'électrolyse parallèle de Mn et MnO_2 il est nécessaire de maintenir des conditions très differentes pour le déroulement des réactions d'électrode. Ainsi, le Mn électrolytique est obtenu industriellment à 35 °C aux densités de courant de 400 —500 A/m^2, à partir des solutions de $MnSO_4$ neutres et dans un réacteur compartimenté, tandis que le MnO_2 électrolytique est obtenu à 90 °C, à une densité de courant de 100 A/m^2, à partir des solutions de $MnSO_4$, acides, dans un réacteur non-compartimenté. Les densités de courant différentes pour les deux processus d'électrode, peuvent être réalisées choisissant un raport adéquat entre les surfaces actives des électrodes. La différence de pH peut-être maintenue utilisant un séparateur interpolaire de porosité et stabilité chimique adéquates. La contrainte la plus difficile est celle dûe a la différence de température d'environ 50 °C, qu'on doit maintenir entre l'espace cathodique et anodique. Ainsi, s'explique les études dédiés à l'obtention du Mn à des températures plus élevées [22, 25]. La présence de $(NH_4)_2SeO_4$ 0,05 —0,1 g/l permet l'obtention catodique (à 80 °C) du Mn avec un rendement convenable et, à la fois, à l'anode, du MnO_2 cristallin. D'autre parte, la présence de $(NH_4)_2SeO_4$ permet d'abaisser le contenu de $(HN_4)_2SO_4$ de 150 g/l à 50 g/l, l'utilisation d'un électrolyte ayant un contenu d'impuretés plus élevé et l'électrolyse à

une densité de courant de 1000 A/m^2 [55]. La cathode peut-être en Al ou en acier inoxydable et l'anode en Ti recouvert d'une couche de MnO_2.

Une autre variante d'obtention parallèle de Mn et MnO_2, recommende une difference de température anolyte-catholyte de 70°C [56]. Le catholyte est refroidit par l'intermédiare de la cathode en Ti, ayant une géometrie tubulaire, qui permet la circulation de l'eau de refroidissement.

L'anode est en graphyte ou en alliage Pb—Ag. Pour éviter la pénétration d'ions NH_4^+ dans anolyte, le niveau de celui-ci dépasse celui du catholyte. La littérature contient peu d'informations rélatives aux séparateurs interpolaires employés. Pour la variante parallèl sont indiqués le polychlorure de vinyl armée aux fibres en verre [56], les permutites, ou les résines synthétiques echangeuses d'ions contenant des groupements NH_3^+ ou S^- [57].

Conclusions. L'électrolyse ignée est energo-intensive (on consomme environ 5,1 kWh/kg Mn uniquement pour la déposition cathodique du Mn, sans compter l'énergie nécessaire pour maintenir l'électrolyte en état fondu) et la pureté du produit obtenu est moderée. L'électrolyse de solutions aqueuses de $MnCl_2$ est caracterisée par une énergie spécifique plus faible (aprox. 4,5 kWh/kg Mn), mais elle pose des problèmes de corrosion très importants, à cause de la présence du Cl^-. Celui-ci empèche la préparation parallèle du MnO_2, à cause de la décharge anodique du Cl_2. En revanche, l'électrolyse des solutions de $MnCl_2$ est recommandable pour l'obtention d'un métal trés pur, destiné par exemple à la fabrication des matrices cathodiques employées dans l'electrolyse des solution de $MnSO_4$.

L'électrolyse de solutions aqueuses de $MnSO_4$ pour l'obtention de Mn métalique, est caracterisée par une consommation d'environ 8 kWh/kg Mn. Elle est la plus repandue pour les raisons suivantes :

— la solubilisation du minerai de MnO_2 avec une solution aqueuse de H_2SO_4 est plus efficace ;

— la corrosion dans l'instalation d'électrolyse est moins accentuée ;

— les solutions de $MnSO_4$ peuvent-être employées simultanément a l'obtentions du MnO_2 ;

— les perfectionnements du procédé, réalisés récemment, permettent la diminution de la consommation d'énergie au dessous de 8 kWh/kg Mn ;

— l'obtention simultané de Mn et MnO_2 à partir de solutions de $MnSO_4$ représente une alternative attrayante pour la rentabilisation du processus anodique. Elle peut mettre en valeur les meilleurs résultats obtennus dans la recherche des deux processus d'électrodes concernés : température élevée et pH acide, en présence des composés de Se pour le processus cathodique, et l'utilissation de d'électrodes électrocatalytiques pour le processus anodique.

BIBLIOGRAPHIE

1. R. D. W. Kemmitt, *Comprehensive Inorganic Chemistry*, Vol. **3**, Perganon Press, New York, 1973, p. 771.
2. R. I. Agladze, Elektrokhim. Margantsa, **3**, 7 (1967).
3. * * * *Statele lumii*, Ed. Ştiinţifică şi Enciclopedică, Bucureşti, 1985, p. 795.
4. B. V. Tilak, J. W. Van Zee, J. Electrochem. Soc., **135**, 279c (1988).
5. J. W. Van Zee E. J. Rudd, J. Electrochem. Soc., **135**, 485c (1988).

6. Kirk — Othmar, *Encyclopedia of Chemical Technology*, Vol. **12**, Interscience Publishers New York, 1967, p. 887.
7. V. S. Savenko, G. N. Baturin, Litol. Polezn. Iskop. **5**, 64 (1981), Chem. Abstr., **95**, 223128 (1981).
8. Brevet France, 1. 463. 101. 1966, Chem. Abstr., **67**, 66756 (1967).
9. Brevet Indie, 150. 471, 1982, Chem. Abstr., **99**, 8867 (1983).
10. R. I. Agladze, V. Yu. Muidin, V. P. Tugushi, Trud. Gruz. Politekh. Inst., **5**, 48 (1970), Chem. Abstr. **75**, 115256 (1971).
11. Brevet R.F.A., 2. 629. 725, 1977, Chem. Abstr. **86**, 109512 (1977).
12. Brevet Hollande, 6. 501 844, 1936, Chem. Abstr. **66**, 7931 (1967).
13. Brevet France, 1. 495. 621, 1967, Chem. Abstr. **71**, 119037 (1969).
14. Brevet U.S.A., 3. 477. 925, 1969, Chem. Abstr. **72**, 50392 (1970).
15. S. N. Basmanova, R. I. Agladze, Isled. V. Obl. Elektrolitm. i Radiats. Khim., **55**, 145 (1965), Chem. Abstr. **64**, 17033 (1964).
16. B. P. Yurbev, S. N. Skolnikov, G. I. Patrova, *Fizikokhimia i metalurghia margantsa*, Mir, Maskva, 1983, p. 66, Ref. Zhur. Khim., 6I,347 (1984).
17. N. T. Kudrayavtseva, *Prikladnava Electrokhimiya*, Khimiya, Moskva, 1975, p. 283.
18. R. I. Areshidze, T. I. Seshav, Soobsheh. Akad. Nauk. Gruz. S. S. R., **33**, 579 (1964), Chem. Abstr. **62**, 2507 (1965).
19. N. A. Shwab, D. P. Zosimovich, *Elektrokhimiya Protsessy Electroasazdenii. Anodnom Rastvorenii Metal*, Nauka, Maskva, 1969, p. 47, Chem. Absrt. **73**, 126369 (1970).
20. A. K. Sulyakas, I. V. Yanitskii, G. Juseviciene, Liet. T.S.R. Mokslu Akad. Darb. Ser. B, **4**, 47 (1973), Chem. Absrt. **80**, 55224 (1974).
21. I. V. Yanitskii, A. K. Sulyakas, M. Kuadyte, idem, **4**, 47 (1983), Chem. Abstr. **100**, 417180 (1984).
22. J. Janickis, A. Suliakas, A. Niaura, *Int. Soc. Electrochem., 37-th Meeting*, Extended Abstr., Vol. II, Vilnius, 1986, p. 127.
23. I. V. Yanitskii, P. I. Vishkyalis, A. K. Sulyakas, Trud. Akad. Nauk. Lit. S. S. R. Ser. B, **3**, 18 (1984).
24. A. R. Tourky, I. M. Issa, I. F. Hewaidy, J. Chem. U. A. R., **5**, 77 (1962), Chem. Abstr. **64**, 3024 (1966).
25. G. Ya. Sioridze, E. D. Tshchikvadze, Elektrokhim. Margantsa, **3**, 390 (1967).
26. C. L. Mantell, G. R. Ferment, Brevet U.S.A., 3. 455. 799, 1969, Chem. Abstr. **71**, 76823 (1969).
27. Y. Amino, Y. Kumano, N. Nishino, R. Hayakawa, Brevet Japon, 7015610, 1970, Chem. Abstr., **73**, 68876 (1970).
28. S. Kiriyava, K. Kanamura, Brevet Japon, 7413011, 1974, Chem. Abstr., **81**, 5362, 1974.
29. V. O. Nwoko, Chem. Age India, **31**, 262 (1980), Ref. Zhur. Khim., 21,274 (1981).
30. S. C. Lai, Brevet U.S.A., 3.686 083, 1972, Chem. Abstr., **77**, 134391 (1972).
31. E. M. Unghiadze, R. I. Agladze, Soob. Inst. Neorg. Khim. Elektrokhim. Akad. Nauk. S. S. R., **7**, 32 (1967).
32. Yu. Yu. Matulis, A. K. Byarnotas, Y. S. Bubyalis, Elektrokhim. Margantsa, **3**, 316 (1967).
33. Yu. Yu. Iurie, *Îndreptar de chimie analitică*, Ed. Tehnică, Bucureşti, 1970, p. 268.
34. O. S. Sadunishvili, N. T. Gofman, R. I. Agladze, T. A. Lomiya, D. Ya. Sepertеladze, Elektrokhim. Margantsa, **7**, 50 (1978).
35. A. K. Sulyakas, J. Jsnishis, M. Viskelis, Isled. Obl. Osazh lenya Metal. Mater., Respub. Konf. Elektrokhim. Litov. S.S.R., **11**, 31 (1971), Chem. Abstr., **77**, 13992 (1972).
36. R. I. Agladze, N. T. Gofman, L. Z. Zadikashvili, O. S. Sadunishvili, Izvest. Akad. Nauk. Gruz. S.S.R., Ser. Khim., **1**, 93 (1975).
37. N. T. Gofman, Yu. V. Abuladze, M. V. Chankashvili, Elektrokhim. Margantsa, **5**, 37. (1975).
38. R. I. Agladze, I. G. Shavoshvili, M. J. Kurashvili, Izvest. Akad. Nauk. Gruz. S.S.R., **5**, 72 (1979).
39. R. I. Agladze, E. M. Unghiadze, Elektrochim. Margantsa, **1**, 421 (1957).
40. D. A. Bogyeradze, idem, **3**, 122 (1967).
41. J. C. D'Abreu, M. L. Torem, Congr. Anu. ABM, 35-th, **2**, 245 (1980), Chem. Abstr., **94**, 38556 (1981).
42. I. V. Gamali, G. E. Rybalskaya, Zhur. Priklad. Khim. **46**, 185 (1973).

43. I. G. Shavoshvili, M. J. Kurashvili, R. I. Agladze, Sob. Akad. Nauk. S.S.R. **93**, 81 (1979).
44. A. M. Suhotina, Spravocinik po elektrokhimiya, Khimia, Leningrad, 1981, p. 137.
45. S. C. Lai, Brevet U.S.A., 3.821.0096, 1974.
46. K. R. Kaziol, E. F. Wenk, *Elektrolyse Nichteisenmet.* Votr. 11 met. Semin, Lüneburg. 22—24 Jan., 1981 Weinheim e.a., 1982, p. 409, Ref. Zhur. Khim. 18L371 (1984).
47. L. Oniciu, P. Ilea, Cs. Bolla, L. D. Boboș, G. Țarălungă, *Cercetări privind obținerea manganului metalic prin electroliză*, Raport de fază, 1986.
48. E. M. Unghiadze, Trud. Inst. Priklad. Khim. i Elektrokhim. Akad. Nauk. Gruz. S.S.R., 3, 87 (1962).
49. P. I. Vishkyalis, I. V. Janitskii, A. K. Sulyakas, Tr. Akad. Nauk. Lit. S.S.R., Ser. B, **4**. 31 (1984), Ref. Zhur. Khim. 3L326 (1985).
50. L. Fekete, Proc. Res. Inst. Nonferrous Metals, 281 (1958). Chem. Abstr. **75**. 136463 (1971).
51. H. Kuodyte, I. V. Janitskii, A. K. Sulyakas, Issled. Obl. Elektroosazhdeniya Met., Mater. Resp. Konf. Elektrokhim., Lit. S.S.R., 15-th, 57 (1977), Chem. Abstr. **88**. 179261 (1978).
52. V. N. Belinskii, *Kinetika i elektrod protsessy v vodnih rastvorah*, Khimia, Kiev, 1983, p. 79.
53. A. K. Sulyakas, I. V. Janitskii, A. Niaura, *Issled. Obl. Osazhdeniya Metal.*, Mater. Resp. Konf. Elektrokhim. Lit. S.S.R., **16**. 45 (1977), Chem. Abstr. **87**. 13382 (1977).
54. R. I. Agladze, N. T. Gofman, Yu. V. Abuladze, Brevet U.S.S., 380742, 1973.
55. Yu. V. Abuladze, N. T. Gofman, R. I. Agladze, Elektrokhim. Margantsa, **7**. 39 (1978).
56. N. S. Goghishvili, R. I. Agladze, Izv. Akad. Nauk. Gruz. S.S.R. Ser. Khim. **12**. 156 (1986).
57. Brevet R.S. Cehoslovacia, 101801, 1961, Chem. Abstr. **58**. 8655 (1963).
58. C. A. Hampel, *The Encyclopedia of Electrochemistry*, Reinhold Publishing Corp. Chapman and Hall, London, 1964, p. 790.

STUDIA UNIV. BABEŞ-BOLYAI, CHEMIA, XXXVII, 1—2, 1992

L'ÉLECTRODÉPOSITION DU MANGANÈSE DE SOLUTIONS AQUEUSES DE $MnSO_4$.

II. Voltammétrie dans le système $MnSO_4 - (NH_4)_2SO_4$ à la présence des certains additifs.

LIVIU ONICIU, PETRU ILEA, IONEL CĂTĂLIN POPESCU et MELANIA URDĂ

Received 21.09.1992

ABSTRACT. The electrodeposition of manganese from aqueous solution of $MnSO_4$. II, Linear sweep voltammetry in the syttem $MnSO_4-(NH_4)_2SO_4$ and some additives. Manganese is an electroactive metal, that is why its electrodeposition from aqueous solutions requires special conditions for counteracting simultaneous discharge of hydrogen ions. Electrolyte composition and the presence of certain additives (Se^{4+}, Se^{6+}, Zn^{2+}, F^-, urea) influences the current efficiency of the electrodeposition process. Using linear sweep voltammetry, the inhibition of the hydrogen discharge reaction by tested additives and the existence of their synergetical action was proved.

Introduction. L'analyse de l'électrodéposition du manganèse de solutions aqueuses de $MnSO_4$ a relevé l'influence de la composition de l'électrolyte $(NH_4)_2SO_4$ [1] et des certains additifs, tel que les composés du Se [2], l'urée [3], l'ion F^- [4] et l'ion Zn^{2+} [5].

Le but de cet étude a été d'éclaircir la specificité d'action des constituants de base et d'additifs mentionnés dans la réaction de décharge de l'hydrogène (*rdH*) [1].

La méthode utilisée a été la voltammetrie au balayaje linéair de potentiel.

Partie expérimentalle. Les mesures voltammétriques ont été effectués dans une cellule compartimentée (Fig. 1) par l'intermédiaire d'une parois en verre fritté (porosité G3). Le compartiment catodique (aprox. 50 *ml*) a été équipé d'un fil en Pt (electrode de travail, ET) ayant $\emptyset = 0{,}5\ mm$ et $S \approx 8\ mm^2$, d'une électrode de calomel saturée (referance, ER) et d'une électrode en verre (EV) pour la mesure du *pH*. Dans le compartiment anodique a été placé une contreélectrode en platine ($S \approx 5\ cm^2$).

La vitesse de balayage et les limites du potentiel exploré sont spécifiées sur les voltammogrames onbtenues. Avant chaque mesure, l'électrode de travail a été nettoyée en HNO_3 conc., lavée à l'eau distillée et puis flambée dans une flame d'alcool éthylique.

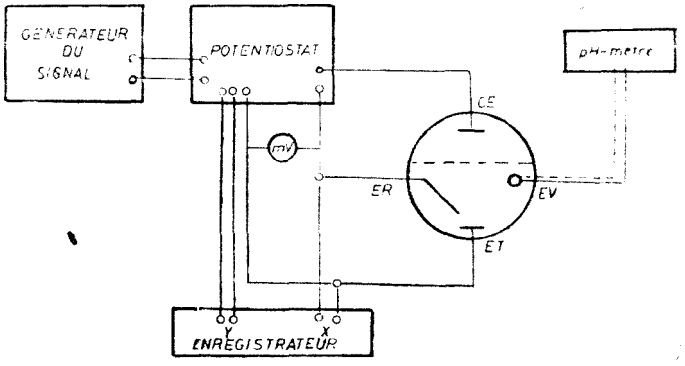

Fig. 1. Le montage expérimental

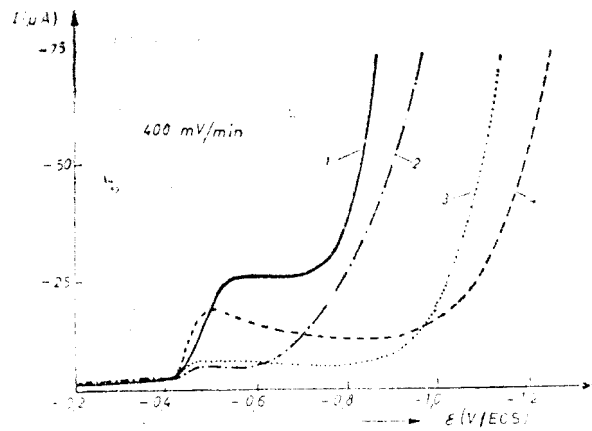

Fig. 2. Voltammogrames des systèmes: $(NH_4)_2SO_4$ 1M (1), NH_4Cl 1M (2), KCl 1M (3) et K_2SO_4 0.5M (4); pH = 3,0.

Résultats et discussions. Dans l'électrodéposition du Mn de solutions aqueuses de $MnSO_4$, la *rdH* est entretenue, plus ou moins, par chacun constituant de la solution d'électrolyte.

Le mode d'action de l'électrolyte support sur la *rdH* (Fig. 2. au pH =3 et Fig. 3, au pH=7) est présenté par comparaison à celui du NH_4Cl, du KCl, et du K_2SO_4.

On constate que tant en milieux acide (pH = 3), qu'en milieux neutre (pH = 7), la *rdH* a lieu aux potentiels de plus en plus negatifs, dans l'ordre: $(NH_4)_2SO_4$, NH_4Cl, KCl, K_2SO_4.

Les deux sauts de courent remarqués sur les courbes 1 et 4 de la Fig. 2 correspondent à la réduction de l'hydrogéne provenant de deux sources protogènes: HCl et H_2O (courbe 1) et respectivement HSO_4^- et H_2O (courbe 4).

Apparément, le meilleur électrolyte support semble être le K_2SO_4. En réalité, au pH = 7 (condition d'opération industrielle), seulement le $(NH_4)_2SO_4$ a un effet tampon efficace pour maintenir le pH dans le domaine 7—8.

La diminution de l'intensité de courant dans la zone de potentiel correspondante à l'électrodéposition du Mn^{2+} déterminée par la présence du H_2SeO_3 (Fig, 4) pourait-être associée a l'empechement de la *rdH* et, par conséquent, à l'augmentation du rendement en courant de l'électrodeposition du manganèse.

Une confirmation indirecte de ce fait nous a fourni l'analyse des surfaces et des hauteurs des boucles anodiques des voltammogrames cycliques (Fig.5) On observe, (la courbe 1 Fig. 5A et la courbe 2 Fig. 5B) que, la présence des ions NH_4^+ dans l'électrolyte support, a aussi un effet bénéfique sur le rendement de deposition cathodique du Mn^{2+}, grace à l'effet tampon du système $NH_4^+/(NH_3)$; ainsi dans le voisinage immédiat de la cat-

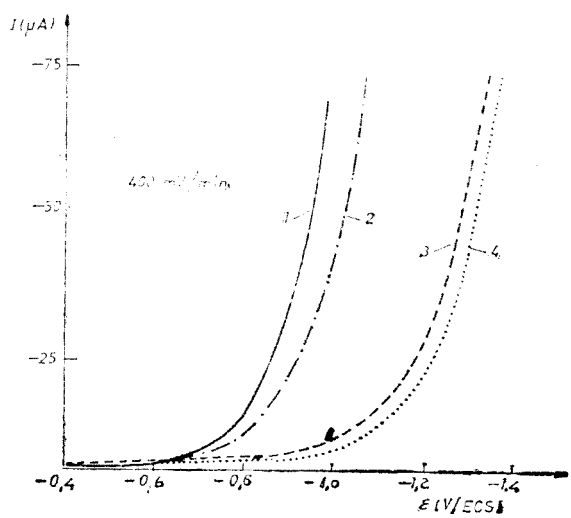

Fig. 3. Voltammogrames des systèmes: $(NH_4)_2SO_4$ 1M (1), NH_4Cl 1M (2), KCl 1M (3) et K_2SO_4 0.5M (4); pH = 7,0.

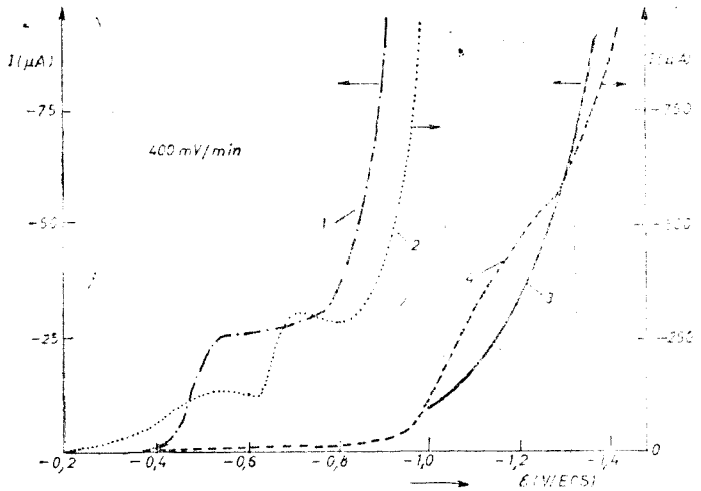

Fig. 4. Voltamogrammes du système $(NH_4)_2SO_4$ 1M: (1) $pH = 3,0$ et (3) $pH = 7,0$ et du système $(NH_4)_2SO_4$ 1M + H_2SeO_4 1,5 mM: (2) $pH = 3,0$ et (4) $pH = 7$

hode, l'augmentation excessive du pH est evitée en assurant ainsi la stabilité des ions Mn^{2+}.

L'effet de H_2SeO_4 dans électrolyte est beaucoup plus faible en comparaison avec le H_2SeO_3 (Fig. 6, les courbes 1 et 2), probablement, à cause de la stabilité électrochimique du SeO_4^{2-} [6].

Les ions Zn^{2+} en concentrations de l'ordre de *ppm*, inhibent la *rdH*, (Fig. 7,

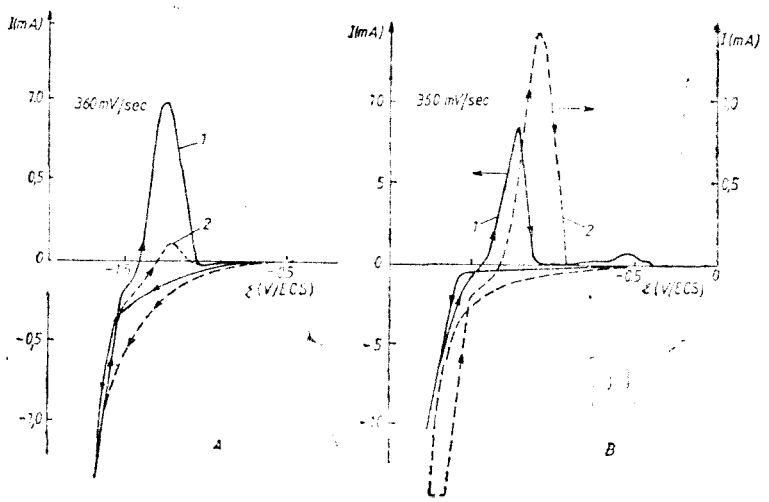

Fig. 5. Voltammogrames cycliques, pH = 7, des systèmes: (A) $MnSO_4$ 1M + $(NH_4)_2SO_4$ 1M (1) et $MnSO_4$ 1M + K_2SO_4 0,5M (2); (B) $MnSO_4$ 1M + $(NH_4)_2SO_4$ 1M + H_2SeO_3 1,5 · 10^{-3}M(3) et $MnSO_4$ 1M + K_2SO_4 0,5M + H_2SeO_3 1,5 · 10^{-3} M (4).

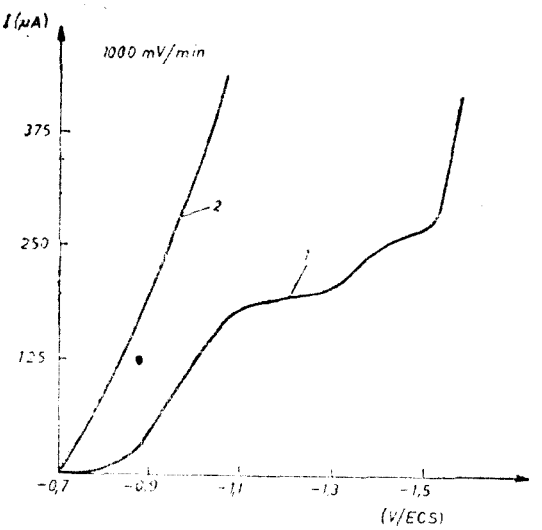

Fig. 6. Voltammogrames des systèmes:
$MnSO_4$ 1M + $(NH_4)_2SO_4$ 1M + H_2SeO_3 $1.5 \cdot 10^{-3}$ M, $pH = 6.8$ (1),
$MnSO_4$ 1M + $(NH_4)_2SO_4$ 1M + H_2SeO_4 $1.5 \cdot 10^{-3}$ M, $pH = 7.0$ (2).

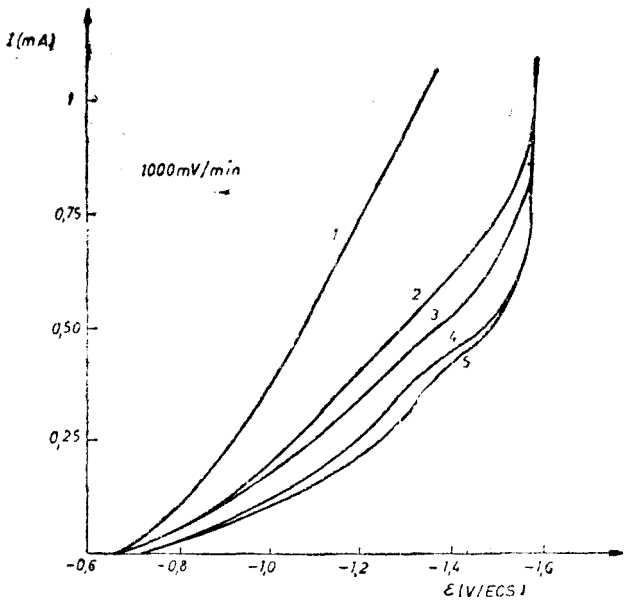

Fig. 7. Voltammogrames, pH = 7, des systèmes:
$MnSO_4$ 1M + $(NH_4)_2SO_4$ 1M, (1);
$MnSO_4$ 1M + $(NH_4)_2SO_4$ 1M + Zn^{2+} 0,31 *ppm* (2);
$MnSO_4$ 1M + $(NH_4)_2SO_4$ 1M + Zn^{2+} 0,62 *ppm*, (3);
$MnSO_4$ 1M + $(NH_4)_2SO_4$ 1M + Zn^{2+} 5 *ppm*, (4);
$MnSO_4$ 1M + $(NH_4)_2SO_4$ 1M + Zn^{2+} 15 *ppm*, (5).

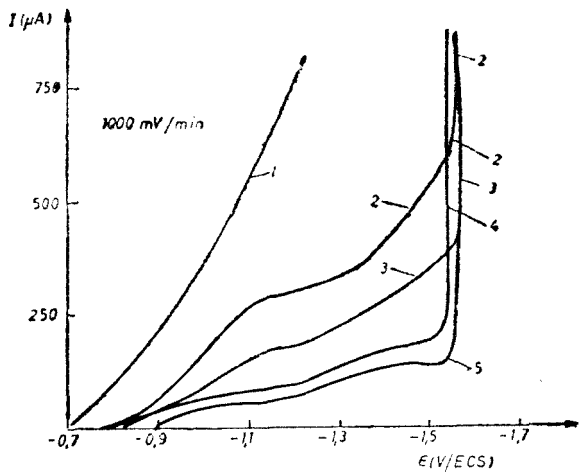

Fig. 8. Voltammogrames, $pH = 7$, des systèmes :
$MnSO_4$ 1M + $(NH_4)_2SO_4$ 1M, (1) ;
$MnSO_4$ 1M + $(NH_4)_2SO_4$ 1M + H_2SeO_3 $1,5\ 10^{-3}$ M, (2) ;
$MnSO_4$ 1M + $(NH_4)_2SO_4$ 1M + urea 1,2 g/l, (3)
$MnSO_4$ 1M + $(NH_4)_2SO_4$ 1M + Zn^{2+} 5 *ppm*, (4) ;
$MnSO_4$ 1M + $(NH_4)_2SO_4$ + F^- 30 *ppm*, (5).

les courbes 1—5, et, par conséquent, la déposition des ions Mn^{2+} se fait avec des rendements meilleurs, aux densités de courant plus petites [5]. L'effet augmente progressivement avec la concetration du Zn^{2+} jusqu'à la valeur de 5 *ppm*, ou il se plafonne.

La Fig. 8 montre l'inhibation de la rdH, due à l'H_2SeO_3, à l'urée, au Zn^{2+} et à la KF.

D'aprés les résultats obtenus l'effet des additifs étudiés, exprimé par la diminution des densités de courant de la *rdH*, peut s'ordoner de la manière suivante :

Se (IV) > Zn^{2+} > urée > F^- (voir Fig. 8 les courbes 2—5).

Si l'électrolyte contient à la fois, à coté de H_2SeO_3, les additifs mentionés (Fig. 9, les courbes 1—5), on constate un effet synergétique qui baisse dans l'ordre :

(F^- + Se (IV)) > (Zn^{2+} + Se(IV)) > (urée + Se(IV)).

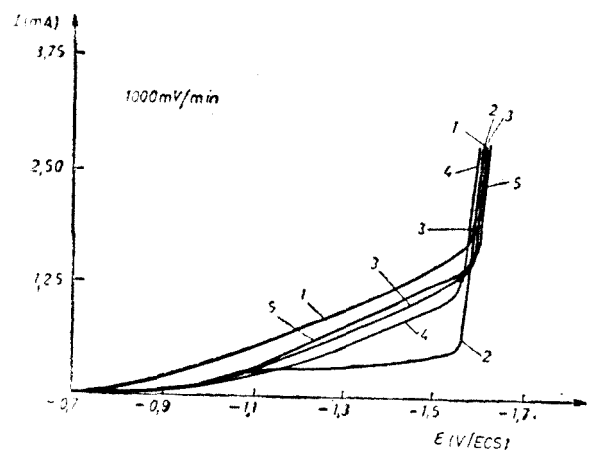

Fig. 9. Voltammogrames, $pH = 7$, des systèmes :
$MnSO_4$ 1M + $(NH_4)_2SO_4$ 1M, (1) ;
$MnSO_4$ 1M + $(NH_4)_2SO_4$ 1M + H_2SeO_3 $1,5 \cdot 10^{-3}$ M, (2) ;
$MnSO_4$ 1M + $(NH_4)_2SO_4$ 1M + H_2SeO_3 $1,5 \cdot 10^{-3}$ M + urée 1200 *ppm*, (3) ;
$MnSO_4$ 1M + $(NH_4)_2SO_4$ 1M + H_2SeO_3 $1,5 \cdot 10^{-3}$ M + Zn^{2+}, (4) ;
$MnSO_4$ 1M + $(NH_4)_2SO_4$ 1M + H_2SeO_3 $1,5 \cdot 10^{-3}$ M + F^- 30 *ppm*, (5).

Conclusions. L'analyse de la voltammograme de l'électrolyte support, $(NH_4)_2SO_4$, montre que dans le domaine de pH neutre-faiblement alcalin, l'ions NH_4^+ constitue une source importante de protons pour la *rdH*, ce qui suggère que les ions NH_4^+ doivent être évités. Mais, en réalité, la basicité induite par NH_3 fourni à la cathode par la déprotonation de l'ion NH_4^+ est favorable pour les conditions de déposition du manganèse.

Des petites quantités du Se (IV), déterminent une augmentation notable du rendement de courant de l'électrodéposition du Mn^{2+}, surtout quand l'électrolyte est $(NH_4)_2SO_4$.

Les effets de certains additifs dans l'électrodépositon du Mn^{2+} de solutions aqueuses de $MnSO_4 - (NH_4)_2SO_4$, montrent que la présence simultanée du Se(IV) $1{,}5 \cdot 10^{-3}$ M et de la F^- à 0,32 *ppm* est la meilleur, à cause de l'effet synergétique.

D'autre part, la présence simultanée du Se(IV) $1{,}5 \cdot 10^{-3}$ M et du Zn^{2+} à 5 *ppm* a un effet positif ; d'ailleurs le minerai de manganèse contient des traces de Zn, ce qui est positif pour l'électrodéposition du manganèse.

BIBLIOGRAPHIE

1. L. Oniciu, P. Ilea, I. C. Popescu, Melania Urdă, Cs. Bolk, Studia Univ. Babeş–Bolyai, Chem., en press.
2. O. S. Sadunishvili, N. T. Gofman, R. I. Agladze, T. A. Lomiya, D. Ya. Seperteladze, Elektrokhim. Margantsa, **7**, 50, (1978).
3. Shavoshvili, I. V., Kuhashvili M. J., Agladze R. I., Sabsh. Akad. Nauk. S.S.R., **93**, 81 (1979).
4. Kiriyama, S., Yamamura, K., Patent Japonia, 743–011 (1974).
5. Lai, S. C. Patent SUA, 3.821.096, (1974).
6. Janickis, P. V., Vishkyalis., P. J. Sulyakas, A. K. Trud. A.N. Lit. S.S.R., Ser. **B**. **3**, 18 (1984).

STUDIA UNIV. BABEŞ-BOLYAI, CHEMIA, XXXVII, 1—2, 1992

CONTRIBUTIONS TO THE KINETICS AND MECHANISM OF THE CHROMATE ACID OXIDATION OF ALCOHOLS. OXIDATION OF CYCLOHEXANOL AND BENZYL ALCOHOL.

IOAN BÂLDEA,* MARIA GIURGIU*

Received: 05.10.1992

ABSTRACT. The kinetics of benzyl alcohol and cyclohexanol oxidation by chromate in strong acid media have been studied spectrophotometrically over a temperature range 10—30 °C and various H^+ and ROH concentrations. Forth-order rate expression

$$-d[Cr(VI)]/dt = k_4\ [HCrO_4^-]\ [ROH]\ [H^+]^2$$

have been determined for both oxidations, with $k_4 = (2.5 \pm 0.1) \times 10^{-1}\ dm^9\ mol^{-3} s^{-1}$ for $C_6H_5CH_2OH$ at 25.5 °C and $k_4 = (4.5 \pm 0.2) \times 10^{-3}\ dm^9 mol^{-3} s^{-1}$ for *ciclo*—$C_6H_{11}OH$ at 25.0 °C. Activation parameters have been calculated. Relative low values of $\Delta H^{\neq}$ and negative and large values $\Delta S^{\neq}$ have been obtained. The proposed mechanism involves the formation of chromic esters, and one- and bi- equivalent redox processes.

Introduction. Chromium (VI) is a well-known oxidizing agent used in chemical analysis and as a common reagent for the oxidation of organic materials. The oxidation of alcohols yields aldehydes, ketones and other products where cleavage of C — C bond takes place, depending on the nature of alcohol and on the concentration of reacting species [1, 2]. Westheimer reviewed chromate oxidation in 1949 [3] concerning himself chiefly with the mechanism of the oxidation of alcohols. The mechanism he elaborated for the oxidation of 2-propanol [3] has served as a model for the oxidation of alcohols, aldehydes or organic acids. The alcohols or other reducing agents having —OH group form esters with $HCrO_4^-$ [4], which undergo internal oxidation-reduction in the rate-determining step to give chromium (IV).

$$R_2CH—OH + HCrO_4^- \rightleftarrows R_2CHOCrO_3^- + H_2O \quad (1)$$

$$R_2COCrO_3^- \rightarrow R_2CO + Cr(IV) \quad (2)$$

Westheimer and Watanabe [3, 5] considered several possible pathways involving subsequent reactions of chromium(IV) as *A* and *B*, *A* being preferred

$$A: \quad Cr(IV) + Cr(VI) \rightarrow 2Cr(V) \quad (3)$$

$$B: \quad Cr(IV) + R_2CHOH \rightarrow Cr(II) + R_2CO \quad (4)$$

$$Cr(II) + Cr(VI) \rightarrow Cr(III) + Cr(V) \quad (5)$$

* *Babeş Bolyai Univesity, Dept. of Chemistry, Cluj-Napoca, 3400, Romania*

Chromium(V) behaves like chromate itself and oxidizes R_2CHOH in a two-equivalent step [6]

$$Cr(V) + R_2CHOH \rightarrow Cr(III) + R_2CO \quad (6)$$

R o č e k and coworkers have presented evidence that chromium(IV) oxidizes the substrate in an one-equivalent reaction [7] forming ketyl free radical

$$C: \quad Cr(IV) + R_2CHOH \rightarrow Cr(III) + R_2CHO^{\cdot} \quad (7)$$

$$R_2CHO^{\cdot} + Cr(VI) \rightarrow Cr(V) + R_2CO \quad (8)$$

W i b e r g and M u k h e r j e e [8] followed the rate of acetone formation from 2-propanol relative to the growth of chromium(V) ESR signal in acetic acid solution, giving support to the *C* pathway of the reaction. Chromium (IV) is considered responsible for the cleavage reaction [9].

Many scientists dealt with the oxidation of alcohols or glycols [10–16], aldehydes [17–20], organic acids [21–27] and some co-oxidation of alcohols and oxalic acid [28, 29] by chromium(VI). Some of them determined activation parametrs [30, 31] and involement of free radicals [9, 32].

The decay of the ester has been the subject of much discussion, mainly concerned with hidride transfer in a two-equivalent rate-determining step, as well as the fate of the intermediate Cr(V) and Cr(IV) oxidation states. Long-lived compounds of Cr(V) have been identified and monitored [27, 33].

The purpose of this paper is to compare the oxidation of benzyl alcohol (primary aromatic) and cyclohexanol (secondary, cyclic) and to search for the involvement of free radicals, under the conditions of strong acid solutions.

Experimental. Chemicals used in this study were of analytical grade purity. Inorganic materials were of E. M e r c k ' s *p.a.* grade and used without further purification. Alcohols were of Reactivul's *p.a.* grade and were distilled prior to use.

Stock solutions of $KHCrO_4$, $HClO_4$, $NaClO_4$ were prepared in twice distilled water and standardized by usual procedure. Aliquots of $NaClO_4$ solution were passed through a column of cationic resign Amberlite IR–120 (H — form) and released $HClO_4$ was then determined. Solutions of alcohols were freshly prepared before each set of runs by measuring a known volume of pure organic substrate to a volumetric flask and making it to the mark with twice distilled water. Benzyl alcohol was used near to its solutibility limit, and diluted to the concentration required by each experiment.

The oxidation reaction was followed spectrophotometrically at 350 *nm* in a cell either of 1 *cm* or 5 *cm* path length, using a Zeiss Spekord spectrophotometer having a cell-holder provided with a temperature jacket. Temperature was kept constant by means of a thermostate to within ± 0.05°C.

The ionic strenght of reaction mixture was adjusted by addition of sodium perchlorate.

Reaction was started by injecting a known volume of acid solution of Cr(VI) into the cell containing a solution of alcohol, sodium perchlorate and perchlorate acid at the temperature of the experiment. Absorbance values wete then read as a function of time.

The stoichiometry of the reaction was determined by extraction of organic materials into ethyl eter after the process was accomplished, when increasing amounts of Chromium(VI) was used, and recording the spectra of the products.

The involvement of free radicals during the oxidation process was checked by using the systems to initiate polymerization of butylacrylate. Some attempts were made using vinyl acetate, but concurernt oxidation of it has occured. Cumulative effect of increasing temperature of the mixture, contained in a small calorimeter, has been used [38].

Results and Discussion. At low chromium(VI) concentration of $\approx 10^{-4}$ $mol.dm^{-3}$ the equilibrium

$$Cr_2O_7^{2-} + H_2O \rightleftarrows 2\ HCrO_4^- \qquad (9)$$

is entirely shifted to the right [35], so that the oxidizing species of chromium (VI) is $HCrO_4^-$ under the conditions investigated. The acid dissociation

$$HCrO_4^- \rightleftarrows H^+ + CrO_4^{2-} \qquad (10)$$

has been completely neglected ($pK_a \approx 6 - 7$ [36]) at $HClO_4$ concentration employed.

The ester formation in the acid catalized condensation equilibrium (eq. 1) is characterized by K, having value of the order of magnitude of $10^0 - 10^1$ [4, 37]. At 350 nm, the molar absorbance for the esters are less than 1560 $dm^3mol^{-1}cm^{-1}$, which is ε_{350} for $HCrO_4^-$ [4,6] To verify the involvement of such an equilibrium, we have recorded the absorbance at around 20 s after mixing when a relative constant value has been maintained for a short time, under the condition where the oxidation process is relatively slow compared to the condensation process. Figure 1 prezents the absorbance values as a function of concentration of chromium(VI). Lambert-Beer law was fulfilled, and a mean molar absorbance $\bar{\varepsilon} = 1470 \pm 10\ dm^3mol^{-1}cm^{-1}$ could be calculated from the slope of the line. Smaller value of $\bar{\varepsilon}$ as compared to that for $HCrO_4^-$, shows the involevment of the equilibrium

$$C_6H_5CH_2OH + HCrO_4^- \rightleftarrows C_6H_5CH_2OCrO_3^- + H_2O \qquad (11)$$

The absorbance measured at 350 nm is a contribution of free $HCrO_4^-$ ion and the ester $ROCrO_3^-$

$$A = d\{\varepsilon_{HCrO_4^-} \cdot [HCrO_4^-] + \varepsilon_{ROCrO_3^-} \cdot [ROCrO_3^-]\} \qquad (12)$$

where d is the path length of the cell. Monitoring the decrease of absorbance with time, correlated with the decay of total Chromium(VI), we were able to obtain pseudo-first-order rate constants from the slope of semilogarithmic plots

$$\ln(A - A_\infty) = \ln(A_0 - A_\infty) - k_{obs}t \qquad (13)$$

where indexes "o" and "∞" denote absorbance values at $t = 0$ and at the end of the run $t = \infty$ respectively. The requirements for that were conditions of low chromium(VI) concentration, to avoid the involvement of dichromate species, and excess con-

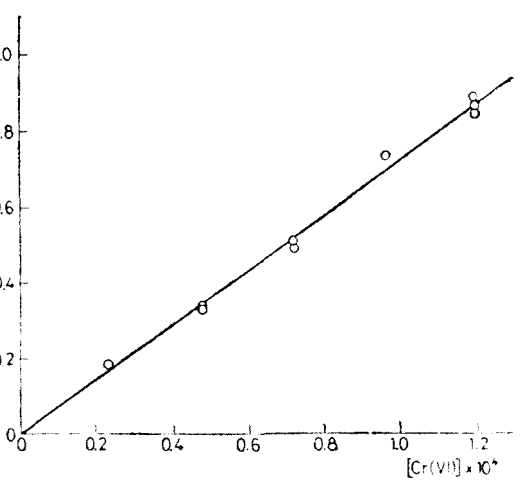

Fig. 1. Absorbance values after about 20 s from the mixing of $C_6H_5CH_2OH$ ($3.85 \times 10^{-2}\ mol\ dm^{-3}$) and various concentrations of Cr(VI). $[H^+] = 0.24$, $\mu = 2.4$, $T = 295$ K

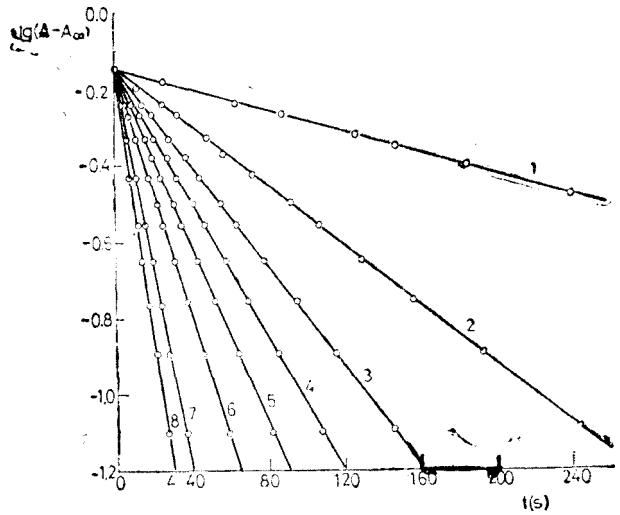

Fig. 2. First-order plots for the oxidation of benzyl alcohol with Cr(VI). Conditions indicated in table 1.

centration of both the alcohol and perchloric acid. First-order plots were linear up to more than 90–95% of reaction. Figure 2 presents some examples in the case of benzyl alcohol. Similar plots were obtained with cyclohexanol.

The order with respect to the substrate and hydrogen ion were determined at constant H^+ concentration and ROH concentration respectively. Table 1 and 2 illustrate dependence of first-order rate constant on concentration of ROH and H^+ respectively, at the oxidation of benzyl alcohol. Each value in the table has been obtained from 2–3 individual runs under the same experimental conditions using a least-square procedure to determine the slope

Table 1

The effect of benzyl alcohol concentration on the rate:

$[HCrO_4^-] = 1.2 \times 10^{-4}$, $[H^+] = 1.44$, $\mu = 2.4$, $T = 309.5$ K

$[C_6H_5CH_2OH] \times 10^2$ $mol \cdot dm^{-3}$	$10^2\, k_{obs}$ s^{-1}	Correlation coefficient
0.38	0,35	0,998
0,76	0,81	0,998
1,62	1,40	0.999
2.30	2.00	0.997
3.08	2.40	0.998
4.14	3.70	0.998
6.16	4.80	0.995
7.70	6.20	0.992

Table 2

The effect of H^+ concentration on the rate at 283.8 K

$[C_6H_5CH_2OH] = 3.08 \times 10^{-2}$ $mol \cdot dm^{-3}$ and $[HCrO_4^-] = 1.2 \times 10^{-4}$ $mol \cdot dm^{-3}$, $\mu = 2.4$

$[H^+]$ $mol \cdot dm^{-3}$	$10^3\, k_{obs}$ s^{-1}	Correlation coefficient
2.40	25.0	0.993
1.46	9.50	0.997
1.36	7.88	0.997
1.09	5.63	0.998
0.93	3.24	0.998
0.82	2.54	0.999
0.56	1.34	0.999

of the lines (eq. 13). Similar behaviour was noticed using cyclohexanol. The dependence shown in Table 1 could be described by the linear relation

$$k_{obs} = (1.3 \pm 1.2) \times 10^{-3} + (0.78 \pm 0.02)\ [ROH] \qquad (14)$$

with a correlation coefficient of $r = 0.994$. Taking into consideration the error of the intercept, as well as the stoichiometry requirements, we considered that zero-order term in eq. 14 could be neglected. A plot of k_{obs} *vs* [ROH] gives a line passing through the origin. On the other hand, using data given in Table 2, a plot of lg k_{obs} *vs.* lg H^+ is a line. A slope of 2.07 ± 0.05 has been found, which is the order with respect of H^+. Consequently, these findings led to the following rate law:

$$-\frac{d[Cr(VI)]}{dt} = k_4[HCrO_4^-][ROH][H^+]^2 \qquad (15)$$

as previously determined for other alcohols.

Table 3 and 4 collect the data for the oxidation of $C_6H_{11}OH$ and $C_6H_5CH_2OH$ under various conditions employed. As seen from the tables, the oxidation of benzyl alcohol is much faster than that of cyclohexanol, with about two orders of magnitude.

From the dependence of forth-order rate constant k_4 with temperature, activation parameters have been determined, as shown in Table 5. Activation parameters for the oxidation of cyclohexanol are very close to those previously determined by Kwart and Nickle [31] ($E_a = 52.8\ kJ.mol^{-1}$), or by Mueller and Perlsberger [30] ($\Delta H^{\neq} = 54.8\ kJ.mol^{-1}$) in acetic

Table 3

Kinetic results under various experimental conditions at the oxidation of cyclohexanol

$[Cr(VI)] = 4 \times 10^{-4}$ $\mu = 1.6$

$T(K)$	$[H^+]$	$10^2[ROH]$ $mol \cdot dm^{-3}$	$10^4 k_{obs}$ s^{-1}	$10^3 k_4$ $dm^9 mol^{-3} s^{-1}$
293.0	0.952	4.60	1.43	3.40
		2.30	0.67	3.18
	0.893	2.88	0.75	3.28
298.0	1.35	2.88	2.28	4.36
	0.952	4.60	1.87	4.49
		2.30	0.95	4.56
303.0	1.35	2.88	3.22	6.13
	0.952	4.60	2.60	6.24
		2.30	1.25	6.33
	0.893	2.88	1.43	6.24
	0.595	2.88	0.62	6.09
	0.388	2.88	0.27	6.23
313.0	0.952	4.60	6.13	14.71
		2.30	3.08	14.79
	0.893	2.88	3.35	14.59
	0.595	2.88	1.47	14.43

acid solutions. We have not found activation data for the oxidation of benzyl alcohol, kinetic being studied in acetic media, where the oxidizing species is acetochromate acid $CH_3COOCrO_3H$.

Measuring the absorbance values of benzaldehyde and cyclohexanone at 283 and 290 *nm* respectively, on the recorded sepctra of the products, and comparing with calibration curves obtained with pure substances, ratios very

Table 4

Kinetic results under various experimental conditions at the oxidation of benzyl alcohol

$[Cr(VI)] = 1.2 \cdot 10^{-4}$ $\mu = 2.4$

$T(K)$	$[H^+]$	$10^2[ROH]$ $mol \cdot dm^{-3}$	$10^3 k_{obs}$ s^{-1}	k_4 $dm^{-2} \cdot mol^{-3} \cdot s^{-1}$
283.8	2.40	3.85	2.70	0.122
		3.08	2.50	0.141
		2.31	1.70	0.128
	1.46	3.08	0.95	0.144
	1.36	3.08	0.79	0.139
	1.09	3.08	0.56	0.154
	0.93	3.08	0.32	0.122
	0.82	3.08	0.25	0.125
	0.56	3.08	0.13	0.139
291.5	2.40	3.85	3.70	0.167
		3.08	3.00	0.167
		2.31	2.20	0.165
	1.59	3.85	1.60	0.164
	1.44	3.85	1.30	0.163
	1.33	3.85	1.16	0.171
	1.22	3.85	0.96	0.166
	1.06	3.85	0.71	0.164
	0.90	3.85	0.53	0.168
	0.69	3.85	0.31	0.169
298.5	2.40	3.85	5.30	0.262
		3.08	4.20	0.237
		2.31	3.28	0.246
		3.08	4.30	0.242
		2.31	3.40	0.255
309.5	2.40	3.85	9.50	0.428
		3.85	8.80	0.396
		3.85	8.40	0.379
		3.08	6.56	0.367
		2.31	5.60	0.420
		1.54	3.50	0.395

Table 5

Activation parameters calculated from the fourth order rate constants

		Cyclohexanol	Benzyl Alcohol
E_a	$kJ \cdot mol^{-1}$	56.8 ± 0.5	31.4 ± 0.6
$\Delta H^{\neq}$	$kJ \cdot mol^{-1}$	54.1 ± 0.5	29.0 ± 0.6
$\Delta S^{\neq}$	$J \cdot mol^{-1}K^{-1}$	-108 ± 6	-159 ± 8

close to 1.5 alcohol : 1 Cr(VI) have been determined, when large excesses of alcohols were used. Carbonyl compounds are produced as main products in these oxidations.

Using the redox cyclohexanol-chromate process to initiate polymerization, increases of temperature of around 1.3°C were measured when mixtures contained butyl acrylate as compared to the systems without monomer. The solution volume in the calorimeter was 15 cm^3 for each experiment ; concentration range was the same as for kinetic runs. No differences of temperature increase was noticed with the system $C_6H_5CH_2OH - Cr(VI)$ in the presence or absence of butylacrilate monomer. The small increase of temperature indicates the involvement of some free radicals at a very low concentration during the oxidation of cyclohexanol.

Kinetic data obtained, stoichiometry, molar absorbante smaller than expected for $HCrO_4^-$ ion at the beginning of the reaction, as well as the activation parameters (relative small $\Delta H^{\neq}$ and negative $\Delta S^{\neq}$) could be rationalized by a Westheimer type mechanisms (eqs. 1 and 2)

$$ROH + HCrO_4^- + H^+ \rightleftarrows H_2O + ROCrO_3H \qquad K_f \tag{16}$$

$$ROCrO_3H + H^+ \rightarrow Cr(IV) + R' = O \qquad k \tag{17}$$

with formation of carbonyl compound and chromium(IV) in the rate—determining step.

Chromium(IV) reacts further through the route A (eqs. 3 and 6) in the case of benzyl alcohol and either through the same route or route C in the case of cyclohexanol. It is also possible that a few free radicals to be formed by some further oxidation, with the last system, with the cleavage of the cycle in a very small proportion (stoichiometric ratios a little bit lower than 1.5 :1).

From the H^+ catalized preequilibrium (16) and the di-equivalent electron transfer step (17), taking into account that the total Cr(VI) concentration has been measured, one can obtain the rate law as :

$$-\frac{d[Cr(VI)]}{dt} = \frac{kK_f[ROH][H^+]^2}{1 + K_f[ROH][H^+]}[HCrO_4^-] \tag{18}$$

Assuming that K_f is of the order of magnitude of unity, as for the other alcohols [37], the proportion of ester from the total Cr(VI) concentration in the mixture is about 8—15%. Therefore, $K_f[ROH][H^+] \ll 1$ at the concentration range used in the study, and a simpler form of the rate could be written :

$$-\frac{d[Cr(VI)]}{dt} = kK_f[ROH][H^+]^2[HCrO_4^-] \tag{19}$$

which is in agreement with the rate law experimentally determined, with $k_4 = k K_f$.

The relative small values of activation energy or enthalpy for the oxidation processes, with major changes of the structure of the reagents in the rate-determining step, could be understood by the involvement of the exothermic preequilibrium.

The difference in the forth-order rate constant for the two studied alcohols with about two orders of magnitude consists of the energy requirements to change sp^3 to sp^2 hybridization at the reaction centre during the rate-determining step. When C atom is involved in a cycle, a higher barrier should be surpassed as compared to the primary benzylic C atom. Some tension is introduced in cyclohexanone ring relative to cyclohexanol, and a higher activation energy and a less negative activation entropy are involved.

REFERENCES

1. K. B. Wiberg *Oxidation in Organic Chemistry* Part A. Acad. Press. New-York, 1965 p. 69
2. J. Hampton, A. Leo, F. H. Westheimer, J. Amer. Chem. Soc., **78**, 306 (1956).
3. F. H. Westheimer, Chem. Rev., **45**, 419 (1949); A. Novick, F. H. Westheimer, J. Chem. Phys., **11**, 506 (1973); F. H. Westheimer, N. Nicolaides, J. Amer. Chem. Soc., **71**, 25 (1949).
4. M. Anber, I. Dostrovsky, D. Samuel, A. D. Yoffe. J. Chem. Soc., **1954**, 3603; F. Holloway, M. Cohen, F. H. Westheimer, J. Amer. Chem. Soc., 75, 4377 (1953); H. H. Zeiss, C. N. Mattews, J. Amer. Chem. Soc., **78**, 1694 (1956); H. Kläning, M. C. Symons, J. Chem. Soc., **1961**, 3204.
5. W. Watanabe, F. H. Westheimer, J. Chem. Phys., **17**, 61 (1949).
6. K. B. Wiberg, H. Schäfer, J. Amer. Chem. Soc., **91**, 933 (1969).
7. J. Roček, A. E. Radkowsky, J. Amer. Chem. Soc., **90**, 2986 (1968); M. P. Doyle, R. J. Swedo, J. Roček, J. Coord. Chem, **92**, 7599 (1970); F. Hasan, J. Roček, J. Amer. Chem. Soc., **94**, 9073 (1972); F. Hasan, J. Roček, J. Amer. Chem. Soc., **94**, 3181 (1972); F. Hasan, J. Roček, J. Amer. Chem. Soc., **94**, 8946 (1972); F. Hasan, J. Roček, J. Amer. Chem. Soc., **95**, 5421 (1973); F. Hasan, J. Roček, J. Amer. Chem. Soc., **97**, 1444 (1975); M. Krumploc, J. Roček, J. Amer. Chem. Soc., **99**, 137 (1977); S. N. Mahapatra, M. Krumploc, J. Roček, J. Amer. Chem. Soc., **102**, 3799 (1980).
8. K. B. Wiberg, S. K. Mukherjee, J. Amer. Chem. Soc., **92**, 7599 (1970).
9. P. M. Nave, V. S. Trahanovsky, J. Amer. Chem. Soc., **92**, 1120 (1970); V. S. Trahanovsky, P. M. Nave, J. Amer. Chem. Soc., **93**, 4536 (1971).
10. W. A. Mosher, F. C. Whitmore, J. Amer. Chem. Soc., **70**, 2544 (1948).
11. J. Lal, S. N. Shukala, A. C. Chatterji, Z. Physik. Chem. (Leipzig), **228**, 173 (1965); A. C. Chatterji, S. N. Shukala, J. Lal, Z. Physik. Chem. (Leipzig), **222**, 303 (1963).
12. M. Doyle, R. Swedo, J. Roček, J. Amer. Chem. Soc., **95**, 8352 (1973).
13. A. C. Chatterji, Indian J. Chem., **10**, 831 (1972), C.A, **78**, 96874 y.
14. V. S. Anantakrishnan, S. Varadaraian, Indian J. Chem., **10**, 66 (1972), C.A. **77**, 18941 g.
15. V. M. Ranmanijan, N. Venkatasubramanian, S. Sundaran, Aust. J. Chem., **30**, 325 (1977).
16. S. P. Wechsler, B. Fuchs, J. Chem. Soc. Perkin Trans. 2, **1970**, 943.
17. A. C. Chatterji, S. K. Mukherjee, Z. Physik. Chem. (Leipzig), **228**, 159 (1958); A. C. Chatterji, S. K. Mukherjee, J. Amer. Chem. Soc., **80**, 3600 (1958).
18. K. B. Wiberg, T. Mill, J. Amer. Chem. Soc., **80**, 3022 (1958).
19. L. E. T. Graham, F. H. Westheimer, J. Amer. Chem. Soc., **80**, 3030 (1958).
20. G. L. Donald, A. U. Spiter, Can. J. Chem., **53**, 3709 (1975).
21. G. H. Bacore, S. Naraian, J. Chem. Soc., **1963**, 3419.
22. K. S. Srivastava, Proc. Nat. Acad. Sci. **39**, 274 (1969), C.A. **93**, 238367 v.
23. F. Mata, M. P. Alvarez, Z. Phys. Chem. N.F., **120**, 155 (1980).
24. G. V. Bakore, A. A. Deshapade, Z. Physik, Chem. (Leipzig), **227**, 14 (1964); G. V. Bakore, S. Narain, Z. Physik. Chem. (Leipzig), **227**, 8 (1964).
25. N. Dahr, J. Chem. Soc., **111**, 707 (1971).
26. J. T. Kemp, W. A. Waters, J. Chem. Soc., **1964**, 1192, 3139.

27. P. P. Haight, G. M. Jursich, M. T. Kelso, O. J. Merill, Inorg. Chem., **24,** 2740 (1985).
28. S. N. Mahapatra, M. Krumploc, J. Roček, J. Amer. Chem. Soc., **102,** 1583 (1980).
29. P. Mueller, J. Blanc, Helv. Chim. Acta., **62,** 1980 (1979).
30. P. Mueller, J. C. Perlberger, Helv. Chim. Acta., **57,** 1943 (1974).
31. H. Kwart, J. H. Nickle, J. Amer. Chem. Soc., **95,** 3394 (1973).
32. M. Rahman, P. Roček, J. Amer. Chem. Soc., **93,** 5455 (1971).
33. Shrinivasan, J. Roček, J. Amer. Chem. Soc., **96,** 127 (1974).
34. *Techniques of Organic Chemistry* Vol. **VII,** 2-nd. edn. Ed. A. Weissberger. Intersci. New York, 1955.
35. J. H. Espenson, R. J. Kinney, Inorg. Chem., **10,** 1376 (1971).
36. G. Schwarzenbach, J. Meier, J. Inorg. Nucl. Chem., **8,** 302 (1958).
37. R. M. Lanes, D. G. Lee, J. Chem. Educ., **45,** 269 (1968).
38. O. Marek, M. Tomka, *Acrilovie Polymeri* Izd. Khim., 1966 p. 80.

STUDIA UNIV. BABEŞ-BOLYAI, CHEMIA, XXXVII, 1—2, 1992

IMMUNOENZYMATICAL CONJUGATES. REMAINING PEROXIDASE ACTIVITY.

GH. COMAN,* S. GOCAN,** R. ZĂBAVĂ,*** C. TEODORU****, P. SZABO*

Received: 05.10. 1992

ABSTRACT. The present paper reports a kinetical study of the free and IgG covalently coupled perosidase. According to our results, it is possible to use immunoenzymatical techniques, in order to design immunochemical reagents, which may be useful in the clinical diagnosis of different kinds of diseases, in humans or animals.

Introduction. Immunoenzymatical techniques have been introduced for a very short time, but they showed a large development, due to their high sensibility and specificity, and easy handling [1]. These techniques enable the studying of the antibody-antigen interaction while one of the two partners is labeled using an enzyme (immunoenzymatical conjugate). The covalentlly bounded enzyme reacts with a specific substrate by modifying its structure and, of course, its physical properties. In some cases the cases the substrate may be chosen so that, following the enzyme action, a change in its spectral properties can be detected. For example, the colour of the solution containing the substrate may change as a result of the enzyme action.

The covalent binding of the enzyme to antibody requires very mild treatment with various reagents. The conformation of the two macromolecules should be least affected, so that the enzymatic antibody activity be maintained.

Immunoenzymatical techniques can be largely applied in virology, bacteriology, pathology and immunopathology, endocrinology etc. [2—6].

The following assumptions were made, in order, to estimate the kinetical parameters of the studied reactions [7]:

a) the enzyme *(E)* and the substrate *(S)* combine at a high rate, forming the enzyme-substrat complex *(ES)*

b) the dissociation of this complex *(ES)* gives a single product and the free enzyme

c) the substrate concentration is much larger than the concentration of the enzyme

d) after a short, prestationary period of time, the *ES* complex will be formed at the same rate as it will dissociate

The enzymatical reaction may be written as:

$$E + S \underset{k_{-1}}{\overset{k_{+1}}{\rightleftharpoons}} ES \xrightarrow{k_2} E + P \qquad (1)$$

* *Centrul de medicină preventivă, Cuca Vodă 20, 2200 Braşov*
* *Univ. Cluj-Napoca, Fac. Tehnologie Chimică, Arany János 11, 3400 Cluj*
** *Institutul Pasteur, Stejarii 8, 2200 Braşov*
**** *Univ „Transilvania" Braşov, Fac. Medicină, Cibinului 3, 2200 Braşov*

Peroxidase takes an oxigen atom from the H_2O_2 molecule, and delivers it to the 5-amino salicilic acid molecule. The oxidation of the last one appears as a change in the colour of solution, which can be measured spectrophotometrically.

According to the above assumptions, we used Michalis — Menten kinetical equation in processing our data:

$$\frac{v_0}{v_{max}} = \frac{[S]}{K_M + [S]} \tag{2}$$

v_0 — the initial reaction velocity, at a certain substrate concentration

v_{max} — the maximum observed velocity

[S] — substrate concentration

K_M — Michaelis — Menten constant:

$$K_M = \frac{k_{-1} + k_2}{k_{+1}} \tag{3}$$

with k_{+1}, k_{-1} the rates for the forward and backward reactions in the reversible step and k_2 the rate for the irreversible step in eq. (1)

Modifying the Michaelis — Menten equation, the Lineweaver — Burk equation may be obtained:

$$\frac{1}{v_0} = \frac{K_M}{v_{max}} * \frac{1}{[S]} + \frac{1}{v_{max}} \tag{4}$$

Thus, the plot (of the function):

$$\frac{1}{v_0} = f\left(\frac{1}{[S]}\right) \tag{5}$$

will be a straight line. Its crossing points with the coordinate axes will give the values: $-1/K_M$ (on the horizontal axis) and $1/v_{max}$ (on the vertical one).

Experimental. We have determined the remaining activity of the peroxidase in imunoenzymatical conjugate obtained in our laboratory, according to a modification [8] of method of Avrameas and Ternyclk [9].

Bovine antibodies were purified by affinity chromatography. Peroxidase and perhydrol were delivered by Merck. The peroxidase substrate, 5-amino salicilic acid, was delivered by Fluka.

The kinetical study has been carried out in a 0.1 *M* phosphate buffer, *pH* 6.95, at a room temperature. The substrate was added in quantities that made possible the enzyme concentration to limit the rate of the reaction. The peroxidase activity was assayed by determining the rate of product formation, monitoring the increase of the absorbance at 405 *nm* with the time.

Results and Discussion. While the enzyme concentration was kept at $3.06 * 10^{-6}$ *mM*, we measured the rate of product formation in solutions in which the 5-amino salicilic acid concentration varied from 2.56 *mM* to 7.68 *mM*. The H_2O_2 concentration was always high enough, so that the reaction rate be independent on it. The kinetical plots shown in Fig. 1. were obtained.

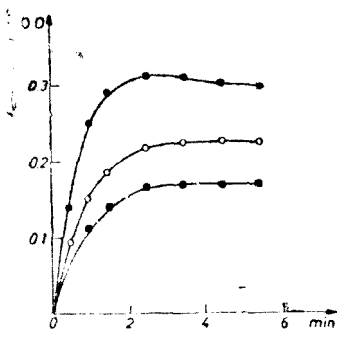

Fig. 1. The kinetical plots for free enzyme

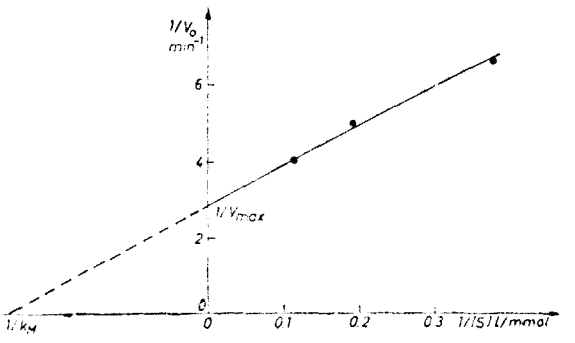

Fig. 2. The Lineweaver—Burk plot for free enzyme

The Lineveaver — Burk (4) plot of our data gave a straight line (Fig. 2). The following values of K_M and v_{max} could be determined:

$$v_{max} = 0.355\ mM/min$$

$$K_M = 3.95\ mM$$

If the whole quantity of the enzyme is catalitically active, the following equation may be written [10]:

$$v_{max} = k_2 * [E] \tag{6}$$

with k_2, the rate constant of the ES dissociation, representing the molecular activity of the enzyme. We obtained:

$$k_2 = 1.16 * 10^5\ min^{-1}$$

The turnover number of the peroxidase was:

$$1/k_2 = 8{,}6 * 10^{-6}\ min.$$

it counting the time the enzyme needs to complete a catalytical act.

The characterisation of the free peroxidase could be completed by determining its enzymatical activity [11]:

$$A.E. = \frac{\Delta A/\Delta t}{\varepsilon * c_E} \tag{7}$$

with: ε — molar absorbance coefficient of the 5-amino salicilic acid oxidation product;

ΔA — increase in absorbance of the product solution during the period Δt of time;

c_E — enzyme concentration (mg/ml)

The free peroxidase activity ($\varepsilon = 11.64\ mM^{-1}\ cm^{-1}$) turned out be 140.83 U/mg, value is that given by Merck (188 U/mg)

The same way, the kinetical parameters and the enzymatical activity of

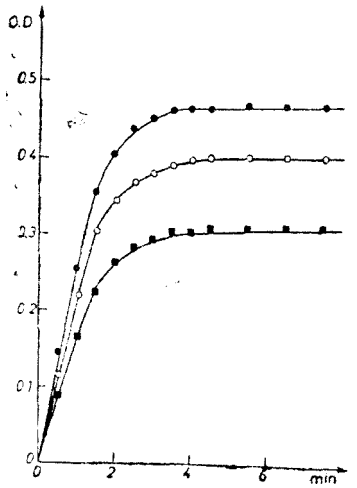

Fig. 3. The kinetical plots for conjugated enzyme

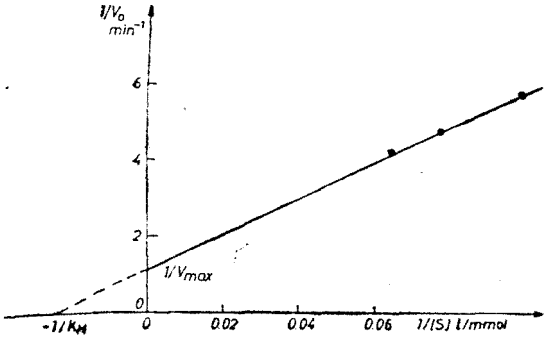

Fig. 4. The Lineweaver – Burk plot for conjugated enzyme

the IgG covalently bounded peroxidase were determined. The kinetical plots are shown in Fig. 3.

The Lineweaver — Burk plot (Fig. 4) led to the following values for the kinetical parameters:

$$v_{max} = 0.25\ mM/min$$

$$K_M = 8.4\ mM$$

Equation (6) led to:

$$k_2 = 0.73 * 10^5\ min^{-1}$$

$$1/k_2 = 1.73 * 10^{-6}$$

The enzymatical activity of the covalently bounded peroxidase was 2.3 *U/mg*, representing 1.65% of the free peroxidase activity.

A remarcable decrease in the enzymatical activity of the IgG antibody bounded peroxidase, as compared with the free peroxidase activity, can be observed. This decrease can be understood, considering the conformational changes which may occur in the enzyme and the possible inactivation of some the peroxidase molecules during the binding to the antibody.

The relative decrease of the peroxidase activity we obserwed, is consistent with the values given in the literature for remaining activities antibody covalently bounded enzymes (0.95 — 5%) [12].

With the decrease in peroxidase activity, k_2 also decreases. The turnover number is larger for the bounded peroxidase than for the free one, so that the time required to complete a catalitical act is longer for the bounded peroxidase.

A increase in the K_M value of the enzyme in the immunoenzymatical conjugate may also be noticed. This demonstrates that affinity of the peroxi-

dase for its substrate decreased during its covalently coupling to the IgG antibody, most probably because of the conformational changes which could modify the shape the catalitical center of the enzyme.

Conclusions. The decrease in enzymatical activity is due not only to inactivation (and therefore loss) of peroxidase during the process of binding, but also to the important conformational changes of its active center. This conclusion is supported by the concomitant decrease in enzymatical activity and increase of the K_M value of the IgG covalently bounded peroxidase.

The changes in the value of kinetical parameters and in the enzymatical activity of the peroxidase in the immunoenzymatical conjugate is consistent with the general data available in the literature on antibody bounded enzymes. Therefore our immunoenzymatical conjugate may be used as immunochemical diagnosis reagent.

REFERENCES

1. E. Engvall, P. Perlman: Immunochemistry, **8**, 871 (1971)
2. M. Calamel: Sci. Vet. Med. Comp., **85**, 4—5, 211 (1983)
3. M. Lambert: Ann. J. Vet. Res., **136**, 4, 303 (1985)
4. I. A. Piffer: Ann. J. Vet. Res., **45**, 1126 (1984)
5. J. Boothby: Ann. J. Vet. Res., **42**, 1242 (1981)
6. P. Chantal: Rev. Med. Vet., **134**, 8—9, 465 (1983)
7. I. H. Segel: *Enzyme Kinetics*, J. Wiley & Sons, New York, 1975, p. 19.
8. Gh. Coman, S. Gocan, R. Zabava, C. Teodoru: Studia, (in press).
9. S. Avrameas, T. Ternyck: Immunochemistry, **8**, 1175 (1971)
10. I. H. Segel: *Enzyme Kinetics*, J. Wiley & Sons, New York, 1975, p. 33.
11. L. M. Shannon: J. Biol. Chem., **241**, 2166 (1966).
12. T. H. Adams, G. Wisdom: Biochem. Soc. Trans., 7, 55 (1971).

STUDIA UNIV. BABEŞ-BOLYAI, CHEMIA, XXXVII, 1—2, 1992

IMMUNOCHEMICAL DIAGNOSIS REAGENTS. USING OF ELISA IN THE SELECTION OF VIRUS RESISTANT WHITE BEET VARIETIES

GH. COMAN*, S. GOCAN**, R. ZĂBAVĂ***, C. TEODORU****, C. HENEGAR*****

Received: 05.10.1992

ABSTRACT. Saples from the 40 groups of white beet, each of them consisting of 25 individuals, have been assayed using ELISA for the degree of infection with the BNYVV virus. The immunoenzymatical reagents used during the assay were prepared in our laboratories. It is possible to select BNYVV-resistant individuals, which should be further analised for their root productivity and sugar content.

Introduction. Viral diseases in white beet are extremely important because of the remarcable decrease in sugar content of the roots of the affected plants, which may even drop to zero. The Beet Necrotic Yellow Vein Virus (BNYVV) [1] is one of the viruses affecting the white beet sugar content, causing the Risomania diseases.

ELISA (Enzyme Linked Immunosorbent Assay) is one of the most frecvently used immunoenzymatical techniques. Because of its sensibility and specifity, it is largely applied in the diagnosis of different microorganism infections in humans and various species of plants and animals [2].

The present paper reports the usage of ELISA in studying the BNYVV infection of different varietes of white beet. The results of this study, together whith the sugar content analisis of each variety, should be used in selecting virus-resistant varieties, which are to be cultivated over the contaminated areas.

Experimental. The immunoenzymatical reagents used during the ELISA test were prepared in our laboratories [3]. The enzyme used for antibody labeling was alcaline phosphatase. 4-Nitrophenil phosphate was used as substrate. The „sandwich" alternative was chosen in order to assay the presence of BNYVV. Product concentration was measured by monitoring the optical density at 405 *nm* [4].

The study was extended over 40 groups of the white beet, each of them including 25 samples.

Results and Discussion. The results of the ELISA are shown in Fig. 1, for two of the 40 gropus of white beet studied.

The differences in virus infection degree among the groups, and even within each group, is large enough to permit the selection of virus resistant plants.

* *Centrul de medicină preventivă, Cuza-Vod 20, 2200 Braşov*
** *Univ. Cluj-Napoca, Fac. Tehnologie Chimică, Arany János 11, 3400 Cluj-Napoca*
** *Institutul Pasteur, Stejăriş 8, 2200 Braşov*
**** *Univ. „Transilvania" Braşov, Fac. Medicină, Cibinului 3, 2200 Braşov*
***** *Staţiunea de cercetări pentru sfeclă de zahăr Arad Splaiul Mureşului 10, 2900 Arad*

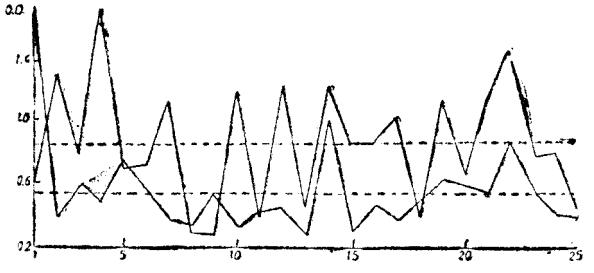

Fig. 1. The test of ELISA. Relationships between optical density and the number of the sample for two groups of white beet

Fig. 2 presents the differences observed among the average values of the observed optical density (and therefore different average infection degrees) among groups. Considering that all groups have been cultured on the same infected soil, we could distinquish the groups 8, 15 and 16 which showed minimum optical densities and, therefore, are least infected. Most infected showed up to be groups 1, 37 and 40.

The main statistical parameters (the standard deviation s, the variance s^2 and the variance coefficient $s\%$) of the studied groups were determined. The values obtained are synthetically shown in Fig. 3.

The standard deviations and the variations are, as expected, similar among the studied groups, but their values are specific for each one. This finding proves that each group is different from all the others in its behaviour towards the virus.

Differences among the variance coefficient values for different groups can also be noticed. The large values of this synthetic parameter, which best expresses the dispersion of the particular optical density values, prove that a strict selection among individuals within each group is necessary.

Conclusions. The groups taken as samples and immunoenzymatically assayed showed different degrees of viral infection. Some of them seemed to be virus — resistant more than the others.

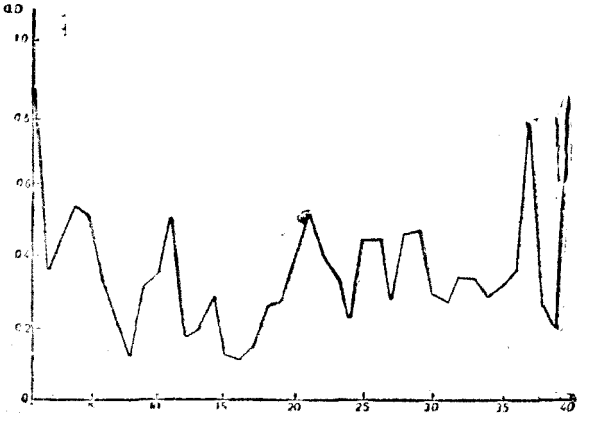

Fig. 2. Average values of the observed optical density for the 40 groups of white beet

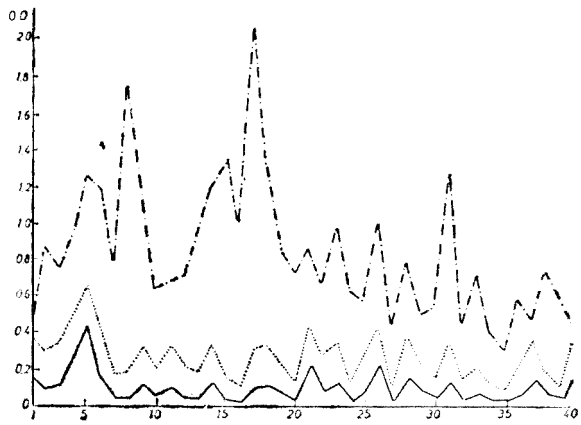

Fig. 3. The main statistical parameters of the studied groups
a) . . . standard deviation (s)
b) — variance (s^2)
c) —·— variance coefficient ($s\%$)

The next step in selecting a BNYVV resistant white beet variety should follow, with assaying the root production over a certain unit of land surface and the sugar content of each variety.

REFERENCES

1. A. Macovei: Buletin de protecţia plantelor, **2**, 7 (1989).
2. R. Piroid, M. Lombard: Rev. Med. Vet., **131**, 1, 25–40 (1983).
3. Gh. Coman, R. Zabava, V. Ciochia, C. Henegar: *Lucrările celei de a doua Conferinţe Naţionale de Protecţia mediului prin metode şi mijloace biotehnice*. Martie 1992.
4. M. F. Clark, A. Adams: J. Gen. Virol., **34**, 475–483 (1977).

STUDIA UNIV. BABEŞ-BOLYAI, CHEMIA, XXXVII, 1—2, 1992

THE STUDY OF LEAD SULFIDE FILMS. III. THE ADHESION OF PbS LAYERS ON GLASS

CRISTINA NAŞCU*, ILEANA POP*, VIOLETA IONESCU* and VALENTINA VOMIR*

Received: 05.10.1992

ABSTRACT. The study of PbS layers adhesion on glass, deposited by chemical methods was realized through FTIR spectroscopy. It was established that in the first phase of chemical deposition process, lead hydroxide and lead carbonanates are forming, which are responsible for the PbS adhesion on glass.

Introduction. To obtain micro and optoelectronical components by deposition of metallic or semiconducting layers (in our case PbS [1]) is necessary to assure a good adhesion of the layer on support.

In that purpose it must be considered a few aspects connected with the structure and the physico-chemical properties of the glass. A fresh formed glass surface reacts with atmospheric water vapors covering itself with a neutral layer of OH groups. A unique characteristic of this exposed hydroxyl layer is its ability to retain neutral water molecules by covalent hydrogen bonds. Due to this ability to form hydrogen bonds with polar molecules the glass surface, free of physically adsorbed gases, may be completely wetted by water and other substance having OH or NH_2 groups [2, 3]. This property is used to test the cleaning grade of the glass which will be the support for deposition of thin layers. The cooled surface of the glass may be covered with a few adsorbed gases monolayer whose thickness varies between 15 to 30 $\AA$ or more [4]. The nature of the gases and the proportion in which they are mixed was determined by Langmuir [5]. The gases adsorption in glass surface is caused by the presence of microscopic inhomogeneities varying in size from 0.01—0.1 μm [6].

Due to the glass surface reactivity a special care will be accorded to the glass cleaning methods before the deposition of the thin layers. It is important to do "water break" test [7], used to establish if gross contaminants have been removed from a glass surface. The glass surface cleaning grade determines the adhesion and the quality of the deposited layer.

According Mattox [8] the adhesion mechanism is correlated with the structure of the interfacial regions between the film and the support.

As in the literature was not found references regarding the adhesion of PbS layers on glass we proposed ourselves the study this subject that has an especially interest for us.

Experimental. On plates of Mediaş glass sized at 25 × 25 × 0.17 *mm* was deposited PbS layers using solutions of $Pb(NO_3)_2$ 0.12 *M*, thiourea $SC(NH_2)_2$ 0.48 *M*, sodium hydroxide 1.32 *M*, and hydroxylamine hydrochloride $NH_2OH \cdot HCl$ 0.43 *M* at 25 °C [1]. Before that the plates were extremely well cleaned according [1].

* *Institute of Chemistry Cluj-Napoca, 30 Fântânele Str., 3400 Cluj-Napoca, Romania*

In the same time at Institute of Isotopic and Molecular Technology (ITIM) Cluj-Napoca was deposited PbS layers on same size plates by vacuum evaporation.

IR transmission spectra of PbS layers (obtained by chemical deposition and vacuum evaporation) was realized with a FTIR spectrometer Bruker, which assures vanishing of glass effect, and with a spectrophotometer Specord 75 IR.

Because in documentary material which was avaible for us we have not found IR spectrum of lead hydroxide, this was prepared from a solution containing lead salt and sodium hydroxide (the same reagents that we have used for PbS deposition), after that taking IR spectrum (in KBr).

Results and Discussions. To establish the nature of PbS layers adhesion on glass, it must be considered the layer forming reaction mechanism. After Kitaev and co-workers [9] PbS layer fromation takes place by decomposing of thiourea hydroxocomplexes with lead in alkaline medium. In the system containing lead salts, thiourea and alkalies, it may be found in balance, depending of the components concentrations ratio, the following species: $Pb(OH)_2$, $Pb(N_2H_4CS)_3^{2+}$ and $Pb(OH)_4^{2-}$.

The forming reaction of PbS layers is catalysed by $Pb(OH)_2$ particles which are deposited on the plates and also on the walls of the bottle in which the reaction takes place. This affirmation does not infirm the explanation of the activation process with $SnCl_2$ solutions, which leads to the formation of hydrolysis products with the same effect.

K i t a e v and coworkers [9], have established that in the range of $pOH = 2-0.5$, particles of $Pb(OH)_2$ are forming in the system as nucleation centers. In the same time important quantities of lead remain in solution as soluble plumbite. At $pOH < 0.5$, the quality of layers go wrong, concerning both adhesion and aspect. It may be considered that formation of PbS layers on glass is realized through a $Pb(OH)_2$ layer adsorbed on glass. The lead hydroxide particles dimensions must be correlated with microcavities existing on the surface of the support, $0.01-0.1\ \mu m$ [6].

The existence of the lead hydroxide layer presumed by these authors [9] have been distinguished by us using FTIR transmission spectroscopy.

In Fig. 1 it is presented FTIR transmission spectrum of a PbS layer deposited on glass by vacuum evaporation, in Fig. 2 — FTIR transmission spectrum of the layer obtained by chemical deposition and in Fig. 3 — IR transmission spectrum of $Pb(OH)_2$ prepared by us and carefully handled to avoid decomposing in $Pb_3O_2(OH)_2$ [10].

We mention that lead sulfide presents absorption peaks in far IR spectrum ($<400\ cm^{-1}$).

In the case of PbS layer deposited by vacuum evaporation (Fig. 1) there are not absorption peaks to show the presence of impurities. In the spectrum of PbS obtained by chemical deposition (Fig. 2) there are absorption peaks similar with these observed in $Pb(OH)_2$ spectrum (Fig. 3), at $480\ cm^{-1}$. There are also peaks for lead carbonate $PbCO_3$ (at $660\ cm^{-1}$ and $840\ cm^{-1}$) and for basic lead carbonate $2\ PbCO_3 \cdot Pb(OH)_2$ (at $660\ cm^{-1}$) [11]. Lead carbonates formation is explained by CO_2 absorption from atmosphere [12].

The spectra shown in Fig. 1 and 2 proves that in PbS layers deposited by vacuum evaporation, an interlayer between glass and PbS does not form.

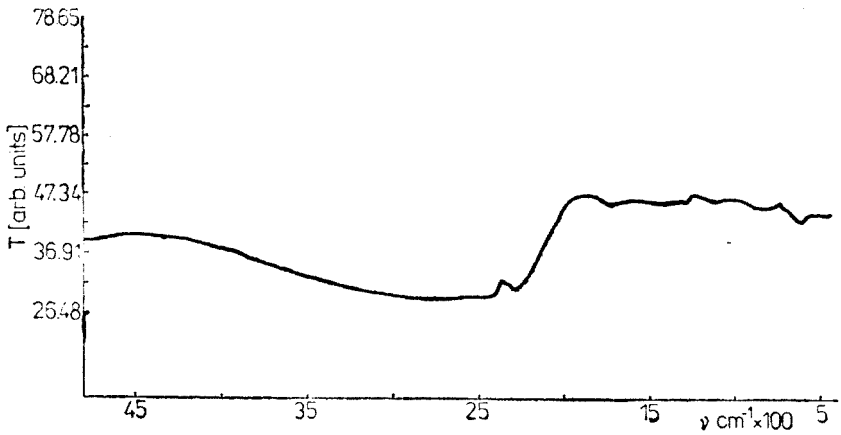

Fig. 1. FTIR transmission spectrum of PbS film deposited in vacuum, on glass plate

For that reason the PbS layers deposited by vacuum evaporation are not adherent to the glass surface and can be easily removed.

By chemical deposition of PbS from alkaline solutions, a lead hydroxide and lead carbonate layer is formed, which gives the adhesion to the support. Its existance concords with the mechanism of PbS and PbSe forming on glass support [9, 13].

The forming of lead hydroxide takes place in the initial phase of the deposition process when Pb(II) concentration in solution is higher and the reaction of forming PbS doesn't take place being characterized by an induc-

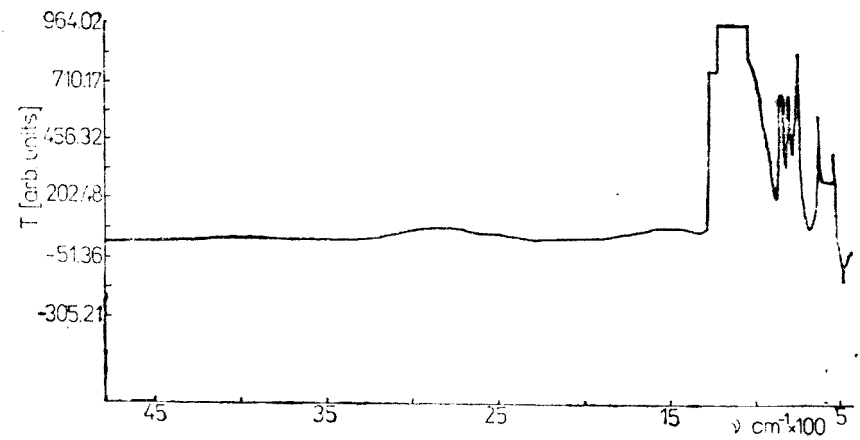

Fig. 2. FTIR transmission spectrum of PbS film chemically deposited on glass plate

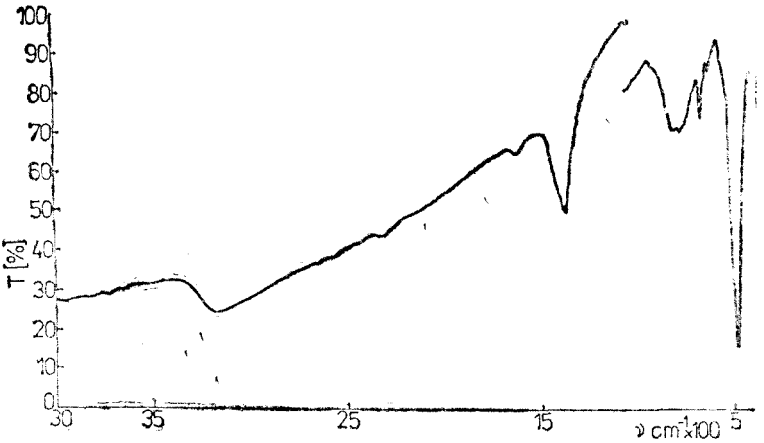

Fig. 3. IR spectrum of $Pb(OH)_2$

tion period necessary to form those nuclei which will act as catalyst for further deposition of PbS.

The adhesion degree of PbS layers was evaluated semiquantitatively by tape test [14]. The scotch tape test is utilised to give a quick measure of thin film adhesion. A piece of mylar-base tape is pressed on to a freshly deposited thin film and then removed by a snap action. If the film remains completely on the substrate it has an adhesion greater than 300 to 500 *psi* (pound square inch). In general, the minimum adhesion requirement for most thin film applications is that the film pass this tape test.

The PbS layers exceeds this test even if it is done immediatelly after preparation. It may be observed a growth of adhesion in time.

Conclusions. Through IR spectroscopy in the case of chemically deposited PbS layers, the existence of a layer composed from lead hydroxide and lead carbonates was shown, which is considered the cause of the film adhesion on glass. In the case of PbS layers deposited by vacuum evaporation there are not distinguished any other species and that is why the adhesion of these layers is much weaker.

The authors express their gratitude to dr. Emil Indrea from Institute of Isotopic and Molecular Technology Cluj-Napoca, for preparation of the PbS films by vacuum evaporation and for recording FTIR transmission spectra.

REFERENCES

1. C. Naşcu, V. Vomir, V. Ionescu and I. Pop. Submitted to Rev. Roumaine Chim.
2. S. Bateson, Vacuum, **2**, 365 (1952).
3. P. J. Hazdra, Ceramic Industry, **5**, 45 (1963).
4. W. D. Harkins and F. E. Brown, J. Amer, Chem. Soc., **41**, 499 (1919).
5. J. Langmuir, J. Amer. Chem. Sec., **40**, 1361 (1918).
6. L. Holland, *The Properties of Glass Surface*, Chapman and Hall, London (1966), p. 367.
7. D. O. Feder and D. E. Koontz, *Symposion on Cleaning of Electronic Device Components and Materials*, AST Special Tech. Pub. No. 246, 40 (1959).

8. D. M. Mattox, Sandia Corp. Reprint SC-R-65-997 (1966).
9. G. A. Kitaev, G. M. Fofanov and A. B. Lundin, Izv. Akad. Nauk SSSR, Neorg Mater., **3**, 473 (1967).
10. D. Negoiu, *Tratat de chimie anorganică*, vol. **II**, Ed. Tehnică Bucureşti (1972), p. 1125.
11. R. A. Nyquist and R. O. Kagel, *Infrared Spectra of Inorganic Compounds*, Academic Press, New York and London, (1971), p. 83.
12. V. N. Vertsner, G. P. Tihomirov, M. S. Davidov, V. S. Kosnirev, Izv. Akad. Nauk SSSR, Seria Fizic 27, **9**, 1228 (1963).
13. R. C. Kainthla, D. K. Pandya and R. L. Chopra, J. Electrochem. Soc., **127** (2), 277 (1980).
14. G. G. Paulson, Ph. D. dissertation (University of Illinois) 1969 p. 25 University Microfilms Inc. Ann. Arbor, Michigan.

STUDIA UNIV. BABEŞ-BOLYAI, CHEMIA, XXXVII, 1—2, 1992

ON THE USE OF METHANE-AIR FLAME IN FLAME SPECTROMETRY I. THE BURNER.

E. CORDOŞ*, L. KÉKEDY NAGY*

Received: 20.10.1992

ABSTRACT. The use of methane-air flame is proposed to generate emission and/or absorption spectra of analytes in flame spectrometry. The characteristics of a suitable new burner are reported. The translational temperature of the laminar flame obtained in the 12 – 15 *mm* region over the burner is 1875 *K*.

Introduction. Flame spectrometry is a widespread method for the determination of some analytes in low concentrations [1]. The emission spectra usually are obtained by excitation in acetylene-air, hydrogen-oxygen or acetylene-nitrogen protoxid flames. Considering that the analytical laboratories in our country are supplied with high purity natural methane gas, an attempt is made for the use of the methane-air flame in flame spectrometry in order to reduce the cost of the analysis. Such a procedure is not known in the literature.

The aim of this work and that of the following ones is to investigate the physico-chemical properties of the methane-air flame as well as the possibilities of the determination of some analytes by emission or absorption spectrometry using this flame.

Experimental. For this purpose a suitable methane-air burner was projected considering the physico-chemical properties of the methane-air flame. In the literature there exist a great number of fundamental studies concerning the flame structure as well as the chemistry of combustion [2]. The investigations concerning the methane-air flame are based on the results obtained with different burners used in the industry. The combustion of methane in air:

$$CH_4 + 2O_2 + 8N_2 \rightleftarrows CO_2 + H_2O + 8N_2 \qquad (1)$$

is strongly exothermic with 802.491 *kJ/mol*. The chemical energy is liberated stepwise in the course of many successive elementary reactions and equilibria, supported by some free radicals [2]. The activation energy of the ignition of the methane is high, the burning velocity is slow and the danger of explosion is also small. This simplifies considerably the handling of the gas and the design of the burner. Further it becames superfluous to equip the spectrophotometer with special antiexplosive devices.

The main characteristics of the methane-air (M—A) flame are: limits of ignition between 6.26% and 11.91% methane, temperature of ignition 918 *K* for a stoichiometric mixture in standard conditions [3]. The gas layer before the burning zone, the preheating zone, in our case has a thickness of 0.798

* *Babeş-Bolyai University, Dept. of Chemistry, 3400 Cluj-Napoca, Romania*

mm. The highest temperature of a stoichiometric M—A mixture in the primary reaction zone is 2228 *K* [4]. The burning velocity (the rate of propagation of the chemical reaction zone) for a stoichiometric M—A mixture in standard conditions is 33.8 $cm \cdot s^{-1}$ [5—8]. The increase of the initial temperature of the gas mixture increases considerably the burning velocity [9—10]. The shape and the properties of the flame depend on the flowing conditions of the gases through the burner too. If the Reynold's number is less than 2300 ($R_e < 2300$) the flow of the gases is laminar, yielding a laminar flame. When $R_e > 2300$ the flame becomes turbulent. In flame spectrometry, the most frequently used flames are the so called premixed (the fuel and the oxybant are proviuosly mixed), laminar, stationary flames which can be obtained by a judicious choice of the gas flow velocity as well as by the design and size of the burner. Usually the flame is stationar and laminar if the flow speed of gases in the burner exceeds 3—10 times the burning velocity of the gas mixture. Taking into account all these, a special burner was projected for a M—A mixture with the aim to obtain a premixed laminar flame to be used in flame spectrometry (Fig. 1).

The premixed flames have well defined burning zones assuring optimal excitation conditions. The new burner has the following characteristics:

a) Made of brass, it is provided with 80 bores each bore having 1.5 *mm* diameter. The flame cannot enter in the burner because the diameter of the bores are smaller than the extinction diameter of the flame. Thus the danger of explosion is completelly eliminated. *b)*. The elongated form of the burner allows to be used both in emission and absorption spectrometry. The length of the optical path in the flame is 50 *mm* ensuring an enhanced sensitivity. *c)*. The bores are arranged in four parallel rows thus the flame has 8—12 *mm* width. The cold ambient air cannot reach the central zone of the flame, thus the temperature in the central zone of the flame, in a 1—2 *mm* width, is practically constant. As a result of this design the danger of selfreversal of the lines decreases, but the possibility of autoabsorption increases. *d)*. The burner was made of a 10 *mm* thick brass block providing a rapid preheating of the

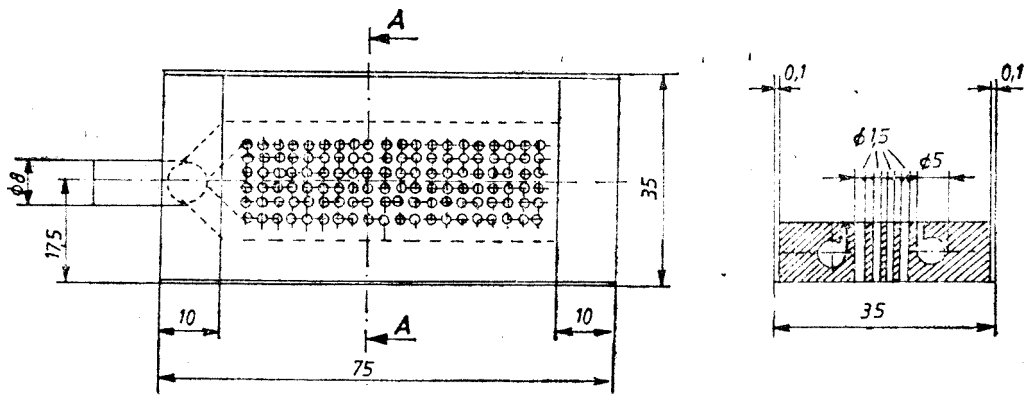

Fig. 1. Schematic diagram of the burner for a laminar M—A flame

gases, which increases the burning velocity and the stability of the flame. *e)*. The number of the bores have been determined considering the flow rate of the gases, determined mainly by the nebulizer whose optimal efficiency is at a flow rate of the air of 500 *l/h*. *f)*. In order to isolate the flame from the ambient air with an inert gas, the burner was provided with two peripheral rows of bores. Thus an excess of oxygen can be introduced in the flame in order to increase its temperature, without the danger of explosion [11, 12]. *g)*. The laminar flame with a low burning velocity exhibits fluctuation due to the influence of the ambient air. To reduce this effect, the burner was provided alongside with a protection mase made of a thin brass sheet.

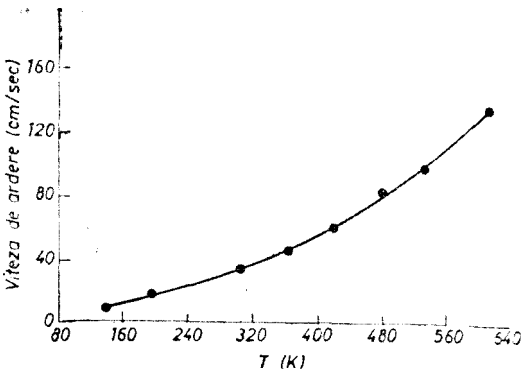

Fig. 2. The burning velocity of a stoichiometric M—A mixture versus the initial temperature of the mixture [2]

The burner was settled on a mixing chamber of an AAS—1 Carl Zeiss atomic absorption spectrophotometer. The flame obtained with this burner is a so-called *flat flame* with separated cones over each bore (the primary combustion zone) and with a single secondary merging combustion zone, respectively. The thickness of the preheating zone extends from 0.4 to 1 *mm* with the increasing methane content of the gas mixture. In the same time, the hight of the cones also increases from 2 to 3 *mm*. The secondary combustion zone extends 100—200 *mm* over the burner head. In work, the burner warms up to 410—440 *K* preheating the gas mixture to 330—350 *K* which increases considerably the stability of the flame (Fig. 2). The stability limits of the flame have been established too. The lower stability limit corresponds to a substoichiometric composition of the M—A mixture at which the flame burns out because of low burning velocity. The upper stability limit corresponds to a gas mixture in which the methane is in excess. In this case the separate cones rise and then merge owing again to the slow combustion velocity. During this investigations, the flow rate of the air was kept constant, and that of the methane was changed. Experimentally it was found that the lower stability limit corresponds to a 0.8, the upper to a 1.24 M—A stoichiometric ratio. In practice one can work between the limits of 0.88 and 1.12, respectively, expressed in the same units. It is advisable to work with the warmed burner, 4—5 minutes after igniting the flame.

As a main characteristic, the translational temperature of the flame has been determined at different heights, from 0 to 18 *mm* over the burner head, in 1 *mm* steps, at three different M—A stoichiometric ratios (0.88; 1.00; 1.12) using the sodium line inversion method [13]. The schematic diagram of the apparatus used is shown in Fig. 3.

For this purpose the intensity of a line of a light source at $\lambda = 589.0$ *nm* has been determined after passing the flame. Afterwards an aqueous

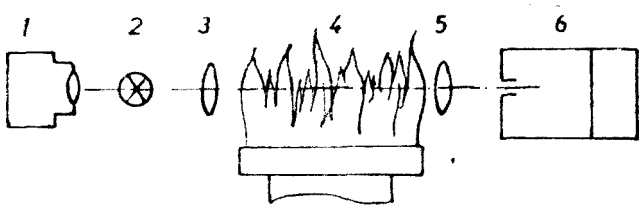

Fig. 3. Schematic diagram of the apparatus used for the determination of the translational temperature of the flame

NaCl solution with 5 *ppm* Na was introduced in the flame and the intensity of the same line was followed. If the temperature of the light source is equal to that of the traslational temperature of the flame, the two intensities remain constant both in the presence or in the absence of Na. The temperature of the light source is varied by the voltage applied to the filament till no variation in intensity is observed. In this moment the translational temperature of the flame is equal to the temperature of the filament, this being determined with an optical pyrometer. The results obtained are shown on Fig. 4.

It can be seen that the translational temperature of the flame increases slowly and non-uniformly with the height of the flame, the maximal value of 1857 *K* being observed at 12 *mm* over the burner head. In the 12—15 *mm* region, the temperature practically is constant. The temperature values obseved are lower than the theoretical ones owing to losses of heat by convection and radiation as well as to the presence of water pulverized in the flame, being lower with approximetely 200 *K* than the temperature of a similar M—A flame enriched with oxygen.

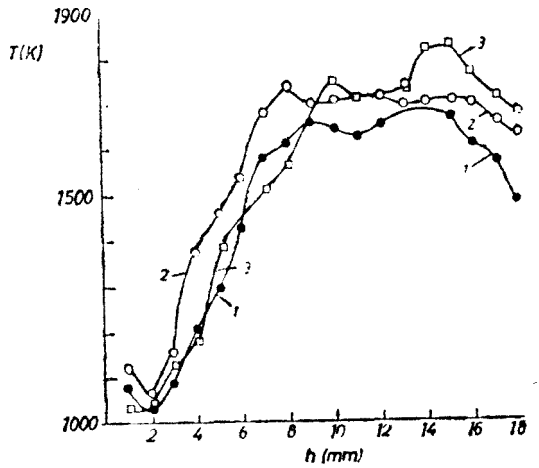

Fig. 4. The translational temperature of the M—A flame versus the distance over the burner head as a function of the gas mixture
1. Stoichiometric ratio 0.88
2. Stoichiometric ratio 1.00
3. Stoichiometric ratio 1.12

Apparatus. The spectrophotometric measurements were carried out with a HEATH—701 spectrophotometer using a HEATH EU—700 grating monochromator and a HEATH EU—700—30 type photomultiplier module. The photomultiplier current was recorded as an ohmic potential drop with a K-201, Carl Zeiss Jena, recorder. The slit width of the monochromator was 0.1 *mm* enabling a spectral resolution of 0.2 *nm*. The spatial resolution in the flame was 1 *mm*. In the spectral range of $\lambda = 200-700$ *nm* an 1P28A (RCA) type photomultiplier was used,

and in a higher wavelengths a M12FC51 (NARVA) one, respectively. The 0.1 *mm* slit width as well as the 700 *V* applied to the photomultiplier ensured the required sensitivity without raising the background noise of the system [14—17]. A pneumatic nebulizer was used with premixing chamber from a AAS-1 Carl Zeiss Jena spectrophotometer. The flow rate of the air was kept constant at 500 *L/h* required for the optimal performance of the nebulizer, the rate of methane being varied as a function of the composition of gas mixture wanted.

REFERENCES

1. J. D. Winefordner, *Spectrochemical Methods of Analysis*, Wiley-Interscience, N.Y., 1971, p. 130.
2. R. M. Fristrom, A. A. Westenberg, *Flame structure*, Mc. Graw Hill, N.Y., 1965, p. 146.
3. R. Mavrodineanu, H. Boiteux, *Flame spectroscopy*, Wiley, N.Y., 1965.
4. see 3, p. 31.
5. A. G. Gaydon, H. G. Wolfhardt, *Flames, their Sstructure, Radiation and Temperature*, Chapman-Hall, 1970, p. 81.
6. P. Bashu, A. Ghosh, Indian J. Tehnol, **10**, 215 (1972).
7. I. O. Moen, Comb. Inst. Can., **27**, 1 (1979).
8. B. Osawa, K. A. Ghashi, J. Fire Flam., **11**, 106 (1979).
9. J. R. Creighton, A. K. Oppenheim, *Report UCRL* 82816 (1979); cf. Chem. Abstr. **93**, 50074 (1980).
10. G. L. Dugger, I. Heimel, *5-th Symp. Comb.*, p. 589, (1952).
11. E. Cordoș, L. N. Kékedy, I. Marian, Brevet RSR, 67866/30.12.1977.
12. E. Cordoș, L. N. Kékedy, R. Hui, Brevet RSR, 67867/30.12.1977.
13. A. Hubaux, G. Vos, Analyt. Chem., **42**, 849 (1970).
14. J. D. Winefordner, C. Veillon, Analyt. Chem., **37**, 416 (1965).
15. J. D. Ingle, S. R. Crouch, Analyt. Chem., **43**, 1331 (1971).
16. J. D. Ingle, S. R. Crouch, Analyt. Chem., **44**, 1709 (1972).
17. E. D. Salin, G. Horlick, Analyt. Chem., **52**, 1578 (1980).

STUDIA UNIV. BABEŞ-BOLYAI, CHEMIA, XXXVII, 1—2, 1992

ON THE DIOXIMINE COMPLEXES OF TRANSITION METALS (LXXXIX)

Study of some mixed azido-complex acids and nonelectrolytes of cobalt(III) with aliphatic α—dioximes

CSABA VÁRHELYI*, FERENC MÁNOK**, DIDINA OPRESCU***, GABRIELA HORVÁTH** ZSUSZANNA SZEKERES**

Received: 20.10.1992

ABSTRACT. New diazido-complex acids of cobalt(III) with aliphatic α-dioximes: $H[Co(Glyox.H)_2(N_3)_2]$, $H[Co(DH)_2(N_3)_2]$ and $H[Co(Propox.H)_2(N_3)_2]$ ($Glyox.H_2$ — glyoxime, DH_2 — dimethylglyoxime, $Propox.H_2$ — methyl-isopropyl-2,3-dione dioxime) were obtained by oxidation of the components. $[Co(DH)_2(N_3)Cl]^-$, $[Co(DH)_2(N_3)(CN)]^-$ and 14 new nonelectrolytes $[(Co(DH)_2(N_3)(amine)]$ were obtained by substitution reactions. The composition of the azido-acids was proved also by isolation of a number of 27 new binary salts by double decomposition reactions.

The azido-complexes were characterized by UV and IR spectra, thermal-, potentiometric and polarographic measurements.

Introduction. The azide ion (N_3^-) with large nucleophylic properties reacts easily with various transition metal complexes and substitutes the halogen, H_2O, other acidic ligands and neutral groups. "Mixed" classical complexes and chelate compounds with N_3^- ligand are known in a considerable number (e.g. $[Co(NH_3)(N_3)]^{2+}$ [1], $(Co(en)_2(NO_2)(N_3)]^+$ [2], $[Cr(en)_2(N_3)_2]^+$ [3], $[Fe(o\text{-}phen)_2(N_3)_2]$ [4], $[Rh(NH_3)_5(N_3)]^{2+}$ [5], $[Co(ec)(N_3)(Ph_3P)]$, $[Co(salen)(N_3)Py]$ [6—8].

The formation of homogeneous azido-complexes $(M(N_3)_n^m$ (n = 1..6, m = = +3,..0..—4) in aqueous solutions and in nonaqueous media has been investigated by means of spectrophotometric, potentiometric and electric conductance measurements [9—10]. We have observed that the azide ion enters easily in various dioximino-chelates of cobalt (III) and rhodium (III) [11—13]. The anation and other substitution reactions of $[Co(Diox.H)_2(H_2O)X]$ and $[Co(Diox.H)_2X_2]^-$ (X = Cl, Br, I, NCS, NCSe, NO_2) with N_3^- leads to the formation of mixed complex acids.

Results and discussion. In the present paper various aliphatic α-dioximes: glyoxime, dimethylglyoxime and propoxime (methyl-isopropyl-2, 3-dione dioxime) were used for the synthesis of azido- cobalt (III) — complexes.

The starting compound for the synthesis of mixed azido-dioximino-complexes is the dichloro- acid: $H[Co(DH)_2Cl_2]$ (and the analogous derivatives with other dioximes). With stoechiometrical N_3^- -ion (molar ratio 1:1) the chloro-azido derivative is formed:

$$H[Co(DH)_2Cl_2] + NaN_3 = H[Co(DH)_2Cl(N_3)] + NaCl$$

* *Dept. of nat. sciences and mathematics, Transilvanian Museum Association, Cluj-Napoca, Romania*
** *Faculty of Chemistry, Babeş-Bolyai University Cluj-Napoca, Romania*
*** *Polytechnical Institute, Timişoara, Romania*

Using an excess of NaN_3 (molar ratio 1 : 2—2.5), the main product is the corresponding diazido-acid.

The chloro-azido-bis-dioximino-chelates are suitable for the synthesis of other mixed azido-complexes. The chloro-ligand can be substituted easily by NO_2^-, CN^-, NCS^-, SO_3^{2-}, amines and phosphines.

Like the other $[Co(Diox.H)_2XY]^-$ type anions, the mono- and diazido-acids form characteristic, crystalline, generally slightly soluble precipitates with monovalent metal ions (Cu^+, Ag^+, Tl^+ and with diacido-tetramine type complexes of cobalt(III) — and chromium(III) (e.g. $[M(en)_2X_2]^+$, $[M(NH_3)_4X_2]^+$, $[Co(Diox.H)_2(amine)_2]^+$, etc).

A number of 27 new binary salts of the azido-bis-dioximino-cobalt(III)-acids obtained by double decomposition reactions in aqueous or dil. alcoholic solutions are characterized in Tables 1—4.

Table 1

New salts of the $H[Co(DH)_2Cl(N_3)]$ complex acid

Formula	Appearance	Analysis (%)	Caled.	Found
$[Co(DH)_2(o\text{-anisidine})_2] \cdot A$	brown prisms	Co	13.06	12.68
		N	20.19	20.44
$[Co(DH)_2(o\text{-ethylaniline})_2] \cdot A$	brown dendrites	Co	13.12	13.14
$[Co(DH)_2(p\text{-ethylaniline})_2] \cdot A$	brown dendrites	Co	13.12	13.20
		N	20.28	19.92
$[Co(DH)_2(thiouree)_2] \cdot A$	brown prisms	Co	14.59	14.48
		S	7.94	8.15

A = $[Co(DH)_2Cl(N_3)]$

Table 2

New salts of the $H[Co(DH)_2(CN)(N_3)]$ complex acid

Formula	Appearance	Analysis (%)	Caled.	Found
$[Co(DH)_2(aniline_2] \cdot B$	yellow dendrites	Co	14.15	13.89
		N	23.55	23.90
$[Co(DH)_2(m\text{-xylidine})_2] \cdot B$	yellow dendrites	Co	13.26	13.30
$trans\text{-}[Cr(en)_2(NCS)_2] \cdot B$	yellow needles	Co+Cr	17.19	17.45
		S	9.93	9.72

B = $[Co(DH)_2(CN)(N_3)]$

Table 3

New derivatives of the H[Co(Propox.H)$_2$(N$_3$)$_2$] and H[Co(Glyox.H)$_2$(N$_3$)$_2$] complex acids

Formula	Appearance	Analysis (%)	Calcd.	Found
H[Co(Glyox.H)$_2$(N$_3$)$_2$] · 2H$_2$O	brown irreg. cryst	Co	16.64	16.50
		H$_2$O	10.17	9.88
		N	39.56	39.19
[Co(DH)$_2$(pyridine)$_2$] · D. 1.5 H$_2$O	short, light brown prisms	Co	13.04	13.49
		H$_2$O	2.99	2.97
[Co(DH)$_2$(pyridine)$_2$] · E. 1.5 H$_2$O	short, brown prisms	Co	14.89	14.64
		H$_2$O	3.41	3.27
[Co(DH)$_2$(aniline)$_2$] · D	brown hexagonal plates	Co	13.03	13.17
		N	24.77	24.42
[Co(DH)$_2$(aniline)$_2$] · E · H$_2$O	brown, rhomb. plates	Co	14.54	14.68
		H$_2$O	2.22	2.16
[Co(DH)$_2$(thiouree)$_2$] · D · H$_2$O	brown, hexagonal plates	Co	13.26	13.34
		H$_2$O	2.02	2.11
		S	7.22	7.47
[Co(DH)$_2$(thiouree)$_2$] · E · 1.5 H$_2$O	dark brown, short prisms	Co	15.01	15.26
		H$_2$O	3.44	3.35
		S	8.16	7.95
[Co(DH)$_2$(m-chloraniline)$_2$] · D	irregular, brown plates	Co	12.26	12.19
		N	23.32	23.19
[Co(DH)$_2$(NH$_3$)$_2$] · E · H$_2$O	short, brown needles	Co	17.91	17.84
		H$_2$O	2.74	2.63
trans-[Cr(en)$_2$(NCS)$_2$] · D · 3H$_2$O	light brown microcryst.	Co—Cr	14.38	14.75
		S	8.31	8.55
		H$_2$O	7.00	8.07
trans-[Co(en)$_2$Cl$_2$] · E · H$_2$O	gold yellow irreg. cryst.	Co	20.15	19.80
		H$_2$O	3.08	2.88
		N	33.52	34.00
trans-[Co(en)$_2$Br$_2$] · E · H$_2$O	olive yellow dendrites	Co	17.49	17.35
		H$_2$O	2.67	2.52
		N	29.10	28.60

D = [Co(Propox.H)$_2$ N$_3$)$_2$]$^-$; E = [Co(Glyox.H)$_2$(N$_3$)$_2$]$^-$; Co = Cr detn as sum of Co_3O_4 + Cr_2O_3 900° C, 2 hr

New derivatives of the [H][Co(DH)$_2$(N$_3$)$_2$]-acid

Table 4

Formula	Appearance	Analysis (%)	Calcd.	Found
trans-[Co(en)$_2$(NO$_2$)$_2$)] · C · H$_2$O	dark yellow prisms	Co	17.80	17.35
		H$_2$O	2.72	2.10
		N	33.85	34.19
[Co(DH)$_2$(thiouree)$_2$] · C · H$_2$O	dark yellow dendrites	Co	14.15	13.81
		H$_2$O	2.16	1.92
		S	7.70	7.89
[Co(DH)$_2$(aniline)$_2$] · C	long, brown prisms	Co	13.89	13.78
[Co(DH)$_2$(o-ethylaniline)$_2$] · C · H$_2$O	brown dendrites	Co	12.72	12.87
		H$_2$O	1.95	2.20
[Co(DH)$_2$(p-ethylaniline)$_2$] · C	brown dendrites	Co	13.03	13.17
		N	24.77	25.11
[Co(DH)$_2$(p-chloraniline)$_2$] · C	yellow-brown prisms	Co	12.84	12.79
[Co(DH)$_2$(p-bromaniline)$_2$] · C	yellow-brown dendrites	Co	11.71	11.54
		N	22.27	22.66
[Co(DH)$_2$(o-anisidine)$_2$] · C	brown dendrites	Co	12.97	12.58
		N	24.67	24.29

C = [Co(DH)$_2$(N$_3$)$_2$]; Co detn: complexometrically; S detn. as $BaSO_4$; N detn gazvolumetrically as N.

The halogeno-ligand in the $H[Co(DH)_2Cl(N_3)]$ acid can be replaced by neutral ligands too, e.g. NH_3, pyridine bases, aromatic primary amines (pK_b values: 9—12) and tertiary alkyl-aryl-phosphines.

$$H[Co(DH)_2Cl(N_3)] + \text{amine} = [Co(DH)_2(\text{amine})(N_3)] + HCl$$

The reaction was carried out in ammonium acetate buffer solution by water bath temperature.

Some beautiful, characteristic crystalline products are characterized in Table 5.

Table 5

New nonelectrolytes of the $[Co(DH)_2(N_3)(\text{amine})]$ type

No.	Formula	Appearance	Analysis (%)	Calcd.	Found
	$[Co(DH)_2(N_3)(\text{m-toluidine})] \cdot 2H_2O$	brown prisms	Co	12.42	12.66
			H_2O	7.59	7.33
			N	23.62	24.06
	$[Co(DH)_2(N_3)(\text{m-xylidine})] \cdot 2H_2O$	brown-irregular cryst.	Co	12.07	12.23
			H_2O	7.37	7.18
	$[Co(DH)_2(N_3)(\text{p-phenotidine})] \cdot 2H_2O$	dark brown prisms	Co	11.68	11.54
			H_2O	7.14	7.34
	$[Co(DH)_2(N_3)(\text{p-anisidine})] \cdot 2H_2O$	gold-brown plates	Co	12.02	11.98
			H_2O	7.35	7.21
			N	22.85	22.40
	$[Co(DH)_2(N_3)(\text{p-chloraniline})] \cdot 2H_2O$	sparkling, dark brown plates	Co	11.91	11.75
			H_2O	7.28	6.85
	$[Co(DH)_2(N_3)(\text{m-chloraniline})] \cdot 2H_2O$	sparkling brown plates	Co	11.91	11.84
			H_2O	7.28	6.90
	$[Co(DH)_2(N_3)(\text{p-bromaniline})] \cdot 2H_2O$	brown plates	Co	10.93	10.80
			N	20.78	21.10
			H_2O	6.68	6.40
	$[Co(DH)_2(N_3)(\text{p-jodaniline})] \cdot 2H_2O$	sparkling, dark brown plates	Co	10.05	10.02
			H_2O	6.14	6.50
	$[Co(DH)_2(N_3)(\gamma\text{-picoline})]$	brown prisms	Co	13.89	13.76
	$[Co(DH)_2(N_3)(3,5\text{-lutidine})]$	yellow-brown plates	Co	13.44	13.46
			N	25.57	25.40
	$[Co(DH)_2(N_3)(3,4\text{-lutidine})]$	yellow-brown plates	Co	13.44	13.28
	$[Co(DH)_2(N_3)(4\text{-ethylpyridine})]$	brown plates	Co	13.44	13.50
	$[Co(DH)_2(N_3)(\text{imidazole})]$	yellow-brown plates	Co	14.76	14.71
			N	31.58	32.01
	$[Co(DH)_2(N_3)(2\text{-amin-thiazole})]$	short brown plates	Co	13.66	13.70

Potentiometric measurements. The isolated $H[Co(DH)_2Cl(N_3)]$ and $H[Co(DH)_2(N_3)_2]$ are middle strong monobasic acids.

The dissociation constants (25 °C, ionic strenght: 0.1 m) are: 4.10×10^{-3} and 5.05×10^{-3}. These values were calculated using the *pH* values of the half

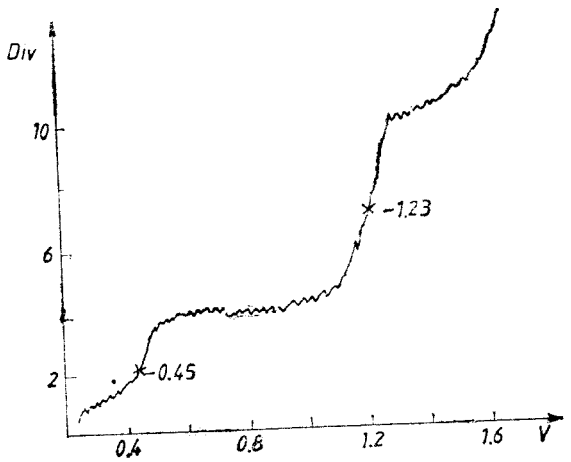

Fig. 1. Polarogram of $[Co(en)_3]Cl_3$ ($pH = 5.02$; gelatine 0.5%)

neutralized aqueous solutions of the complex acids ($c = 1 - 2 \times 10^{-3}$ mole/l), following the equations:

$$K = \frac{[H^+] \cdot [Co(DH)_2XY]^-}{H[Co(DH)_2XY]}$$

$$\log K = \frac{(1 - a)(c - [H^+]) + [OH^-]}{a \cdot c + [H^+] - [OH^-]} + pH$$

(for the neutralization, 0.1 n KOH has been used)
(c — concentration mole/l; a — degree of neutralization)
The azido-cobalt(III) — acids eliberate CO_2 from $NaHCO_3$ HCN from KCN solution. The obtained azido-complexes have not explosive character and can be handled without explosion danger.

Polarographic behaviour. In a previous paper [14] the anodic oxidation of some azido-complexes of the type $[Co(DH)_2X(N_3)]^-$ on the dropping mercury electrode was studied. It was found that the co-ordinated azide is oxidized more easily than the ionic one. The oxidation of the co-ordinated ligands takes place without the change of the oxidation state of the central cobalt atom.

The polarographic reduction of some $H[Co(DH)_2(N_3)X]$ type complexes ($X = Cl$, N_3, NO_2), as compared with those of the $[Co(en)_3]Cl_3$ was studied in Britton—Robinson's buffer solutions. Some typical polarograms are presented in Figs. 1 and 2.
The polarographic data are shown in Table 6.

In the case of the hexamine type complexes ($[Co(en)_3]^{3+}$ and $[Co(NH_3)_6]^{3+}$, respectively) two reduction waves appear corresponding to the following processes: [15].

$$Co(III) \xrightarrow{+e} Co(II) \qquad (I.)$$

$$Co(II) \xrightarrow{+2e} Co(O) \qquad (II.)$$

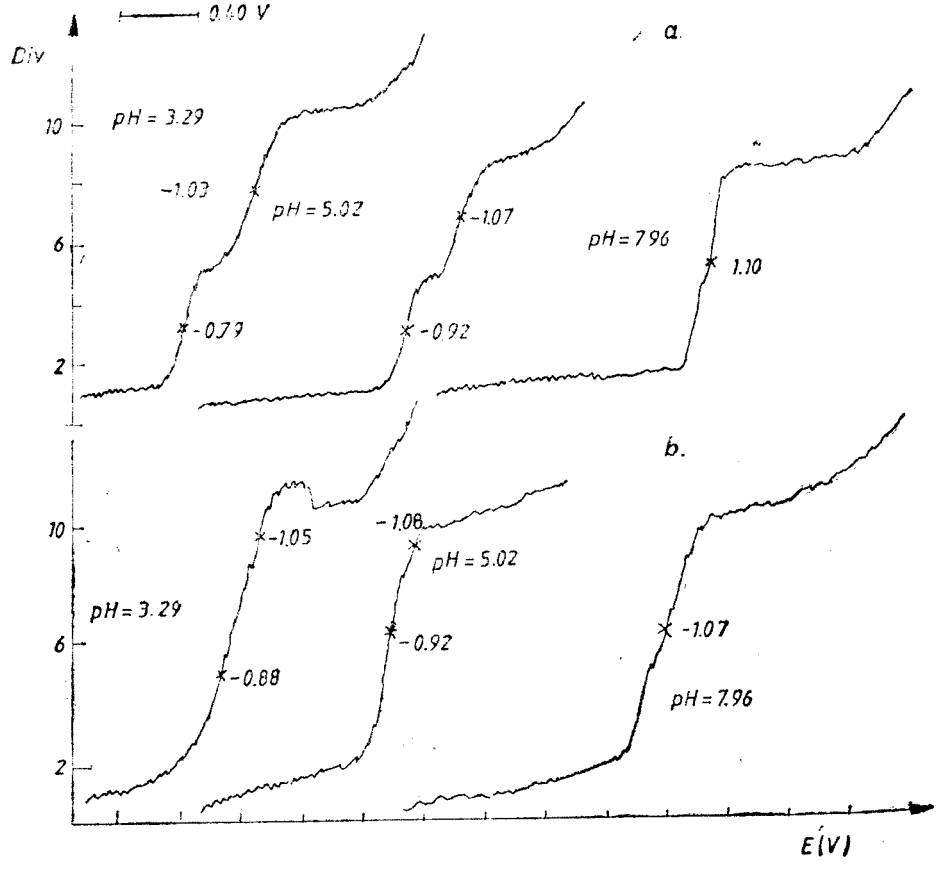

Fig. 2. a) Polarogramms of $H[Co(DH)_2(N_3)_2]$
b) Polarogramms of $H[Co(DH)_2(N_3)Cl]$ (in the presence of gelatine 0.5%)

Table 6

Polarographic data of some cobalt(III)-complexes

Compound	Conc. $\times 10^{-3}$	*pH*	Sensibility A/Div $\times 10^{-7}$	E (vs.SCE) $E^{I}_{1/2}$	$E^{II}_{1/2}$	Height of the wave (Div) I		II
$[Co(en)_3]Cl_3$	0.9	5.02	0.6	−0.45	−1.23	11		22.1
$H[Co(DH)_2Cl(N_3)]$	0.208	3.29	1.2	−0.79	−1.03	15.6		19
		5.02	0.92	−0.92	−1.07	19.0		18.5
		7.96			−1.1		32	
$H[Co(DH)_2(N_3)_2]$	0.23	3.29	1.2	−0.78	−1.02	16.2		17.3
		5.02		−0.91	−1.06	19.0		17.2
$H[Co(DH)_2(N_3)(NO_2)]$	0.284	3.29	2.0	−0.88	−1.05		51	
		5.02		−0.92	−1.08		53	
		7.96		−0.86			40.8	

The height of the second wave is double as compared with that of the first one. The first wave has an irreversible character with $E_{1/2} = -0.4 - -0.6$ *V* (vs. SCE). The half wave value of the second wave is $-1.2 - 1.3$ *V* (vs. SCE).

In the case of the dioximino-chelates, the first wave has a more complicated character with $E_{1/2} = -0.7 - 1.0$ *V* (vs SCE); 5–6 fold higher as by the hexamine-type complexes, and influenced by the *pH* value of the supporting electrolyte. This means, that the reduction of the central cobalt(III) ion is accompanied with the reduction of the oxime groups.

The total reduction of the dioxime ligand is an eight-electronic process:

$$\begin{matrix} R-C=N-OH \\ | \\ R-C=N-OH \end{matrix} + 8e + 8H^+ = \begin{matrix} R-CH-NH_2 \\ | \\ R-CH-NH_2 \end{matrix} + 2H_2O$$

The second wave is shifted towards more positive values as compared with those of the hydrated $[Co(H_2O)_6]^{2+}$ ion (−1.4 V vs. SCE). In the case of the $H[Co(DH)_2(NO_2)(N_3)]$ acid the nitro-group is also reduced (The first wave is higher then by other azido-derivatives studied).

The *IR spectral data* of some new azido-complexes are presented in Table 7.

Table 7

Infrared spectral data of some azido-cobalt(III)-complexes

Characteristic frequency	Azido-complex				
	I.	II.	III.	IV.	V.
ν_{N-H}	—	—	—	3130 m	3130 m
				3030—	3035—
				3070 m	3080 m
ν_{O-H}	2300—	2300—	2300—	2330—	2320—
	2380 s—m	2370 s—m	2300 s—m	2390 s—m	2400 s—m
ν_{asN_3}	2035 v s	2040 v s	2050 v s	2030 s	2045 s
		2120 v s			
$\nu_{O-H..O}$	1750—	1720—	1700—	1740—	1750—
	1770 m	1780 m	1750w	1800 w	1800 w
$\nu_{C=N}$	1540 s	1570 s	1570 v s	1575 s	1575 s
	1570 s				
ν_{sN_3}	1380 m	1360 m	1340 m	1370 m	1360 m
ν_{N-OH} (oxime)	1240 v s	1245 v s	1250 v s	1250 v s	1245 v s
$\nu_{N-O..}$ (oxime)	1085 v s	1100 v s	1090 v s	1100 v s	1100 v s
γ_{O-H}	980 m	960 m	985 s	980 m	975 m
γ_{C-H}	750 m	740 s	750 s	750 s	760 m
ν_{Co-N-N} (azide)	610—	625 m	660 s	630—	610 m
	630 w			580 m	
ν_{Co-N} (amine, oxime)	520 s	515 m	520 m	520 m	515 s
δ_{N-Co-N}	440 m	450 m	440 m	445 m	450 w
				420 m	420 w

I – $H[Co(DH)_2Cl(N_3)]$; II – $H[Co(Glyox.H)_2(N_3)_2]$; III – $[Co(DH)_2(N_3)(imidazole)]$; IV – $[Co(DH)_2(N_3)$ (panisidine)]; V – $[Co(DH)_2(N_3)$(m-xylidine)]. vs – very strong, s – strong, m – medium, w – weak)

The position of the ν O—H and δ O—H..O frequencies show the presence of strong intramolecular O—H..O hydrogen boundings similar to those observed in the case of the analogous H[Co(DH)$_2$X$_2$], [Co(DH)$_2$(amine)$_2$]X type complexes. These hydrogen bridges stabilize the coplanar Co(Diox.H)$_2$ ring system, i.e. the trans-geometric configuration of the azido-bis-dioximino complexes. Therefore ligand exchange reactions occur with retention of the geometric configuration.

The ν C=N, ν N—OH and ν N—O.. frequencies of the coordinated α-dioxime ligands appear at 1550—1570 cm^{-1} (s), 1230—1240 cm^{-1} (v.s.) and 1080—1100 cm^{-1} (s.) showing strong covalent Co—N (oxime) bondings.

The azido-complexes show generaliy 5 characteristic absorption bands at 2030—2080, 1300, 600, 300—400 and 200 cm^{-1}, respectively. These bands can be considered in a first approximation as M—N_3 group frequencies.: $\nu_{as}N_3$ ν_sN_3 stretching vibrations, the δ_{N3} and M—N—N deformation frequencies. [16, 17]. The free, non co-ordinated azide ion is linear and symmetrical with equal N—N atomic distances. By co-ordination appears a symmetry diminishing with M—azide angular bonding $\left(M\diagup^{N-N-N}\right)$ [18].

The increase of the π — interaction between the *p* orbitals of the N-atom and the *d*- orbital of the metal ion leads to the increase of both the N—N atomic distances and of the $\nu_{as}N_3$ value. (in the case of ionic azides, e.g. NaN_3: $\nu_{as}N_3$: 2120—2140 cm^{-1} (v.s.) and δN_3: 643 cm^{-1} (m).

The stretching and deformation vibrations of the co-ordinated azido-groups are shifted as compared to those of the free ionic N_3^-, as seen from Table 7. This phenomenon show the Co—N_3 bond to have strongly covalent character.

The ν N—H stretching frequencies of the co-ordinated primary amines appear at 3100—3200 cm^{-1}, shifted with 200—250 cm^{-1} towards lower frequency values. (The Co-amine bonding is also a strongly covalent bond).

Electronic spectra of the azido-complexes were recorded in methanol. Some spectra are shown in Figs. 3. and 4. and the spectral data are presented in Table 8.

In the case of the diazido-acids two bands appear in the visible region, at 14—16 *kK* and 19 *kK*, respectively.

By substitution of an N_3 -ligand with amines or with other ligands, the band at 14—16 *kK* disappears and the second one is shifted towards higher frequency values (20—21 *kK*). The bands in the 14—20 *kK* region have a ligand field character. The wide, strong band at 39—41 *kK*, overlapped with the charge transfer bands of the N_3^- and of the neutral ligands (amines), is due, probably to the presence of the Co(DH)$_2$, Co(Glyox.H)$_2$ and Co(Propox.H)$_2$ — groups. This band appears in the spectra of the majority of bis-dimethylglyoximino-complexes of cobalt(III) [19].

Thermal behaviour. The binary azido- comples salts and azido-non-electrolytes decompose suddenly on heating. Some derivatographic derivatographic measurements show that the decomposition in air between 150—240 °C is followed by evolution of N_2, NO, CO, CO_2, H_2O in non-stoechiometric ratios. The final residue in the crucible is not a stoechiometric amount of Co_3O_4 be-

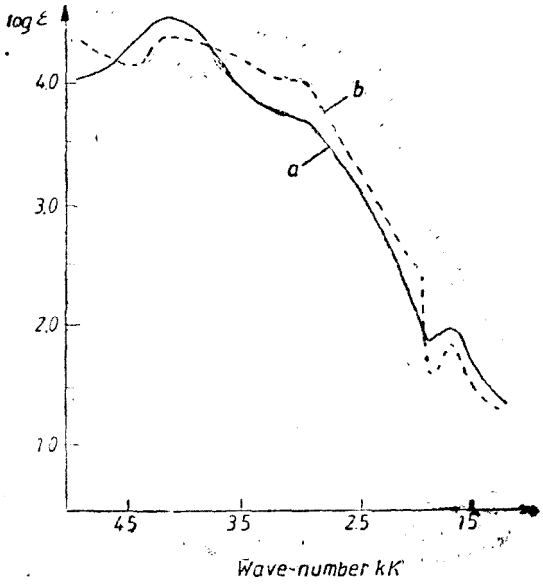

Fig. 3. Electronic spectra of
a) H[Co(DH)$_2$(N$_3$)$_2$]
b) H[Co(DH)$_2$(N$_3$)Cl]

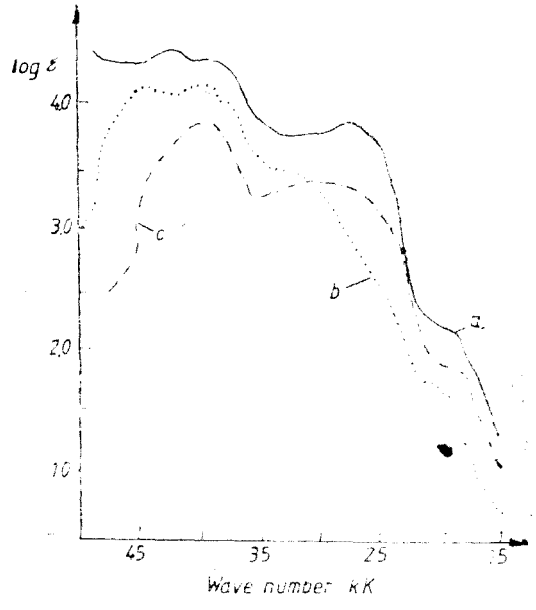

Fig. 4. Electronic spectra of
a) [Co(DH)$_2$(N$_3$)(p-I-aniline)]
b) [Co(DH)$_2$(N$_3$)(3,5-lutidine)]
c) [Co(DH)$_2$(N$_3$)(m-toluidine)]

Table 8

Electronic spectral data of some azido-cobalt(III) complexes

Formula	λ_1	log ε_5	λ_2	log ε_2	λ_3	logε_3	λ_4	logε_4	λ_5	log ε_5
H[Co(DH)$_2$(N$_3$)$_2$]	15.2	1.38	19.0	2.28	31.0	3.82	39.0	4.23	42.0	4.15
H[Co(Glyox.H)$_2$(N$_3$)$_2$]	15.0	1.4	18.8	2.4	32.0	3.9	39.5	4.4	41.0	4.3
H[Co(DH)$_2$Cl(N$_3$)]	15.0	1.45	18.0	1.93	30.0	3.4	40.5	4.5	49.0	4.1
[Co(DH)$_2$(N$_3$)(3.4-lutidine)]	20.0	1.8	30.5	3.4	31.0	3.5	40.5	4.3	43.7	4.3
[Co(DH)$_2$(N$_3$)(m-toluidine)]	20.0	2.02	28.0	3.4	32.0	3.5	39.7	3.9	44.0	3.6
[Co(DH)$_2$(p-anisinine(N$_3$)]	19.0	1.5	25.7	3.8	31.0	3.6	39.8	4.3	43.6	4.3
[Co(DH)$_2$(N$_3$)(p-chloraniline)]	20.0	2.1	22.0	2.3	39.6	4.35	45.2	4.4	49.0	4.5
[Co(DH)$_2$(N$_3$)(p-iodaniline)]	19.8	2.2	27.5	3.8	39.7	4.40	43.5	4.4	49.5	4.4

wave number in *kK*)

cause of a great mass loss during the rapid decomposition processes (explosion in every cases!).

Hot conc. HNO_3 and H_2SO_4 decompose the mentioned substances with formation of $Co(NO_3)_2$ and $CoSO_4$, respectively.

Experimental. Na[Co(Diox.H)$_2$(N$_3$)$_2$]-solutions. 0.1 *mole* cobalt(II)acetate in 150 *ml* aqueous solution were treated with 0.2 *mole* aliphatic α-dioxime (glyoxime, dimethylglyoxime,propoxime) in 200 *ml*. dil. alcohol (1 : 1) and oxidized by air bubbling during 4—5 hours. After addition of 0.22—0.25 *moles* NaN_3 in 50 *ml* water, the oxidation was continued 2 hours. The precipitated dark-

brown by product (azido-aquo-bis-dioximino-cobalt(III): $[Co(Diox.H)_2(N_3)(H_2O)]$) was filtered off. The dark-brown solution was completed with water to 500 *ml* and used for double exchange reactions.

$Na[Co(DH)_2Cl(N_3)]$-solution. 0.1 *moles* $H[Co(DH)_2Cl_2]$ were treated in 200 *ml* water with 0.08–0.09 *moles* NaN_3 in 25 *ml* aqueous solution. By continuous stirring the dichloro-acid dissolves after 5–10 minutes and reddish-violet solution is formed. The mixture was ice cooled, filtered and used for double decomposition reaction.

Free azido-acids. The solutions of $Na[Co(DH)_2(N_3)Cl]$ and $Na[Co(Diox.H)_2(N_3)_2]$ were treated with a large excess of 30–35 per cent sulfuric acid. The crystalline free azido-acids were filtered off washed with ether and dried on air.

$K[Co(DH)_2(N_3)(CN)]$-solution. 25 *mmoles* of $H[Co(DH)_2Cl(N_3)]$ in 100 *ml* water were treated with 25–30 *mmoles* KCN in conc. aqueous solution on a water bath. The brown-violet solution was used for double decomposition reactions.

$[Co(DH)_2(N_3)(amine)]$-nonelectrolytes. 10 *mmoles* $H[Co(DH)_2(N_3)Cl]$ in 60–80 *ml* water were treated with 2 *g* ammonium acetate and 10–12 *mmoles* amine in 10–15 *ml* alcohol. After 15–20 *min.* of heating on a water bath, the characteristic crystalline products separated were filtered off, washed with water and dried on air.

The *IR spectra* were recorded in KBr pellets by means of a UR 20 Carl Zeiss Jena spectrophotometer between 400–4000 cm^{-1}.

UV-spectra were recorded in the 12 and 50 *kK* region in methanol. Concentrations in the visible: $0.5-2 \times 10^{-3}$ *mole/l*; UV region: $0.1-1 \times 10^{-4}$ *mole/l*.

Polarographic measurements. The polarograms were taken with a RADELKIS-TYPE OH–120 polarograph using a conventional polarographic cell with a saturated calomel reference electrode, connected to the cell by means of an agar-agar bridge (1 *M* KNO_3). The oxygen was eliminated from the solution with purified methane.

The supporting electrolytes were prepared from Britton-Robinson solutions with addition of $NaClO_4$ to ensure an ionic strength of approximately 0.1 *M*. The measurements were carried out at 20 °C. *pH-measurements* were carried out at 25 °C with an LPU–0.1 (U.S.S.R.) *p*H-meter having a glass-electrode as indicator and a saturated calomel as standard electrode.

REFERENCES

1. M. Linhard, M. Weigel, H. Flygare, Z. anorg. allg. Chem., **262,** 328 (1950); **263,** 245 (1950); **267,** 121 (1951).
2. P. J. Staples, M. L. Tobe, J. Chem. Soc., **1960,** 4812; **1963,** 3226.
3. M. Linhard, W. Berthold, Z. anorg. allg. Chem., **279,** 173 (1955).
4. W. Beck, K. Madeja, W. Wilke, S. Smidt, Z. anorg. allg. Chem., **346,** 306 (1966).
5. C. S. Davis, G. C. Lalor, J. Chem. Soc. (A), **1970,** 445.
6. W. Beck, E. Schuierer, K. Feldl, P. Pöllmann, W. P. Fehlhammer, Angew. Chem., **77,** 458 (1965); **78,** 267 (1966).
7. W. Beck, W. P. Fehlhammer, P. Pöllmann, E. Schuierer, K. Feldl, Chem. Ber., **100,** 2335 (1967).
8. W. P. Fehlhammer, T. Kemmerick, W. Beck, Chem. Ber., **112,** 468 (1979).
9. R. G. Clem, E. H. Huffman, J. Inorg. Nucl. Chem., **27,** 365 (1965).
10. V. Gutmann, O. Leitmann, Monatsh. Chem., **97,** 926 (1966).
11. Cs. Várhelyi, F. Mánok, S. Kiss, Studia Univ. Babeș–Bolyai, Chem., **18,** (2), 105 (1973).
12. Z. Finta, Cs. Várhelyi, J. Inorg. Nucl. Chem., **36,** 2199 (1974).
13. Cs. Várhelyi, F. Mánok, J. Zsakó, *Proc. XVII. Intern. Conf. on Coord. Chem.*, 6–10 Sept. 1976, Hamburg, F.R.D., *Abstracts of Papers*, p. 337.
14. F. Mánok, Cs. Várhelyi, Rev. Roumaine Chim., **23,** 917 (1978).
15. H. F. Holtzclaw, D. P. Shetz, J. Amer. Chem. Soc., **75,** 3053 (1953).
16. P. Gray, C. Waddington, Trans. Faraday Soc., **53,** 901 (1957).
17. D. Milligan, H. W. Brown, G. C. Pimentel, J. Chem. Phys., **25,** 1080 (1956).
18. D. Foster, W. D. Horrocks, Inorg. Chem., **5,** 1510 (1966).
19. A. V. Ablov, M. P. Filippov, Zhur. Neorg. Khim., **3,** 1565 (1958).

STUDIA UNIV. BABEŞ-BOLYAI, CHEMIA, XXXVII, 1—2, 1992

SOME NEW COBALT(III)-AMINE PERIODATES.
The gravimetric determination of the periodic acid with metal- and metal-amine salts.

FERENC MAKKAY*, CSABA VÁRHELYI** and SÁNDOR GÁL SÉMER*

Received: 20.10.1992

ABSTRACT. A number of 10 new cobalt(III)-amine periodates of the $[Co(Diox.H)_2(Am)_2]IO_4$ type ($Diox.H_2$ — dimethylglyoxime, heptoxime, Am — pyridine bases, tertiary alkyl-arylphosphines) were obtained and characterized by chemical methods, solubility measurements and by IR spectra, respectively.

Some derivatives of this type were used, as compared with the thallium-, silver-, mercury- and lead periodates for the gravimetric determination of the periodic acid. The results were statistically evaluated using the usual methods and programs written in the Turbo-Pascal language.

Introduction. The periodates appear in various forms as: metaperiodates: MIO_4, mezoperiodates: M_3IO_5, dimezoperiodates: $M_4I_2O_9$, orthoperiodates: M_5IO_5 and also in other self condensation products and heteropolyperiodates, depending on the *pH*, the nature of cations and anions present in the reaction's media and the experimental conditions, respectively (reaction in solution or in solid state) [1—3].

The metal salts of these acids, excepting the alkaline — and ammonium salts, are generally sparingly soluble in water. The analogous derivatives of the other oxoacids of the halogens, especially the salts of $HClO$, $HClO_2$, $HClO_3$, $HClO_4$, and in every cases also the bromates and iodates have a higher solubility in analogous experimental conditions.

The periodic acids form also slightly soluble salts with various metal-amines [4—6], e.g. $[Pt(NH_3)_4]^{2+}$, $[Pt(en)_3]^{4+}$, $[Pd(en)_2]^{2+}$, and some chromium(III) — amines.

From analytical point of view one cannot distinguish among the various forms of the periodates. One can determine oxidimetrically only the quantity of I^{7+} in all the periodates present, on the basis of the redox processes:

$$I^{7+} + 2e = I^{5+} \quad (IO_4^- \rightarrow IO_3^-;\ pH = 9-10)$$

and

$$I^{7+} + 8e = I^- \quad (IO_4^- \rightarrow I^-;\ \text{in acidic media}).$$

Following the former equation the periodate can be determined iodometrically in $NaHCO_3$ or borax media in the presence of arsenite [7], manganese(II) [8], H_2O_2 [9], ethane diol and polyalcohols [10], hydroxylamine [11] or hydrazine [12].

* *Babeş-Bolyai University, Faculty of Chemistry, 3400 — Cluj-Napoca, Romania*
** *Transylvanian Muzeum Association, Dept. of Nat. sciences and Mathematics, 3400 — Cluj-Napoca, Romania*

Some non-specific spectrophotometric methods were proposed for the determination of micro amounts of periodates also in the presence of several oxoacids. For spectrophotometric measurements, some amines, oximes, semicarbazones, hydrazones, phenols and dyes were proposed [13—16].

Some metaperiodates and orthoperiodates (unitary, sparingly soluble, easily filtrable precipitates) seem to be suitable for the gravimetric determination of this oxoacid; for this reason, some heavy metal- and cobalt(III)-amine periodates were proved in this paper for the above mentioned purpose.

Results and discussion. In earlier papers [17—25] we studied the formation conditions of the cobalt(III)- and chromium(III)-amine periodates of various types. Thus, the hexamines and monoacido-pentamines form orthoperiodates, mezo- and dimezoperiodates with various number of water molecules, especially at higher *pH*-values have been obtained. The acidic medium promotes the separation of metaperiodates in the case of all cobalt(III)- and chromium(III)-amine bases. The metaperiodate, especially with diacido-tetramine type complexes, are separated, generally, as anhydrous salts.

The metaperiodates are slightly soluble in water. Their solubility is influenced by the composition of the complex cation. The ligands with hydrophobic character diminish the solubility of the corresponding periodates.

In this paper we describe 10 new metaperiodates of the $[Co(Diox.H)_2(Am)_2] \cdot IO_4$ etype (Diox.H_2 — dimethylglyoxime, Heptox.H_2 — heptoxime, Am — pyridine bases and tertiary phosphines). The characteristic data of the new products are summarized in Table 1.

Table 1

New metaperiodates of the $[Co(Diox.H)_2(amine)_2]\ IO_4$ type

Formula	Yield (%)	Appearance		Analysis Calcd.	Found
$[Co(DH)_2(pyridine)_2]IO_4$	90	sparkling, brown rhomb. prisms	Co	9.23	9.11
			I	19.88	19.65
$[Co(DH)_4(3,4\text{-lutidine})_2]IO_4$	90	brown prisms	Co	8.49	8.66
			I	18.28	18.01
$[Co(DH)_2(3,5\text{-lutidine})_2]IO_4$	95	brown microcryst.	Co	8.49	8.38
			I	18.28	17.96
$[Co(DH)_2(3\text{-ethyl-pyridine})_2]IO_4$	85	brown prisms	Co	8.49	8.32
			I	18.28	18.11
$[Co(DH)_2(4\text{-ethyl-pyridine})_2]IO_4$	90	brown microcryst.	Co	8.49	8.55
			I	18.28	17.75
$[Co(Heptox.H)_2(pyridine)_2]IO_4$	95	yellow-brown needles	Co	8.20	8.33
			I	17.66	17.33
$[Co(Heptox.H)_2(\beta\text{-picoline})_2]IO_4$	95	yellow-brown needles	Co	7.89	7.65
$[Co(Heptox.H)_2(3,5\text{-lutidine})_2]IO_4$	96	brown microcryst.	Co	7.61	7.49
			I	16.38	16.32
$[Co(Heptox.H)_2(3,4\text{-lutidine})_2]IO_4$	90	short, brown prisms	Co	7.61	7.54
			I	16.38	16.10
$[Co(DH)_2(diethyl\text{-}phenyl\text{-}phosphine)_2] \cdot IO_4$	yellow-brown microcryst.		Co	7.25	7.03
			I	15.62	16.10

DH — deprotonared dimethylglyoxime: $C_4H_7N_2O_2$; Heptox.H — deprotonated heptoxime (1,2-cycloheptanedione dioxime): $C_7H_{11}N_2O_2$

The solubility in water of the metaperiodates obtained, varies between $10^{-4} - 10^{-5}$ *mole/l* at room temperature. Similar values were obtained also for $Ag_2H_3IO_6$, $Tl_2H_3IO_6$, Pb_2HIO_6 and $Hg_5(IO_6)_2$, respectively. Some solubility data determined gravimetrically and iodometrically are presented in Table 2.

Table 2

Solubility of some metal- and metal-amin-periodates in water

Compound	Solubility (*mole/l*)
Pb_2HIO_6	4.38×10^{-5}
$Hg_5(IO_6)_2$	2.87×10^{-5}
$Ag_2H_3IO_6$	1.45×10^{-4}
$[Co(DH)_2(pyridine)_2]IO_4$	1.10×10^{-4}
$[Co(DH)_2(\beta\text{-picoline})_2]IO_4$	1.15×10^{-4}

The cobalt(III)-amine periodates were characterized also by *IR* spectral measurements.

The *IR* spectra show, that the new obtained salts are metaperiodates. The νI—O valence vibrations appear in all cases at 840—860 cm^{-1}, as strong bands, not influenced by the various deformation vibrations of the co-ordinated oxime, amine or phosphine ligands. In the case of other periodates these frequencies are shifted towards lower values: orthoperiodates: ~ 700 cm^{-1}, mezoperiodates: ~ 750 cm^{-1}, dimezoperiodates: 785—790 cm^{-1} [26, 27].

Gravimetric determination of the periodic acids as $Ag_2H_3IO_6$, $Tl_2H_3IO_6$, $Hg_5(IO_6)_2$, Pb_2HIO_6 and $[Co(DH)_2(pyridine)_2]IO_4$.

The aqueous solution of periodic acid was treated with an excess of a soluble silver-, thallium-, lead-, mercury- or other complex salts of the type $Co(DH)_2(amine)_2$acetate (amine = pyridine, β-picoline), at room temperature. The crystalline precipitates formed were filtered off, washed with ice cooled water and dried. The results are presented in Table 3.

The results were statistically evaluated with the known methods [28]. For the linearization of the experimental data the LIN—EXE program written in the Turbo-Pascal language was used. This program is based on the least square method [29]. For the determination of the accuracy of the new gravimetric methods a series of 10—10 determinations were made with identical H_5IO_6 amounts (50—50 *mg*). The mean values and the statistical data were calculated using a MEDIA—EXE—program [30] written also in the Turbo-Pascal language (Table 4).

The accuracy of the gravimetric determinations is approximately the same in all the examined cases. The interference of the other oxoanions of the halogens, following our qualitative observations, seems to be the less in the case of $[Co(DH)_2(amine)_2]IO_4$.

Experimental. Periodic acid (H_5IO_6) was obtained from KIO_4 according to the reactions [31]:

$$2KIO_4 + 4KOH + 3Ba(NO_3)_2 = Ba_3H_4(IO_6)_2 + 6KNO_3$$

$$Ba_3H_4(IO_6)_2 + 6HNO_3 = 2H_5IO_6 + 3Ba(NO_3)_2$$

Table 3

Gravimetric determination of the periodic acid

m (IO_4^-) *g* sample weighed for all determin. forms	0.0150	0.0300	0.0500	0.0750	0.1000
Determination form: $Ag_2H_3IO_6$					
m (IO_4^-) *g* calculated	0.0149	0.0301	0.0498	0.0747	0.09998
s_{xy}	2.7476E−03				
Γ_{xy}	0.99998				
Equation of the straight line: Y = −0.0000051 + 1.9349 * X					
Determination form: $Tl_2H_3IO_6$					
m (IO_4^-) *g* calculated	0.0148	0.0295	0.0500	0.0751	0.1001
s_{xy}	3.2522E−03				
Γ_{xy}	0.99998				
Equation of the straight line: Y = −0.00052 + 2.2903 * X					
Determination form: $Hg_5(IO_6)_2$					
m (IO_4^-) *g* calculated	0.0149	0.0300	0.0498	0.0748	0.09999
s_{xy}	3.1836E−03				
Γ_{xy}	0.99999				
Equation of the straight line: Y = −0.000044 + 2.2419 * X					
Determination form: Pb_2HIO_6					
m (IO_4^-) *g* calculated	0.0148	0.0300	0.0500	0.0749	0.1000
s_{xy}	3.2626E−03				
Γ_{xy}	0.99999				
Equation of the straight line: Y = −0.000154 + 2.2976 * X					
Determination form: $[Co(DH)_2(py)_2]IO_4$					
m (IO_4^-) *g* calculated	0.0149	0.0297	0.0501	0.0749	0.1001
s_{xy}	4.6921E−03				
Γ_{xy}	0.99999				
Equation of the straight line: Y = −0.00046 + 3.3042 * X					

Table 4

Statistical dates on the accuracy of the gravimetric determinations

Determination form	m (IO_4^-) *g* weighed	m (IO_4^-) *g* calculated	$\bar{X}$	$s_{\bar{x}}$	$\bar{X}_{P(95\%)}$
$Hg_5(IO_6)_2$	0.0500	0.0499 0.0498 0.0497 0.0498 0.0498 0.0498 0.0497 0.0497 0.0499 0.0498	4.979E−2	2.33E−5	4.979E−2 ± 5.3E−5
$Ag_2H_3IO_6$	0.0500	0.0499 0.0498 0.0501 0.0498 0.0499 0.0500 0.0499 0.0500 0.0498 0.0499	4.991E−2	3.14E−5	4.991E−2 ± 7.1E−5
Pb_2HIO_6	0.0500	0.0501 0.0500 0.0500 0.0499 0.0501 0.0500 0.0500 0.0499 0.0500 0.0500	5.000E−2	2.11E−5	5.00E−2 ± 4.8E−5

$\bar{x}$ = average; $s_{\bar{x}}$ = standard dev. of mean; P = con idence limits. t (Student distribution) = 2.26

[Co(Diox.H)$_2$(amine)$_2$]IO_4 · 10 *mmoles* of [Co(Diox.H)$_2$(amine)$_2$] acetate [32] in 100 *ml* water were treated with 11–12 *mmoles* of H_5IO_6 in 50 *ml* aqueous solution. The crystalline products formed were filtered off after 15–30 *min.* standing, washed with water and dreid on air.

Analysis. Cobalt was determined complexometrically and the IO_4 content iodometrically in the usual way.

Solubility determinations. I. *Method.* 100–200 *ml* saturated aqueous solution of $Ag_2H_3IO_6$, $Tl_2H_3IO_6$, Pb_2HIO_6, $Hg_5(IO_6)_2$, [Co(DH)$_2$(pyridine)$_2$]IO_4, [Co(DH)$_2$(β-picoline)$_2$]IO_4 etc. were evaporated to dryness in a crucible and dried at 120 °*C* during 2 hours. The solubility was calculated from the net weight.

II. *Method.* 100 *ml* saturated aqueous solution of the corresponding periodate were treated with 10 *ml* 10% KI and 25 *ml* 10% HCl and the eliberated iodine titrated whit 0.01 *n* $Na_2S_2O_3$ on the usual way.

The IR spectra were recorded in KBr pellets with an UR 20 spectrophotometer (Carl Zeiss Jena, Germany).

Gravimetric determination of the periodic acid (General procedure): 15—100 *mg* of periodic acid in 50 *ml* aqueous solution were treated with an excess of 0.1 *n* $AgNO_3$, Tl(acetate), $Pb(acetate)_2$, $Hg(NO_3)_2$ or 2% $[Co(DH)_2(amine)_2]$acetate, respectively. After about 30 *min.* standing the precipitates formed were filtered off on a G_4 glass porous crucible, washed with 3×5 *ml* ice cooled water and dried at 110—120 °C during 2 hours.

REFERENCES

1. P. Souchay, A. Hessaby, Bul. soc. chim. France, **1953**, 589, 614.
2. J. Crouthamel, A. Meek, D. Martin, J. Amer. Chem. Soc., **71**, 3031 (1949); **73**, 82 (1951).
3. C. Rammelsberg, Pogg. Ann. Chem., **134**, 372 (1868); **137**, 309 (1869).
4. N. I. Lobanov, Zhur. neorg. Khim., **5**, 565 (1960); **6**, 830 (1961); **7**, 48 (1962); **8**, 1112 (1963).
5. L. Szekeres, Magyar Kém. Folyóirat, **63**, 273 (1957).
6. L. Maros, J. Molnár—Perl, E. Schulek, Acta chim. Acad. Sci. Hung., **26**, 475 (1969); **27**, 367 (1961).
7. P. Fleury, J. Lange, J. Pharm. Chim., **17**, 107 (1933).
8. S. Hara, Analyst, **5**, 163 (1956).
9. L. Szekeres, Annal. Chim. (Roma), **51**, 200 (1961).
10. P. Norkus, J. Jankauskas, Zhur. analit. Khim., **27**, 2421 (1972).
11. C. D. Neniţescu: Chimie organică, Vol. I. p. 459, Ed. Didactică şi Pedagogică, Bucureşti, 1980.
12. A. Berka, J. Zyka, Ceskosl. Farm., **8**, 136 (1959).
13. A. K. Hareez, W. A. Bashir, Mikrochem. J., **31**, 375 (1985).
14. M. Callejon Mochon, J. A. Munoz Leyva, Analyst, **109**, 951 (1984).
15. J. J. Berzas Nevado, P. Valiente Gonzales, Analyst, **114**, 243 (1989).
16. K. H. Verma, D. Gupta, S. K. Saughi, A. Jain, Analyst, **112**, 1519 (1987).
17. R. Ripan, Cs. Várhelyi, Acad. RPR, Studii şi Cercetări Chim. Fil. Cluj, **10**, (1), 43 (1959).
18. R. Ripan, Cs. Várhelyi, Acad. RPR, Studii şi Cercetări Chim. Fil. Cluj. 10, (1), 51 (1959).
19. Cs. Várhelyi, E. Kékedy, A. Götz, Acad. RPR. Studii şi Cercetări Chim. Fil. Cluj, **10**, 251 (1959).
20. I. Soos, Cs. Várhelyi, E. Stoicovici, Acad. RPR, Studii şi Cercetări Chim. Fil. Cluj, **11**, (2), 249 (1960).
21. Cs. Várhelyi, M. Kézsmárky, E. Borovszki, Studia Univ. Babeş—Bolyai, Chem., **4**, 47 (1959).
22. I. Soós, Cs. Várhelyi, J. Treiber, Studia Univ. Babeş—Bolyai, Chem., **5**, 88 (1960).
23. I. Soós, Cs. Várhelyi, Studia Univ. Babeş Bolyai, Chem., **5**, 95 (1960).
24. R. Ripan, I. Soós, Cs. Várhelyi, Studia Univ. Babeş—Bolyai, Chem., **6**, 53 (1961).
25. Cs. Várhelyi, J. Horvát, J. Treiber, E. Hamburg, Studia Univ. Babeş—Bolyai, Chem., **12**, (1), 23 (1967).
26. H. Siebert, Z. anorg. allg. Chem., **303**, 162 (1960); **304**, 266 (1960).
27. P. Natalis, Ann. soc. sci. Bruxelles, Ser. I., **73**, 261 (1959).
28. D. Ceauşescu: *Utilizarea statisticii matematice în chimia analitică*. Ed. Tehnică, Bucureşti, 1982, p. 205.
29. L. Ács: *Turbo Pascal kezdőknek*, Novotrade Kiadó, Budapest, 1990.
30. J. Pirkó: *Turbo Pascal* 5.5. *LSI* Oktatóközpont, Budapest, 1990.
31. H. A. Willard: *Inorganic Syntheses*, Vol. I. New York, London, 1939. p. 171.
32. Cs. Várhelyi, S. Kövendi, J. prakt. Chem. **4**, **34**, 209 (1966).

STUDIA UNIV. BABEŞ-BOLYAI, CHEMIA, XXXVII, 1—2, 1992

CATIONIC TENSIDES BASED ON ALIPHATIC ACIDS AND ALIPHATIC DIAMINES

ION ILIUȚĂ*, LAURENȚIU LAZĂR*, MARIAN BULEARCĂ*

Received: 20.10.1992

ABSTRACT. The present work deals with the synthesis of several cationic tensides (quaternary ammonium salts) starting from aliphatic acids, ethylenediamine, acrylonitrile, acrylamide and the corresponding agents to obtaine the quaternary salts. The reaction parameters for the synthesis of amidoamines and tertiary amines are discussed; the quaternary ammonium salts have been tested as corrosion for steel, in hydrochloric and sulphuric acid solutions. All the compounds have been proved to be efficient as corrosion inhibitories (their efficacity being 48—89%).

Cationic tensides, due to their specific properties, are of practical use in various fields such as corrosion inhibitories, flotation agents for clays, additives for cationic emulsions containing bithums etc. The great majority of cationic tensides consists of long chain aliphatic and naphtenic amines, or their derivatives, mainly the quaternary ammonium salts.

The classical path in obtaining long chain aliphatic amines is that starting from aliphatic acids, which react with ammonia in order to obtain nitriles, followed by hydrogenation, resulting in aliphatic amines; in turn, these amines can be alkylated forming secondary and tertiary amines, or even quaternary ammonium salts. This process presents the disadvantage of using high temperatures (300—320 °C) for nitrile syntheses, as well as relative difficulties in operating specific reactors.

In the present work, we report on different ways to obtain cationic tensides, avoiding the above-mentioned difficulties. Thus, staring from long chain aliphatic acids and ethylene diamine, the following reactions have been carried out:

1. The synthesis of amido-amine:

$$R_1-COOH + H_2N-CH_2-CH_2-NH_2 \rightleftarrows R_1-CO-NH-CH_2-CH_2-NH_2 + H_2O$$

2. Alkylation of amido-amine in order to obtain a tertiary amine:

a) with acrylonitrile:

$$R_1-CO-NH-CH_2CH_2NH_2 + 2CH_2=CH-CN \rightleftarrows$$

$$\rightleftarrows R_1CO-NH-CH_2CH_2N\begin{matrix}\diagup CH_2CH_2CN\\ \diagdown CH_2CH_2CN\end{matrix}$$

* *Polytechnical Institute of Bucharest, Calea Victoriei 149, Romania*

b) with acrylamide (AA):

$$R_1CO-NH-CH_2CH_2NH_2 + 2CH_2=CHCONH_2 \rightleftarrows$$

$$\rightleftarrows R_1CONHCH_2CH_2N(CH_2CONH_2)_2$$

3. Quaternization of tertiary amine using the corresponding agent:

$$R_1CONHCH_2CH_2N(R_2)_2 + R_3Cl \rightleftarrows \left[R_1CONHCH_2CH_2-N(R_2)(R_2)(R_3)\right]^+ Cl^-$$

As quaternization agents, monochloracetic acid (ClAc), benzyl chloride (BzCl) and dichloretane (DCE) respectively, have been used. In this way, a number of six quaternary ammonium salts have been obtained, according to the scheme given below:

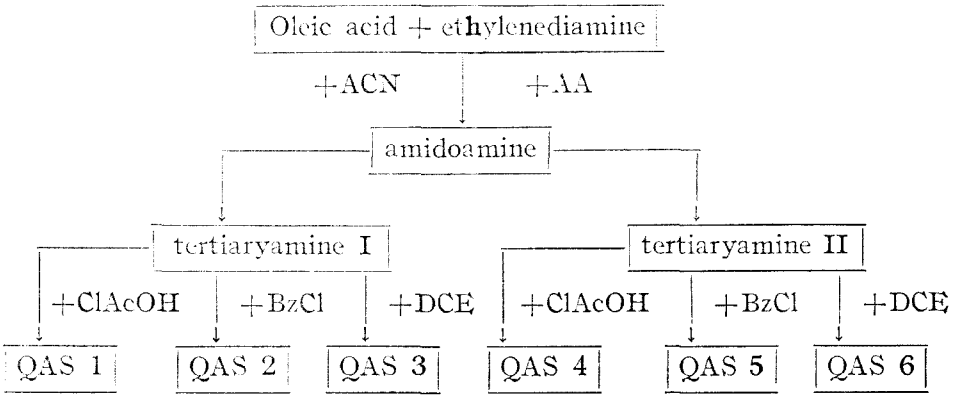

Thus, the general formula for the synthesized quaternary salts is:

$$\left[R_1CONHCH_2CH_2-N(R_2)(R_2)(R_3)\right]^+ X^-, \text{ where } R_1 = C_{11}H_{33};\ R_2 = CH_2-CH_2-CN$$

or $CH_2-CH_2-CONH_2$; $R_3 = CH_2-COOH$, C_6H_5 or CH_3-CH_2Cl; $X = Cl$

We have studied the influence of the molar ratio of reactants on reaction selectivity, as well as the time dependence in all reaction steps.

The synthesis of amino-amine takes place in a round bottom flask equipped with thermometer, stirring and heating systems: an ASTM device allowed water removal from the reaction medium, as azeothrope (with xylene). After introducing the reactants as well as the solvent (xylene), we have started the stirring and heating systems. The first vapour amounts have appeared around 110 *C*; after condensation, they have been collected in the ASTM

device. The bottom layer consists of a mixture of water-ethylene diamine (totally miscible), while the upper layer contains xylene (refluxed in the flask). The reaction kinetics was put in evidence in an indirect way, by measuring the volume of the homogeneous mixture water-ethylene diamine. During the reaction process, the temperature has been gradually risen up to 230—240 *C*. After an appropriate time, considering the solvent, as well as the excess of ethyl diamine (obviously without refluxing). Then the reaction mass has been washed by an alkalyne solution, which, in turn, removes the unreacted acid (as water-soluble salt); finally, the volatile fractions are distiled under vacuum. In this way, the reaction product remains in the flask and can be analysed.

When synthesizing the amido-amine in order to obtain the monoamide, the reactants' molar ratio must be favourable with regard to diamine. Carrying out experiments at different molar ratios, we have found as the most favourable situation the ratio ethylene diamine/oleic acid = 1.2/1 (this value has been established by analysing the content of diamine in the final mixture (see Fig. 1).

Accordingly, during the next tests, we have used the above-mentioned molar ratio. In Fig. 2 we present the evolution of conversion versus time; one can see that after 240 *min.* the maximum conversion (95—96%) has been reached.

The second step, namely the obtaining of tertiary amine, takes place in a polar solvent, preferably isopropanol, at 75—90 *C*, under vigouros stirring; acrylonitrile is added gradually, finally a certain time is provided in order to get a high conversion. A small excess of acrylonitril (5—10%) is needed; this unreacted excess is subsequently removed by distillation. We have found that the condensation reaction of amine takes place with a somewhat slower rate than the first step, a conversion of approx. 84% being reached after 7—8 hours.

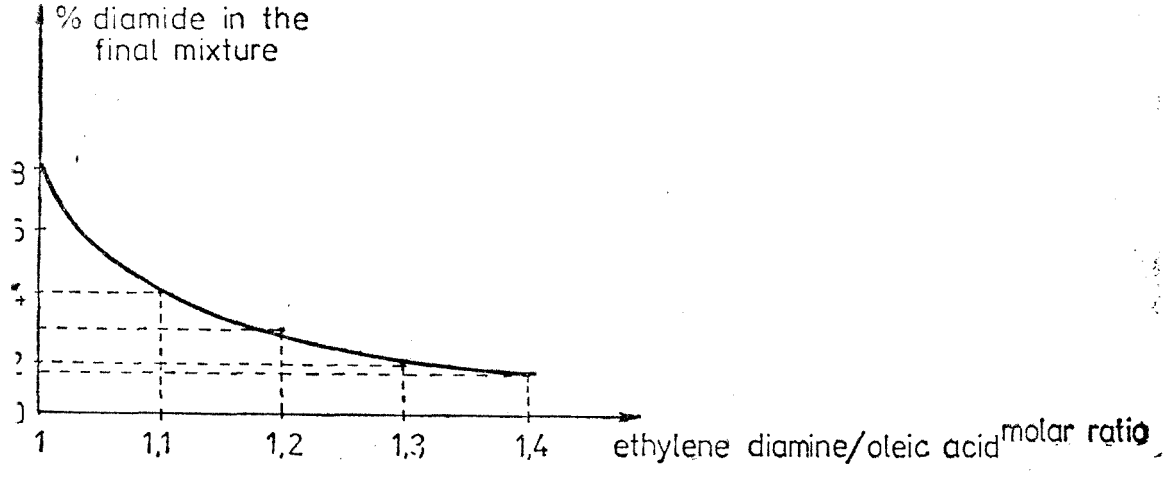

Fig. 1. — The influence of reactants molar ratio on the composition of reaction products.

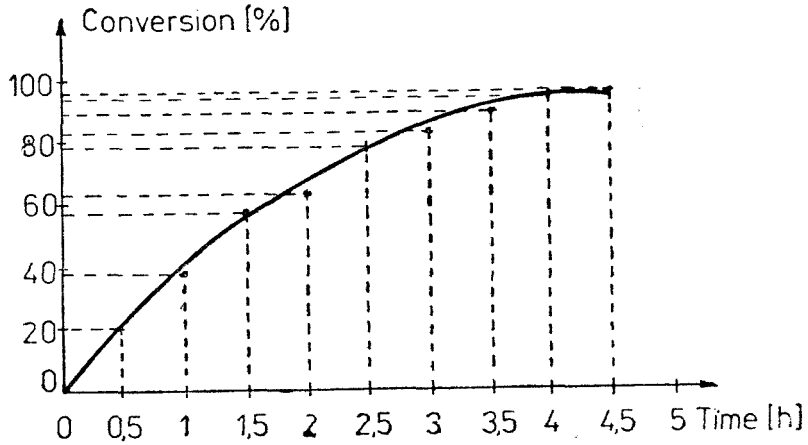

Fig. 2. — The evolution of conversion as a function of time for amido-amine synthesis.

When synthesizing the tertiary amine using acrylamide, a polymerization inhibitory (preferably hydroquinone or phenothiazine) is, obviously, needed. The procedure is similar to that used in the condensation with acrylonitrile; nevertheless, the maximum conversion is somehow higher (approx. 88%).

The last step, quaternization, is carried out also by refluxing in a polar solvent (isopropanol) with a molar ratio tertiary amine/quaternization agent = = 1/1.5, during 12—14 hours, thus obtaining a conversion between 75 and 85%.

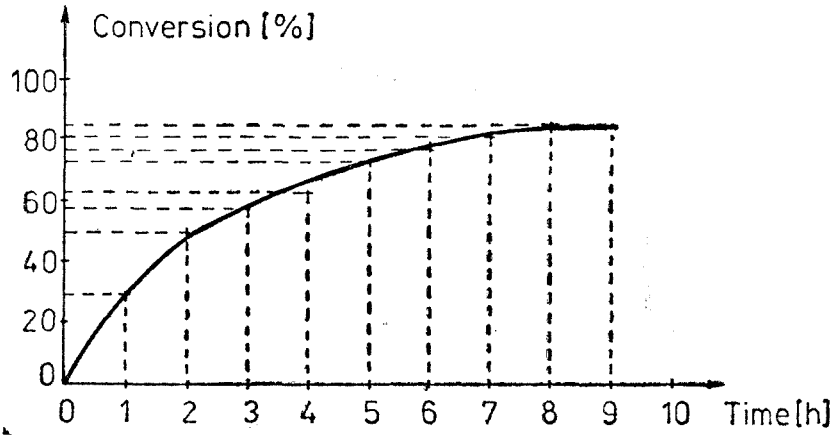

Fig. 3. — The evolution of conversion as a function of time for the synthesis of tertiary amine with acrylonitrile.

The synthesized products have been submitted to various physico-chemical analyses (IR, NMR); they have proved the proposed structure. The products are paste-like, coloured in various brown shades, soluble in alcohols (the solubility in isopropanol is, for instance 25%), in acetone (up to 1%) and less water soluble (under 0.1%).

The resulted quaternary ammonium salts have been tested as corrosion inhibitories for steel, in aqueous media containing mineral acids (HCl or H_2SO_4), at room temperature as well as at higher temperature (60 C). The degree of corrosion has been estimated by gravimetric measurements. The obtained results have an orientating value. It has been shown that the new products present a strong inhibition effect; at very low concentrations (20—60 *ppm*) in corrosive media they provide a very effective protection (up to 85% at room temperature and up to 67% at higher temperature). These results are presented in Tables 1 and 2.

Table 1

The results of corrosion tests in HCl sol. (15%)

Product	Inhibitor concentration [ppm]	Corosion rate [mm/year] at 20 C without inh.	with inh.	Efficiency [%]	Corosion rate [mm/year] at 60 C without inh.	with inh.	Efficiency [%]
1	20	7.22	2.7	62.6	135	70.03	48.1
	40	7.22	2.47	65.8	135	62.77	53.5
	60	7.22	2.09	71.0	135	54.27	59.8
2	20	7.22	2.6	64.1	135	68.44	49.3
	40	7.22	2.42	66.4	135	67.36	50.1
	60	7.22	2.5	65.3	135	66.55	50.7
3	20	7.22	3.1	57.3	135	65.07	51.8
	40	7.22	2.71	62.1	135	61.83	54.2
	60	7.22	2.67	63.0	135	60.75	55.0
4	20	7.22	3.05	58.2	135	77.2	43.2
	40	7.22	2.74	61.8	135	71.5	47.5
	60	7.22	1.98	73.5	135	66.8	50.3
5	20	7.22	3.5	51.4	135	82.0	38.9
	40	7.22	3.06	58.0	135	79.2	41.5
	60	7.22	2.46	76.4	135	55.0	58.9
6	20	7.22	2.90	60.3	135	65.2	51.3
	40	7.22	2.52	65.2	135	58.3	57.1
	60	7.22	1.58	78.3	135	50.5	62.3

Table 2

The results of corrosion tests in H_2SO_4 sol. (15%)

Product	Inhibitor concentration [ppm]	Corosion rate [mm/year] at 20 C without inh.	with inh.	Efficiency [%]	Corrosion rate [mm/year] at 60 °C without inh.	with inh.	Efficiency [%]
1	20	1.37	0.450	67.1	88.3	35.4	59.9
	40	1.37	0.304	77.8	88.3	33.5	62.0
	60	1.37	0.223	83.7	88.3	30.1	65.9
2	20	1.37	0.225	83.5	88.3	29.2	66.9
	40	1.37	0.267	86.5	88.3	28.5	67.7
	60	1.37	0.220	83.9	88.3	28.1	68.2
3	20	1.37	0.371	72.9	88.3	34.5	60.9
	40	1.37	0.263	80.8	88.3	32.2	63.5
	60	1.37	0.258	81.2	88.3	32.9	62.7
4	20	1.37	0.470	65.3	88.3	38.6	58.3
	40	1.37	0.391	71.4	88.3	33.6	61.8
	60	1.37	0.232	82.9	88.3	29.6	66.4
5	20	1.37	0.562	58.9	88.3	43.0	51.3
	40	1.37	0.413	70.3	88.3	31.4	64.6
	60	1.37	0.211	84.8	88.3	27.8	68.5
6	20	1.37	0.392	71.5	88.3	38.2	58.0
	40	1.37	0.304	78.0	88.3	40.2	64.5
	60	1.37	0.202	85.3	88.3	27.0	69.3

A better characterization for the newly synthesized products will be continued by electrochemical measurements.

Conclusions.

1. Six new quaternary ammonium salts, unknown in the literature, have been synthesized;
2. The products have been characterized;
3. The synthesized products act as effective corrosion inhibitories.

REFERENCES

1. Rosenfeld, I. L., *Atmospheric corrosion of metals*, nat. ASS Corrosion, Houston, Texas, 1972, p. 57.
2. Crețu, S., Iliuța, I Avram, R., Crîngus, E., Rev. Chim. (Bucharest) 36(5), 435, (1985)
3. Frank, C., J. Amer. Chem. Soc., 66, 725, (1974)
4. Romania Patent 8556/1984.
5. U.S.A. Patent 4420414/1983.
6. U.S.A. Patent 3893935/1975.
7. Romania Patent 82359/1983.

STUDIA UNIV. BABEŞ-BOLYAI, CHEMIA, XXXVII, 1—2, 1992

ELECTRON BEAM EVAPORATION — A SUITABLE METHOD TO OBTAIN MAGNETIC RECORDING MEDIA

ANCA D. SILVESTRU*

Received: 20.11.1992

ABSTRACT. Thin magnetic films may possess longitudinal or vertical magnetic properties. From the first class, the most used material is the CoNi alloy (80/20), and from the second one the CoCr alloy. A very suitable method to obtain a tape as registering media is the vacuum deposition of the mentioned material, using an electron beam equipment.

During the experiments, the process was driven at a pressure of about 10^{-5} *torr*, with an acceleration rate of the electrons of 6/10 *KV*, at a current intensity of 0.1 — 1.0 *A*. There were obtained various deposition rates, according to the process parameters and the source that is used. The obtained films are of homogeneous structure, adherente to the targets and of a good purity.

There is made a study upon the deposition conditions and their influence for the magnetic properties of the film. There are investigated: rate of deposition, substrate temperature, incidence angle of deposition, composition and thickness of the film, the most suitable substrate and intermediar layer, in order to obtain a film with good magnetic properties useful as registering media. There are analysed the possibilities to protect the magnetic film either against corrosion or friction.

1. **Introduction.** The electron beam evaporation method is based upon the principle of bombarding the evaporating material with an energetic electron beam produced by an electron beam gun. When the energetic electrons meet the evaporating material, their cinetic energy is changed into termic energy, that determins the heating of the material untill it melts and, moreover, it boils and goes into vapors. The vapors possess sufficient cinetic energy for noving as a divergent beam to the target on which we want to deposit the material by condensation.

The electron beam gun equipment allowes the evaporation of a large scale of materials and a good deposition of thin, adherente layers on different supports.

As evaporation sources, there were used different metals and alloys (Cu, Al, Ti, Ni, CrNi, CoNi) which were deposited on polyesteric and polyamidic folie.

The process was driven at a pressure of 6×10^{-5} *torr*, and an acceleration voltage of 10/15 KV. The obtained films were of homogeneous structure, adherente to the support and of a good purity.

2. **CoCr films.** The CoCr films are still used on a large scale because of their good magnetic properties, high registering density and, not on the last time, because of the better characteristics offered by a perpendicular registering medium in comparison with a longitudinal one. [3]

* *Babeş-Bolyai University, Dept. of Chemistry, RO 3400 Cluj-Napoca, ROMANIA*

CoCr films can be obtained either by vacuum evaporation or by sputtering. In the first case, using an electron beam gun equipment, in order to obtain good magnetic properties ($H_c > 500\ Oe$), the target had to be heated to 250 °C. [4]

The process was realised in an evaporation equipment with two electrons beam guns. The deposition was made onto a polyimidic folio having a thickness of 15—20 μm. Between the support and the magnreic film it was deposited a titanium layer of 0,03 μm. The CoCr film was of a 0,25 μm thickness. The target's temperature was increased from 70° C to 300° C and, according with this increasing, there were obtained H_c values of about 200 Oe at 70° C and 900 Oe at 300°C [5].

The quality of the registering realized with such kind of tapes is determined by:

— the perpendicular anizotrop field (H_{keff}); — the coercive force H_c; — the saturation magnetization M_s; — the thickness of the deposited film.

a) *The perpendicular anizotrop field* In Fig. 1 is presented the characteristic curve of the registering density. H_{keff}, $H_{c\perp}$, $H_{c//}$, M_s and the thickness of the film were about: 2,2 KOe, 500 Oe, 330 Oe, 570 emu/cc and, respectiv, 0,23 μm.

It can be seen that the reproduced voltage is much greater at 100*kFRPI* than at 10 *kFRPI* and it lowers very rapidely upon 150 *kFRPI*. This is a characteristic behaviour for the perpendicular media and can not be find to the longitudinal ones.; it is determined by the reduced demagnetization field at high liniar density [6].

b) *The coercive force* Fig. 2 showes the $H_{c\perp}$ dependence of reproduced voltage at 10 *kFRPI* and at 100 *kFRPI*. It is obviously that the recording density is not limited by the coercive force for the perpendicular registering media [7, 8].

c) *The saturation magnetization*, As we can see from Fig. 3, at high values of M_s, the reproduced voltage decreases, may be because of the changes

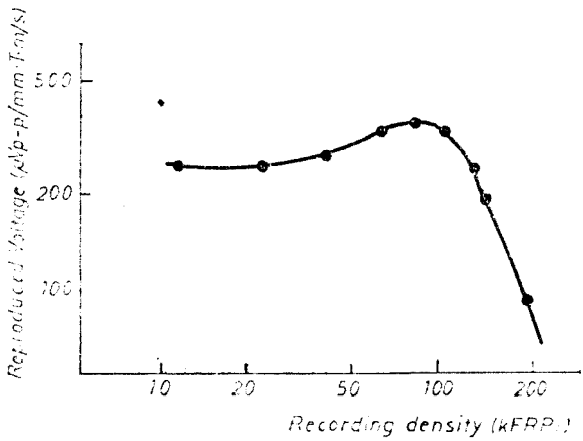

Fig. 1. Recording density characteristics

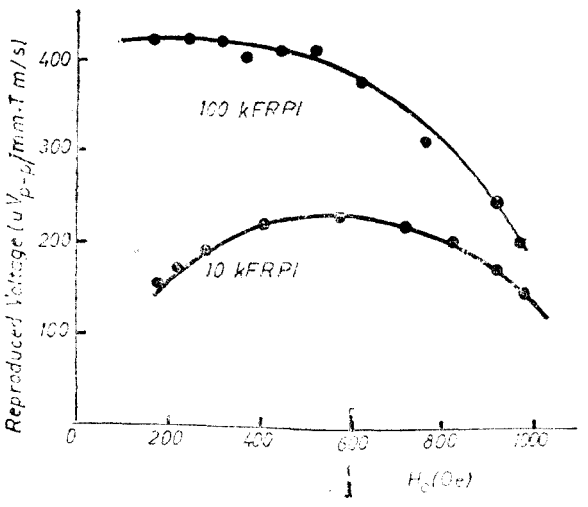

Fig. 2. Dependence of reproduced voltage on H_c

that occure into the perpendicular anizotropic properties. For a CoCr film with a thickness of 0,2—0,23 μm the, reproduced voltage has a maximum around the value of 500 *emu/cc* [9,10].

d) *The CoCr film thickness.* From fig. 4 it appears obviously that the reproduced voltage arises with the thickness if the film till around the value of 0,2 μm. Upon this value it remains the same [11].

The magnetic properties of the CoCr films can be improved by a termic treatment in air at 400 °C. The cromium is preferentially oxidized and is converted into Cr_2O_3 which has antiferomagnetic properties [12].

3. **CoNi films.** Acording with its good magnetic properties that allowed to obtain great recording densities, the CoNi alloy (80/20) is a suitable mate-

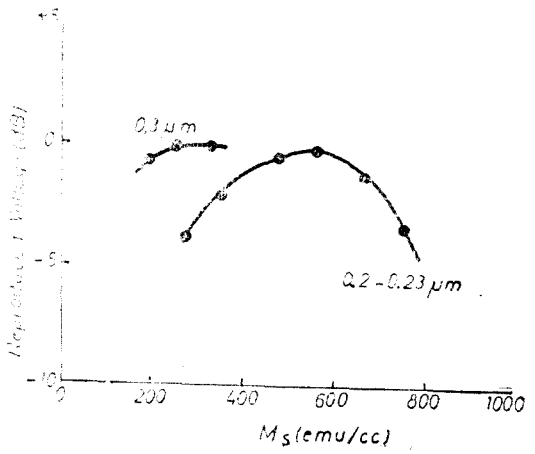

Fig. 3. Dependence of reproduced voltage on M_s

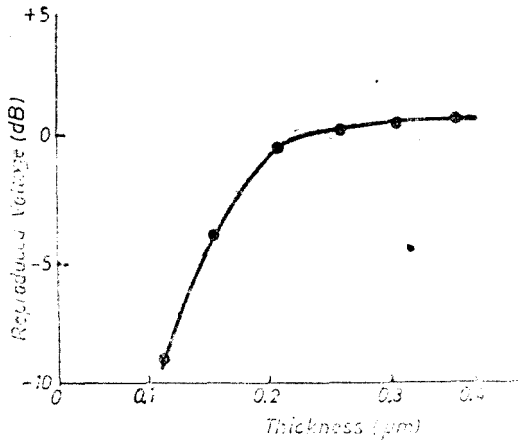

Fig. 4. Dependence of reproduced voltage on thickness

rial for recording media. This material is considered to be a medium with longitudinal magnetization, altough the films possess the perpendicular component too and they behave as multicomponent media [13].

In order to obtain good magnetic properties and, related to these, a good recording density, it has to be used an oblique incidence technique of deposition. The deposition may be at fix angle of incidence or at a continue varying incidence angle.

At incidence angles less than, 60°, the structure of the films is different from that of films obtained at incidence angles greater than 60°. This fact determines important changes in the magnetic properties of the deposited film [14].

The increase of the recording density is supposed to be due to the perpendicular magnetic properties that appear near the main longitudinal properties, when the process takes place at incidence angles greater than 60°.

The magnetic properties of the layer are dependent on the target temperature, rate of deposition, the layer deposited between the support and the magnetic film and on the composition and thickness of the film [15].

Co and Ni having vapours pressure nearly the same, the deposited film will keep, in a good aproximation, the same composition whith the source.

4. The influence of the deposition-conditions on the magnetic properties and the structure of the film. The properties of the magnetic film deposited on the tape are influenced either by the parameters at which the process takes place, or by the quality of the evaporation source. The deposition rate, support temperature, incidence angle composition and thickness of the film determine, by their variation, changes into the magnetic and structural properties of the film.

a) *Rate of deposition.* The coercivity of the deposited films is strong dependently on the deposition rate. H_c increases while the deposition rate is diminished and the temperature of the target arises. As it can be seen from Fig. 5, a notable increase of the H_c value takes place on a narrow domain of

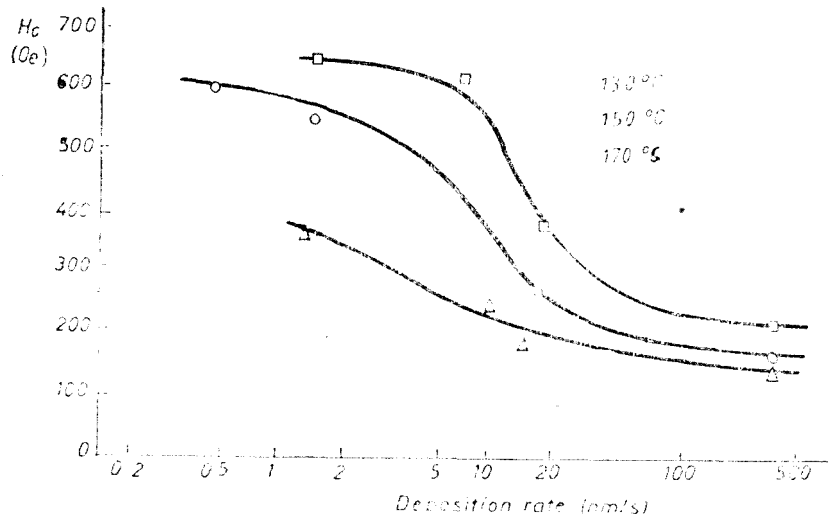

Fig. 5. Deposition rate dependence of H_c

lowering of the rate of deposition, for a given target's temperature. With the increase of the temperature, the notable increase of the H value takes place at greater evaporation rates. There is possible to obtain films with high H values at low temperature of the targets and using small evaporation rates. [16]

b) *The substrage temperature.* Figure 6 presents the dependence of the coercivity on the substrate temperature for CoCr films deposited at (a) 400 *nm/s* and (b) 2 *nm/s*. At the same temperature, a smaller rate of deposition generates films with higher coercivity [17]

c) *The incidence angle.* The structure of the CoNi films and their magnetic properties are strongly influenced by the values of the incidence angle [14].

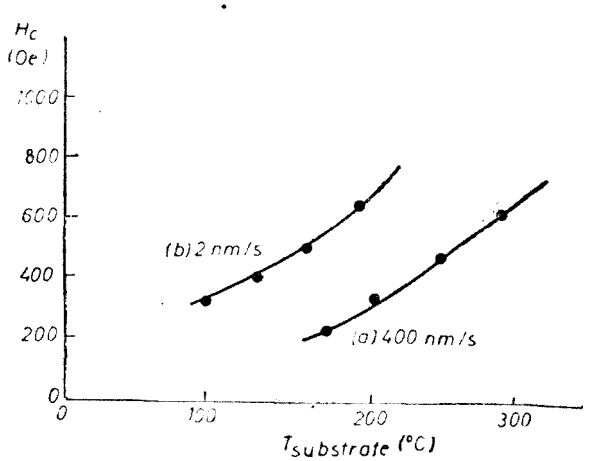

Fig. 6. Substrate temperature dependence of H_c for a deposition rate of (a) 400 *nm/s* and (b) 2 *nm/s*.

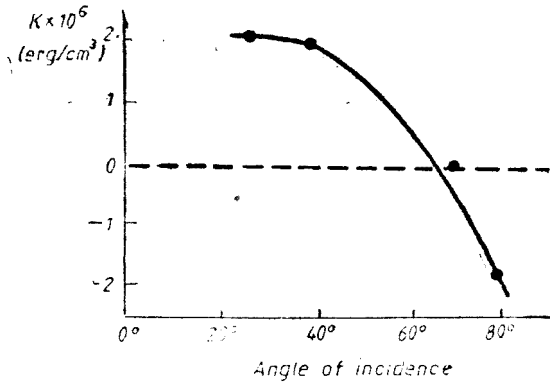

Fig. 7. Anisotropy constant K as a function of incidence angle

c) *The incidence angle.* The structure of the CoNi films and their magnetic properties are strongly influenced by the value of the incidence angle [14].

As it can be seen from Fig. 7, around the value of 60° is a change of sign for the anizotropy constant K. For values greater than zero, the anizotropy axis is perpendicular on the vapors plane and for negative values of K it is parallel with this plane.

Around the value of 60° of the incidence angle takes place a change in the structure of the film; for incidence angles less than 60°, the deposited criystals are of a platelike structure, while at incidence angles greater than 60° the crystals are of a rodlike structure. This change in the structure of the film determins variations of the anisotropy and, related to this, variations of the coercivity.

The CoNi films deposited at angles of incidence greater than 60° present, near the main longitudinal magnetic properties, also enough strong vertical magnetic properties, that improve their recording characteristics.

d) *Composition and thickness of the film.* For CoNi films, the magnetic properties increase while the tickness of the film decreases. Good magnetic and recording properties are obtained when is used a CoNi alloy with 20% Ni [18].

e) *The oxygen content.* The presence of oxygen in the CoNi films deposited by evaporation influenced strongly the structure and the magnetic properties of the film. The films deposited in the presence of oxigen present a columnar structure, the size of the crystalites being dependent on the oxygen content. Without oxygen the film has a desordered structure, with long crystals [19].

f) *The intermediar layer.* To improve the aderence of the magnetic film on the polyestheric or polyimidic substrat, it is useful to deposit a thin intermediar layer of a nonmagnetic material (Al, Ti, Ri, etc.). This intermediar layer influences very strongly the structure of the magnetic film [20, 21].

The magnetic properties of a CoCr film deposited on a polyimidic support with and without an intermediar layer of titanium are presented in Figures 8 and 9.

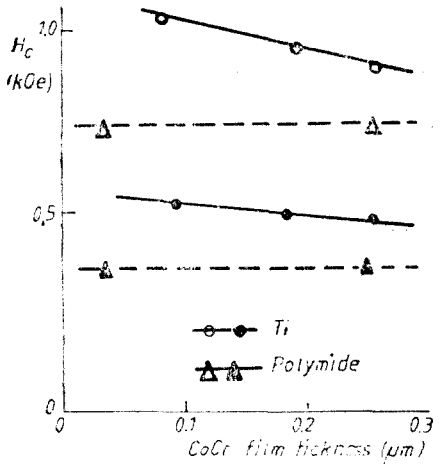

Fig. 8. Perpendicular magnetic properties of CoCr films deposited on Ti underlayers and on a substrate without any underlayer.

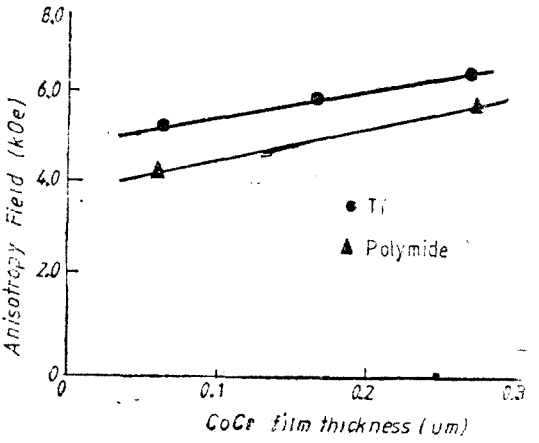

Fig. 9. Anisotropy field of CoCr films

The increase of the values of H_c and H_K (the anisotropy field) is obvious in the presence of the Ti underlayer [22—24].

The intermediar layer influences more the form of the crystals and only a little their orientation. The intermediar layer has a notable influence at any thickness of the magnetic field.

5. *Mechanic properties and corrosion prevention.* The thin metalic films, used as recording media, envolv two problems to be solved: — the resistence to friction — corrosion prevention.

To solve these two problems, is very useful to deposit a protective coat upon the magnetic film. Silicon and carbon are very suitable materials for this purpose.

The durability of a tape is determined by the magnetic head material or by the system "Magnetic head + protective coat". The protective coat must be chosen so, that, together with the magnetic head material to offer the optimum solution for maximum durability of the magnetic layer [25].

Fig. 10 shows the dependence of the durability for a CoCr film on the thickness of a silicon layer. The durability of about 10^3 times when a 20 *nm* silicon layer is deposited.

The DLC films are the most suitable to improve the durability of the magnetic

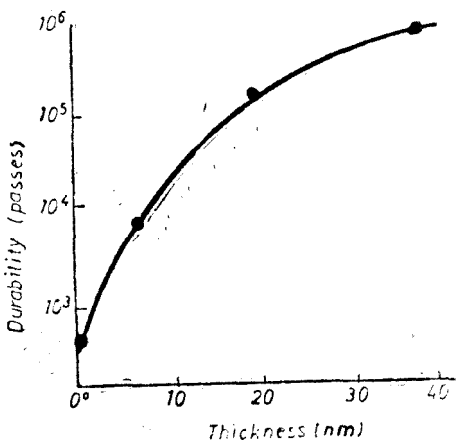

Fig. 10. Durability dependence on protective layer (Si) thickness. Slider: Mn - Zn ferrite

layers; they are characterized by a low coefficient of friction and a good chemical stability. Their structure is a proper one, different either from that of graphite or diamond, containing a small amount of hidrogen.

In table no 1. are presented the properties ef a DLC film in comparison with other inorganoc protective films [26].

Table 1

Coefficient of friction and Knoop hardness

Film	Knoop hardness (Kg/mm²)	Coef. of friction	
Si_x	1200	1 pass	0.16
	1200	1 pass	0.16
		10 pass	0.22
Al_y	1000	1 pass	0.12
		10 pass	0.12
Si_z	3000	1 pass	0.16
		10 pass	0.50
DLC	2800	1 pass	0.08
		10 pass	0.08

The high hardness and the low coefficient of friction make the DLC films very suitable for protective layer of magnetic recording media.

Fig. 11 shows the results of a friction test for a tape with CoNi magnetic film, without protective coat and with DLC coat [26].

The tape with 100 Å DLC film presents no degradation of the output level after 100 hours of activity (friction), while the tape without protective coat presents a fall after 2 hours.

The magnetic head shows no scratches after passing on a DLC layer; the magnetic head which passed on a tape without protective coat, presents scratches and adhesions of metallic powder of the magnetic layer.

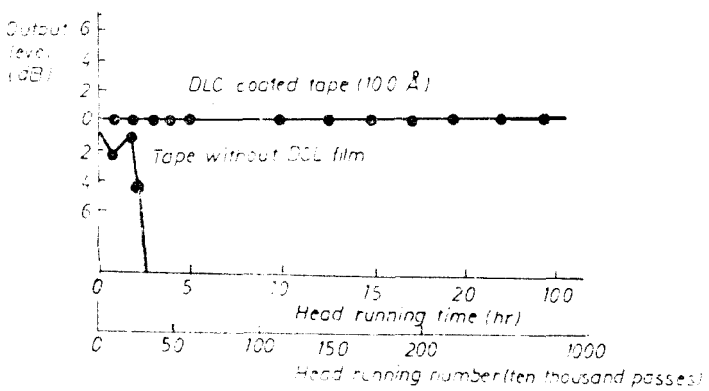

Fig. 11. Still durability on rotary-head tester

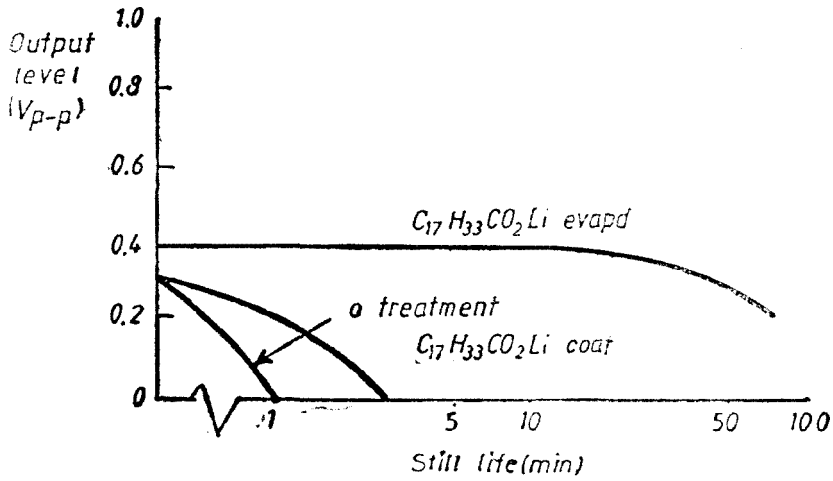

Fig. 12. Still life of films coated with $C_{17}H_{33}CO_2Li$

The amorf carbon (graphite) can also be used to improve the durability The carbon layer gives a resistence to corrosion to the magnetic film too. It protects the tape againts corrosive media (SO_2, O_2. Cl^-. umidity) [27].

The durability of the magnetic layer can also be improved by the deposition of a lubrifiant coat (greasy acids or their salts). The deposition of a lubrifiant coat (greasy acids or their salts). The deposition can be realîsed either by a chemical method or by vacuum evaporation. The second one gives continuous adherente films that ptotect against friction either the tape or the magnetic head.

Fig. 12 shows he behaviour of a magnetic tape with a protectivé layer of $C_{17}H_{33}CO_2Li$ (litium salt of the oleic acid) deposited (a) from a solution of $C_{17}H_{33}CO_2Li$ in *n*-hexane and (b) by evaporation [28].

It is obvious that the properties of the tape with an evaporated coat are greatly improved.

The CoNi films can be protected against corrosion by a wet oxidation (the tape must be mentained for 150 hours at 60°C and 10% umidity). The corrosion prevention is realised in this case by the formation of a Co(III) oxyhidroxyde amorf layer, with a small content of Co^{2+} ions [29].

5. **Conclusions.** The evaporation of different materials with the aid of an energetic electron beam generated by an electron beam gun is a very suitable method to obtain recording media with good magnetic properties.

According to the literature and the experimental data it was realized an equipment for recording tapes, having the following characteristics: 1. Substrate material: polyimidic or polyestheric folio; 2. Thickness of the substrate: 6—20 μm; 3. Underlayer material: aluminium or titanium; 4. Thickness of the underlayer: 200 Å; 5. Magnetic material: CoNi (80/20) or CoCr (70/20) alloy; 6. Thickness of the magnetic material: 1000 Å; 7. Incidence angle: 600—90°, 8. Uniformity of the deposition: 5—10%; 9. Protective

layer: Litium salt of the oleic acid; 10. Process gas: oxygen + specific additives; 11. Predeposition unit: electron beam gun 12. Coating unit: electron beam gun; 13. E-beam gun's power: 10—15 KW; 14. Folio's breadth: 100—200 *mm* — 15. Rolling rate: 2—10 *m/min.*

REFERENCES

1. T. Suzuki, IEEE Trans. Mag., MAG—**20** (5), 675, 1984.
2. M. Wright, J. Vac. Sci. Technol., **A5** (1), 57, 1987.
3. R. Sugita, T. Nambu and Y. Sakamoto, IEEE Trans. Mag., MAG—**23,** 2449, 1987.
4. K. Nakamura, K. Mamono, H. Kawamura, Y. Ota, A. Itan and C. Hayashi, IEEE Trans. Mag., MAG—**20**, 833, 1984.
5. Y. Uchiyama, K. Ishibasi, H. Sato, U, Hwang and T. Suzuki, IEEE Trans. Mag., MAG—**23,** 2058, 1987.
6. S. Iwasaki and K. Takamura, IEEE Trans. Mag., MAG—**11**, 1173, 1975.
7. S. Iwasaki, K. Ouchi and N. Honda, IEEE Trans. Mag., MAG—**16**, 1111, 1980.
8. K. Ouchi, S. Iwasaki, IEEE Trans. Mag., MAG—**18,** 1110, 1982.
9. K. Ouchi and S. Iwasachi, J. Appl. Phys., **57,** 4013, 1985.
10. S. L. Zeder and J. F. Silvain, J. Appl. Phys. **61,** 3804, 1987.
11. K. Röll, J. Vac. Sci. Technol., **A4** (1), 14, 1986.
12. J. C. Loder, T. Wielinga and J. Worst, Thin Solid Films, 101, 61, 1983.
13. K. Shinohara, H. Yoshida and M. Odagiri, IEEE Trans. Mag., MAG—20, 824, 1984.
14. J. S. Gau and W. E. Yetter, J. Appl. Phys., 61, 3807, 1987.
15. M. Kitada, N. Shimizu, J. Appl. Phys., 54, 7089, 1983.
16. D. Baral and H. Lee, J. Appl. Phys., 61, 3828, 1987.
17. K. Honda, R. Sugita and Y. Sakamoto, IEEE Trans. Mag., MAG—23, 2040, 1987.
18. K. Yazawa and H. Masuya, IEEE Trans. Mag., MAG—20, 818, 1984.
19. Y. Nishikawa and W. Ueno, IEEE Trans. Mag., MAG—**23,** 2389, 1987.
20. R. Sugita, IEEE Trans. Mag., MAG—**20,** 687, 1984.
21. O. Kitakami, K. Ojima and Y. Ogawa, IEEE Trans. Mag., MAG—**23**, 2797, 1798.
22. A. Kouchiyama, I. Sumita, Y. Nakayama and N. Asanuma, IEEE Trans. Mag—**23,** 2791, 1987.
23. D. O. Smith, M. S. Cohen and G. P. Weiss, J. Appl. Phys., 31, 1755, 1960.
24. P. Guohong and W. Quintang, IEEE Trans. Mag., MAG—**23,** 2806, 1987.
25. S. Saito, M. Futamoto and Y. Honda, IEEE Trans. Mag., MAG—**23,** 2398, 1987.
26. H. Kurokawa, T. Mitani and T. Yonezawa, IEEE Trans. Mag., MAG—**23,** 2410, 1987.
27. K. Wakai, J. Appl. Phys., 61, 3822, 1987.
28. M. Nagao, K. Sano and M. Kojima, IEEE Trans. Mag., MAG—**23,** 2395, 1987.
29. A. Awano and H. Masayua, IEEE Trans. Mag., MAG—**23,** 2067, 1987.

STUDIA UNIV. BABEŞ-BOLYAI, CHEMIA, XXXVII, 1—2, 1992

KORINDONISCHE UNTERLAGEN FÜR MALEISCHSAUEREANHYDRID KATALYSATOREN

LIVIU LITERAT*

Received: 10.11.1992

ABSTRACT. Corund Supports for Maleic Anhydride Catalists. Based on literature data and personal experiments one provide some new recipes for anhydrous maleic acid catalysator supports. Using indigenous raw-materials, one sat down new prescriptions for obtaining fire-proof binder-materials. One made also experiments and description of mechanical, optic and structural characteristics of the obtained refractory superaluminous. materials.

Einleitung. Den Unterlagen für Katalysatoren (aktive Komponente V_2O_5 und MoO_3) im Falle der Oxidierung mit Luft des Benzols zu Maleischsäureanhydrid, werden strenge Erfordernisse verlangt, in was die Zusammensetzung (Al_2O_3 min. 86,5%; Na_2O max. 0,1%; Summe Na_2O und K_2O max.0,5%), die Porosität (überwiegend Poren zwischen 10 und 100 μm) und die Form (Zylinder mit dem Verhältnis l/d zwischen 1,2—1,5) betrifft. Diese Erfordernisse beeinflussen die Rohstoffe, die Massen von feuerfesten Bindemittel, die Technologie und die Rezepte in derselben Massregel.

Rohstoffe und Basisrezepte für feuerfeste Bindemasse

Wenn wir berücksichtigen dass die maximale Grenze für Na_2O 0,1 ist, aus Gründen der katalytischen Selektivität, muss die Struktur der Unterlagen ein Mehrheitskomponent aus reinem Korund (Elektrokorund, tabellarische Tonerde) enthalten, mit einer passenden Kornzusammensetzung in der Bildung eines porösen Skeletts, befestigt durch Sinterisierung in eine feuerfeste Masse so dass es in derselben Zeit die Texturerfordernisse beantwortet [1].

In diesem Zweck wurde als Strukturmaterial körniges Elektrokorund (Österreich) und tabellarische Tonerde (ICITPR-Plloieşti) verwendet. Als feuerfeste Bindemassen wurde Kaoline aus Aghireş und Harghita, Tonerde Typ Nitrat (VEGA-Ploieşti), Dolomit aus Voşlobeni und Rutyl (TiO_2) verwendet.

Die Rohstoffe und ihre oxidische Zusammensetzung sind in Tabellel gestellt.

Bei der Anpassung der beiden Sorten von Kaolin ist man aus technologischen Gründen angekomen, gebunden an die Gestaltung der Produkte (Plastizität) und weniger aus Gehaltgründen an Alkalien der Kaoline. Die Plastizitätziffer für den Kaolin aus Aghireş war 47,1 und für den Kaolin aus Harghita 64,1.

Zusammensetzungen für die feuerfeste Bindemasse

* *Universität „Babeş-Bolyai" Facultat der Chemische Tehnologie' 3400 Cluj-Napoca, Romania*

Tabelle 1

Rohstoff	Oxidische Zusammensetzung (%)								
	SiO_2	Al_2O_3	Fe_2O_3	TiO_2	CaO	MgO	Na_2O	K_2O	KV
Kaolin (Aghireş)	53,60	30,85	0,98	0,40	0,59	0,32	0,22	1,02	9,50
Kaolin (Harghita)	49,94	29,32	1,52	0,36	3,10	0,85	0,46	2,16	12,36
Tonerde (VEGA)	0,31	65,36	0,29	0,05	0,24	0,12	0,06	0,02	33,49
Dolomit (Voslobeni)	6,25	0,12	0,15	—	29,96	19,80	—	—	43,94
Elektrokorund (import)	—	99,75	—	—	—	—	—	—	—
Rutil	—	—	—	99,82	—	—	—	—	—

Die Schlussfolgerungen eines faktorialen Experiments haben bestimmt, dass die Zusammensetzung und Texturbedinungen erfüllt sind für die Verhältnisse von 55—60%, Elektrokorund oder tabellarische Tonerde und 40—45% Bindemittel durch Sinterisierung. Infolgedessen wurden mehrere Rezepte für die Bindemasse zusammengestellt, welche, unter Form von Paste neben den Porengeneratoren und den Verarbeitungszusätzen (Fassonierung) den Ausgangspunkt in die Realisierung der Produkte Typ Komposit konstituiert haben. Die gebildeten Varianten sind in Tablle 2 dargestellt.

Mit den Pasten AM_1 und AM_2 wurden die Basisrezepte in der Forschungstechnologie gebildet. Die Verhältnisse aus den Komponenten für einige aus diesen, sind in den Tabelle 3 und 4 dargestellt.

Tabelle 2

Rohstoff	Rezeptsymbol und Massenverhältnisse						
	AM_1	AM_{1a}	AM_{1b}	AM_{1c}	AM_2	AM_{2a}	AM_{2b}
Kaolin (Aghireş)	10	—	—	10	5	5	5
Kaolin (Harghita)	5	20	20	5	10	10	10
Nitrate Tonerde	24	10	10	24	24	20	20
Dolomit	2	2	1	4	2,5	2,5	2,0
TiO_2	2	2	2	2	1,5	1,5	1,0

Tabelle 3

Rezeptvarianten auf Basis von AM_1 Bindemittel

Komponenten	Rezemptsymbol and Massenverhältnisse							
	AM_{11}	AM_{12}	AM_{13}	AM_{14}	AM_{15}	AM_{16}	AM_{17}	AM_{18}
Paste AM_1	43	43	43	43	43	43	43	43
Elektrokorund	57	—	57	57	57	57	—	—
Tabelarische Tonerde	—	57	—	—	—	—	57	57
Polystyrolperlen	—	—	—	—	20	—	20	—
Zeamil	—	—	—	—	—	20	—	20
Stärke	—	—	30	30	30	40	30	30
Wasser	20	20	20	20	25	40	30	30

Tabelle 4

Rezepte auf Basis von AM_2 Bindemittel

Komponenten	Rezeptsymbol und Masseverhältnisse			
	AM_{23}	AM_2	AM_{26}	AM_{27}
Paste AM_2	43	43	43	43
Elektrokorund	57	57	57	—
Tabelarische Tonerde	—	—	—	58
Polystyrolperlen	—	20	—	20
Zeamyl	—	—	20	—
Stärke	30	30	40	30
Wasser	15	20	30	20

In den Tabellen 3 und 4 die Pasten AM_1 und AM_2 repräsentieren den massischen Inhalt von Trockenmaterial (43%) und die Verhältnissen von Zeamyl und Polystyrolperlen, in Volumen.

Elemente aus der Formgebungs und Brennungstechnologie der Feuerfesten Unterlagenmassen

Auf der Basis der gebildeten Rezepte wurden die plastischen Rohstoffe (Kaoline) einer Feuchtmahlung ausgesetzt. Die hydrate Tonerde, das Dolomit und TiO_2 vorher dosiert, wurden trockengemahlen, durch ein Sieb 009 STAS 1077-67 gebracht und nachher zusammen mit dem Kaolin 16 Stunden feuchtgemahlen. Der Schlicker wurde nachher 6—10 Tage mazeriert. Aus den mazerierten Teilen wurden Muster für die rohen Unterlagen gebildet, entsprechend den Tabellen 3 und 4. Die Wasser und Stärkeverhältnisse wurden beigebracht in Funktion der Notwendigkeit einer leichten Extrusion.

Die Feuchtigkeit verändert sich nach den Rezepten und ist zwischen 20—40% für AM_1 Rezepte und zwischen 15—30% für die AM_2 Serie enthalten.

Die Trocknung der Zylinder wurde in zwei Etappen gemacht. Eine langsame Etappe von 24 Stunden bei der Mediumtemperatur und die andere wurde durch Heizug in dem Trockenschrank bei 120°C, 8 Stunden gemacht und nachher noch 4 Stunden bei dieser Temperatur gehalten.

Die Brennung der Proben wurde im Tunnelofen bei 1530, 1580 und 1620°C (Zeitpallier 1,5 Stunden) gemacht. Gleichzeitig wurden die Kalzinierungen in den Elektrischofen mit Stagen aus Superkantal KO—II verfolgt. Das Brennungsdiagram in dem elektrischen Ofen 1550°C und 6 Stunden ist im Bild 1 dargestellt.

Bei der Feststellung des Diagrams wurden die polymorphen Verwandlungen des Siliziumdioxyds (Krsytobalit-Tridimit-Quarz) berücksichtigt um die Zerbrechlichkeit der Produkte zu vermeiden.

Die Prüfung des Fertigprodukts hat die mechanische Festigkeit, die Porösität, die Zusammensetzung der Mikrophasen durch elektronische und optische Mikroskopie und X Diffraktometrie [2, 3], verfolgt.

Die texturale Charakteristiken, gefolgert aus der Adsorbtion des Stickstoffes (SORPTOMATIC-1800, Karlo Erba) [4], sind in Tablle 5 dargestellt.

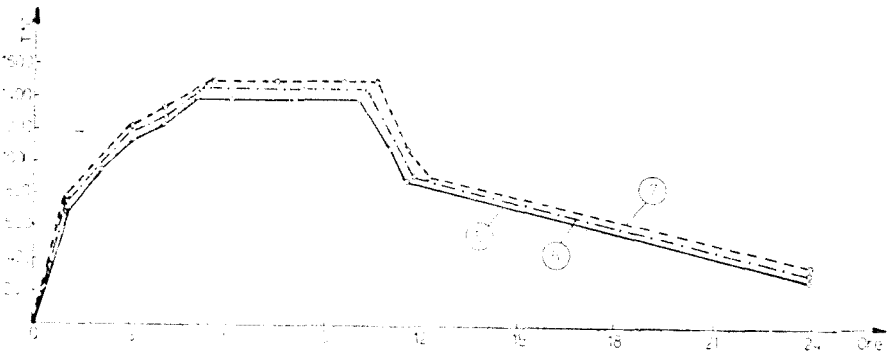

Abb. 1. Brennungsdiagram in elektrischen Ofen.

Tabelle 5

Struktural-textuarl Karakteristiken von AM_1 und AM_2 Proben

Karakteristik	Probe				
	AM_{13}	AM_{15}	AM_{16}	AM_{17}	AM_{22}
Gesamtvolumen der Poren ml/g	0,2309	0.1712	0.2477	0.3189	0.3202
Porenvolumen unter 75 Å	0.1936	0.1222	0.1971	0.2652	0.2618
Porenvolumen $75-10^4$ Å	0.0378	0.0492	0.0650	0.0537	0.0584
Porenverteilung (Mikroporen)					
0.1 – 1 µm (%)	20.77	5,89	26,84	20,75	—
1 – 10	58,67	74,88	37,74	32,58	—
10 – 100	20,56	19,23	35,82	47,17	—
über 100	—	—	—	—	—
Maximaler Radius Å · 10^6	1,14	1,58	1,90	2,27	1,75
Reale Dichte g/ml	3,63	3,79	3,70	3,74	3,51

Die strukturalen und texturalen Charakteristiken der AM_1 *und* AM_2 *Massen*

Für die Muster AM_{2-2} mit Hochstleistungen vergleichbar mit Importkatalysatoren sind die texturalen Charakteristiken in was die Verteilung der Mikroporen betrifft in Tabelle 6 dargestellt.

Die Beugung X Analyse (Diffraktometer PHILIPS PW-750 mit Eintragzähler) auf die integralen Pulver aus Katalysatorenunterlagen hat grosse Korundverhältnisse, mittlere aus Mullit und Silimanit und kleinere aus α-Quarz gezeigt.

Die chemische Zusammensetzung der Muster, erlangt aus den erprobten Rezepten AM_1 und AM_2 entspricht den verlangten Erfordernissen. Für einen Vergleich sind in Tabelle 8 die Daten nach einem LONZA Patent dargestellt.

Schlussbemerkungen

Die realisierten Unterlagen sind im Ganzen vergleichbar mit den Referenzmustern in was den Aspekt, die Festigkeit, die Pöräsität und die minerale Zusammensetzung betrifft.

Tabelle 6

AM_{22} Katalysatorunterlagen. Die strukturale und texturale Charakteristiken

Charakteristik:	
Gesamtvolumen der Poren	0,320 *ml/g*
Porenvolumen unter 75 *Å*	0,2618
Porenvolumen zwischen $75-10^4$ *Å*	0,0584
Makroporen Verteilung (75—75.000 *Å*)	
75—100 *Å* (%)	17,12%
100—300	31,17
300—600	13,70
60 1000	3,42
1000—5.000	27,57
5000—10.0000	3,60
10.000—100.000	3,42
Verteilung des Gesamtvolumen ($75-10^6$ *Å*)	
$75-10^5$ *Å*	23,89%
10^5-10^6	57,24
über 10^6	18,87
Maximaler Radius der Poren	1,75 10^6 *Å*
reale Dichte	3,51 *g/ml*
scheinbare Dichte	2,66 *g/ml*
Porosität (%)	24,22

Table 7

Beugung X Linien auf Unterlagen AM

Nr. der Linie	d/n (Å)	I (%)	Mineralkomponent
1	5,3594	4,76	Silimanit
2	3,4634	34,76	Korund
3	3,4112	5,71	Silimanit
4	3,3731	8,57	Mullit
5	2,6883	3,33	Mullit
6	2,5404	18,09	Mullit
7	2,3719	8,09	Korund
8	2,2046	4,76	Mullit (Silimanit)
9	2,0832	77,14	Korund
10	2,0770	41,75	Korund
11	1,7384	10,47	Korund
12	1,5988	37,14	Korund
13	1,5466	3,33	Mullit(-Quarz)
14	1,5299	100	Mullit
15	1,5255	60,00	Silimanit
16	1,3757	33,33	Mullit

Table 8

Oxidische Zusammensetzung der Unterlagen für Katalysatoren

Muster	SiO_2	TiO_2	Al_2O_3	Fe_2O_3	CaO	MgO	Na_2O	K_2O
AM_1	9,10	2,31	86,64	0,21	0,92	0,53	0,06	0,24
AM_2	8,79	1,20	88,68	0,27	1,14	0,62	0,08	0,31
LONZA	9,63	0,85	87,02	0,52	1,38	0,12	0,21	0,27

Die Diagramme der elektronischen und optischen Mikroskopie, die nicht dargestellt wurden aus technischen Gründen, bestätigen makroporöse Strukturen, gebildet aus eckigen Kristallen und Korundfragmenten zementiert bei den Kontaktpunkten mit der mullitischen Masse.

Die Porengrösse, die Form und das Hohlräumeverhältnis sind variebel und abhänging in einigen Grenzen von dem porogenen Zusatz und dem thermischen Zustand.

Hinsichtlich der phasichen Zusammensetzung (Tabelle 8) stellt man fest Verhältnisse von Na_2O und K_2O unter dem Wert des LONZA Musters, dass was die Selektivität in dem Verfahren der katalytischen Oxidierung versichert.

In was die Mehrheitskomponente Al_2O_3 und SiO_2 betrifft, sind die Rezepte praktisch untereianderliegend, wichtige Unterschiede sind im Fall des TiO_2 verzeichnet. Spätere Studien werden zwischen anderen, die Reduzierung des Rutylverhältnisses unter 1% verfolgen.

LITERATUR

1. Patent Ch. 592 474/24.07.1974, Lonza, Schweis.
2. Bechereseu, D., Menesy, F., Marx, W. *Physikalische Methoden in der Silikatenchemie*, Wissentschaftlicher und Enziklopedischer Verlag, Bukarest, 1977.
3. Solacolu, S., *Physikalische Chemie der technischen Silikate* Technischer Verlag, Bukarest, 1968.
4. Literat, L., *Baumateriale*, vol. XIX nr. 4, 246, 1989.

STUDIA UNIV. BABEŞ-BOLYAI, CHEMIA, XXXVII, 1—2, 1992

ETHYLBENZENE DEHYDROGENATION ON Fe-Cr-K CATALYST. III. Catalyst Modification by Addition of Used Materials with Vanadium

N. DULĂMIȚĂ, M. STANCA, F. BUCIUMAN, I. HOPÂRTEAN, F. IRIMIE*

Received: 15.1 .1992

ABSTRACT. — In this paper the catalytic performance of the Fe—Cr—K catalyst in the ethylbenzene dehydrogenation to styrene are compared to those of Fe—Cr—K—V_2O_5/SiO_2 catalyst.

1. **Introduction.** The styrene is one of the oldest and most important raw material utilised in the manufacturing of plastics, mainly for the polystyrene and synthetic rubber. Industrially, styrene is obtaind through ethylbenzene dehydrogenation using a catalyst based on ferric oxide, with promotor additions. Preponderantly, the research tends to improve the yield and selectivity in styrene by adding promotor substances to the Fe_2O_3-Cr_2O_3-K_2CO_3 catalyst with a view to intensifying the etylbenzene dehidrogenation process and to reducing the specific consumption of raw materials, utilities and energy [1, 2].

This paper studies and compares the performances of the Fe_2O_3-Cr_2O_3-K_2CO_3 catalyst, with or withowt addition of residual vanadic materials (used vanadium catalyst, unwashed or washed with water to $pH = 6$) in the reaction of ethylbenzene dehidrogen ation to styrene.

2. **Experimental.** 2.1. *Catalyst preparation.* The compositions of catalysts are given in Table 1. The Fe_2O_3, Cr_2O_3 and K_2CO_3 powders were supplied by Borzești Chemical Plant. In catalyst no 2 was introduced used and dried catalyst from the sulphuric acid plant of Baia Mare; in catalyst no. 3 the same material was introduced, but it was previously washed to $pH = 6$ and dried. Similarly, in catalyst no. 4 was introduced Wolffen-tyep catalyst, used, respectively washed in catalyst no. 5 (provided by the sulphuric acid plant of Copșa Mică). In the materials containing vanadium, no arsene was identified. The granulation of powders was about 2—10 microns. In a stirrer were introduced and mixed for 30 minutes, the Fe_2O_3, Cr_2O_3 and V_2O_5/SiO_2 dried (catalysts no. 2 and 4)

Table 1

Catalyst composition and mechanical strength

Cat No.	Composition (wt. %)				Compression strenght (kg/pellet)
	Fe_2O_3	Cr_2O_3	K_2CO_3	V_2O_5/SiO_2	
1	87	3	10	—	7.0
2	60	3	10	27	12.5
3	61	3	10	26	14.6
4	59	3	10	28	13.1
5	60	3	10	27	15.7

* *University „Babeș-Bolyai", Department of Technological Chemistry, 3400, Cluj-Napoca, Romania*

and washed (catalysts 3 and 5, respectively) powders, then the K_2CO_3 solution was added and the mixing continued for another 30 minutes. The humidity of the fluid paste was 25—35% as compared to the solid mass. The wet paste was extruded in cylinders of 4 *mm* diameter and 5—6 *mm* lenght. The pellets are dried at room temperature for 4—5 hours, at 110—120 °*C* for 5—6 hours, then calcinated at 700 °*C* for 1—2 *h*. The rate of heating is 100 °*C/hour* to avoid the crushing of the pellets.

2.2. *The mechanical strength*. The components of the enhancement of the compressive strenght as one can see in Table 1.

2.3. *Ethylbenzene dehydrogenation*. In a tubular isothermal reactor, 40 cm^3 catalyst, with granulation in the range of 0.8—1 *mm*, were loaded, placed betwen two beds of silicon carbide of same granulation. Over the catalyst, a mixture of ethylbenzene and steam in a mass ratio of $H_2O/EB = 3/1$ passed, the space velocity, in rapport to the liquid ethylbenzene is 0.5 h^{-1}. The ethylbenzene used had the composition, in weight %: EB — 99.08; benzene + toluene — 0.40; styrene — 0.40; diethylbenzene — 0.10. The reaction gases were cooled and condensed, the organic product was separated from water, measured and the liquid yield was calculated. The product composition was analysed by gas-chromatography and the catalytic performances, for the work temperature, were calculated.

Table 2

Experimental results and catalytic performances

Cat. No.	Temp. (°C)	Composition of the product (wt. %)			Performances (wt. %)		
		B+T	EB	St	R	C	S
1	520	3.94	54.62	41.44	40.68	47.72	85.25
2	620	6.14	51.98	41.88	40.10	49.57	80.90
1	540	4.59	47.67	47.74	46.24	55.29	83.63
2	640	8.70	41.00	50.30	47.11	60.40	78.00
1	560	9.05	29.79	61.16	56.06	72.80	77.00
2	660	15.02	31.80	53.18	59.04	82.00	72.00

B + T — sum benzene + toluene; EB — etylbenzene; St — styrene; R — yield; C — conversion; S — selectivity.

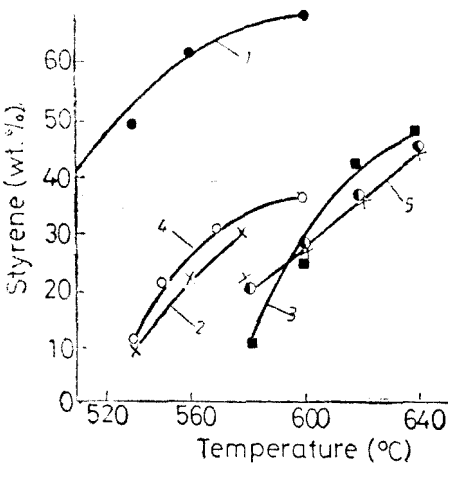

Fig. 1. The variation of styrene content in the product according to temperature.

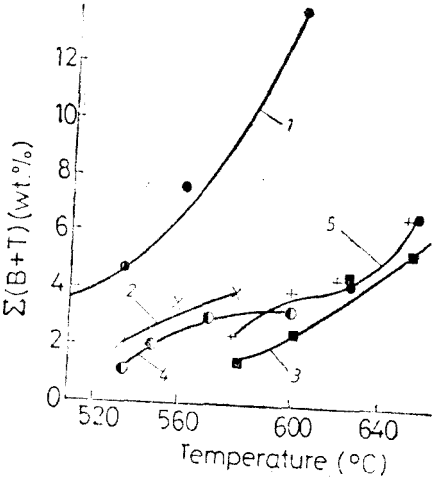

Fig. 2. The content of light hydrocarbons (sum B+T) in the product function of temperazure.

3. Results and discussions. The performances of catalyst no. 1 (with no V_2O_5/SiO_2) are compared with the performances of catalysts no 2—5 (containing V_2O_5/SiO_2 dried or washed) in the reaction of ethylbenzene dehydrogenation with steam dilution. The experimental results are shown in Table 2; Fig. 1 and 2 show the variation, according to temperature, of styrene content and light hydrocarbons (i.e. benzene + toluene = B + T), in the organic product. At 520°C on the catalyst no. 1, 41—43% styrene was produced, and 4% light hydrocarbons simultaneously. At a near content of styrene in the product (see Table 2), the thermal level increases with 100°C for catalyst no. 2, wihch brings the decrease of the selectivity with 4—6%.

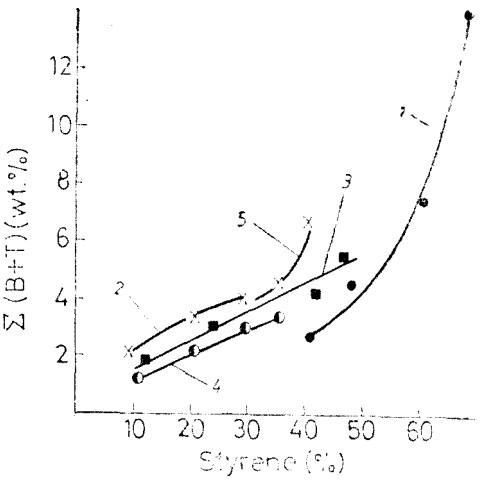

Fig. 3. The variation of sum (B+T) with the styrene content in the product at differentt emperatures.

Irrespective of its treatment (dried or washed), the V_2O_5/SiO_2 added to catalyst no. 1 decreases the performances, i.e. the styrene content in the product, in the same work conditions. For example (see Fig. 1.), at 600°C the styrene content is 68% for catalyst no. 1, 36% for catalyst no. 4, 27—29% for catalysts no. 5 and 3. At the same temperature, the content of light hydrocarbons (see Fig. 2) is 14% for catalyst no. 1 and at most 4% for catalysts no. 2—5. The variation of (B + T) sum with the styrene content, at different temperatures, is presented in Fig. 3. Catalyst no. 1 is the most selective at a high content of styrene in the organic product. The addition of dried vanadium materials (catalysts no. 2 and 4) is more active at temperatures below 600°C. while the washed material lead to a styrene content of 40% at 620—630°C. The dried material from the Wolffen catalyst seems to be more active than the Romanian one (catalyst no. 2.). The situation is inverse for the washed material (see Fig. 1.).

The performances of catalysts no. 2—5 decreased because the irreversible poisoning of the active centers on the Fe-Cr-K system surface, due to the silicovanadates and sulphovanadates of the used catalysts. Catalysts no. 3 and 5 prepared with washed material present the lowest performances in ethylbenzene dehydrogenation, although their mechanical strenght is double in comparison to catalyst no. 1.

The results of the test of ethylbenzene dehydrogenation to styrene allow the following observations:

— the performances of catalyst no. 1 decrease when any of the presented vanadium materials is added;

— the thermal level increases with at least 100°C to achieve the same styrene content in the product, which affects negatively the selectivity;

— the addition of V_2O_5/SiO_2 dried ot washed in the Fe-Cr-K catalyst has an inhibitory effect on the catalytic activity, although the mechanical strength doubles.

4. **Conclusions.** Irrespective of the provenience and treatment, the used vanadium materials studied led to a lower catalytic activity of the Fe-Cr-K catalyst to which they were added. The washed vanadium material presented an even lower activity than the dried material.

Consequently, the utilisation of used V_2O_5/SiO_2, dried or washed in order to promote and enhance the mechanical strength of the Fe-Cr-K catalyst is not recommended.

REFERENCES

1. N. Dulămiță, M. Stanca, F. Buciuman, *React. Kinet. Catal. Lett.*, in press.
2. N. Dulămiță, G. Csomortányi, I. Hopârtean, M. Fodorean, F. Irimie, *Al IV simpozion național de ingineria proceselor chimice*, Piatra Neamț, 1988, p. 313.

STUDIA UNIV. BABEŞ-BOLYAI, CHEMIA, XXXVII, 1—2, 1992

ON THE USE OF METHANE-AIR FLAME IN FLAME SPECTROMETRY. II. THE EMISSION SPECTRUM OF THE METANE-AIR FLAME.

L. KÉKEDY NAGY*

Received: 15.12.1992

ABSTRACT. The emission spectrum of the methane-air flame in the spectral domain $\lambda = 190-800$ *nm* consists of the molecular emission bands of the radicals OH, CN, CH and C_2 and of the stable molecules CO and O_2, respectively. The intensity of the emission spectrum (the concentration of the radicals), varies strongly with the composition of the gas mixture and with the height over the burner head. Its maximum value lies between 3—6 *mm* over the burner head and increases with the methane content of the gas mixture.

Introduction. The emission spectrum of the flame consists of emission bands of different radicals and molecules. It plays an important role in the flame photometrical determinations, being the background of the flame. The spectrum could overlap with the spectral line of the analyses, resulting the so called spectral interference [1—3]. The fluctuations of the background increase considerably the noise level of the analytical signal, decreasing at the same time the signal-to-noise ratio. On the other hand the emission spectrum provides useful information on the mechanism of the combustion reactions, the equilibria in different zones in the flame as well as on the excitation conditions of different elements.

In order to establish the conditions of the determination of different elements in the methane-air (M-A) flame using our new type burner [4], first of all the emission spectrum of the flame was recorded. There have been identified the emittent species as well as the correspondent transitions between the different energetic states. The variation of the flame spectrum as a function of the distance from the burner head has been determined too in order to draw some semicantitative conclusions on the kinetics of burning rections, on the concentration of different radicals and molecules in the flame.

Experimental. The apparatus used was the same as described in our previous paper [5]. The emission spectrum of the M—A flame was recorded in the 190—800 *nm* range, the most frequently used in the flame spectrometry. In order to obtain a maximum concentration of different species in the flame, a fuel rich flame was used (stoichiometric ratio 1.12). The observation zone was fixed experimentally: 4 *mm* above the burner head, in the middle of the flame. Here the emission signal was found to be maximum. The monochromator slit width was 0.1 *mm* corresponding to a spectral resolution of 0.2 *nm* over the entire spectral domain, allowing to record the weak lines too. The sweep rate of the monochromator was of 0.05 *nm/sec*. The sensitivity of the recorder, *S(A/div)*, was chosen in accordance to the line intensities in the given spectral domain. The emission spectra of the M—A flame at 4 different wavelength domain between $\lambda = 190-620$ *nm* are represented in Figures 1—4.

* *Babeş-Bolyai University, Dept. of Analytical Chemistry, 3400 Cluj, Romania*

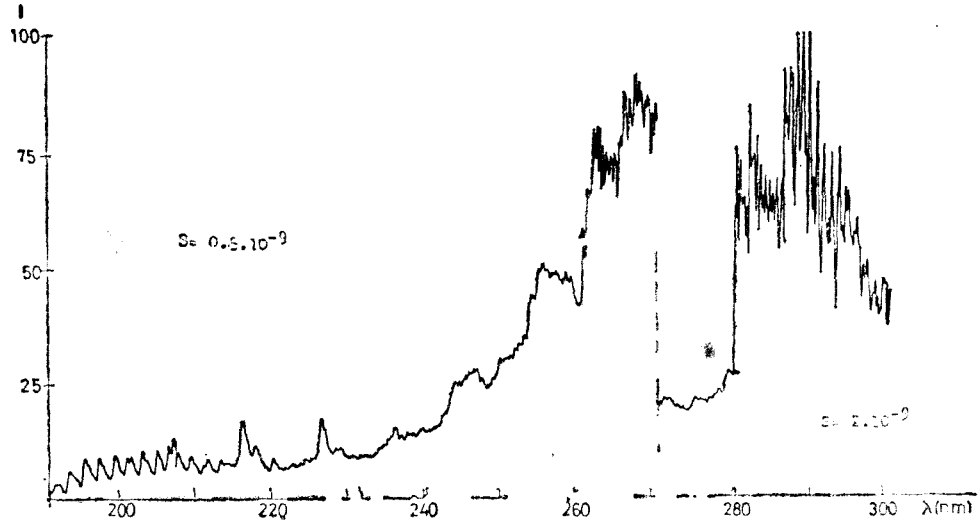

Fig. 1. The emission spectrum of the M—A flame in the spectral domain $\lambda = 190-300$ *nm*

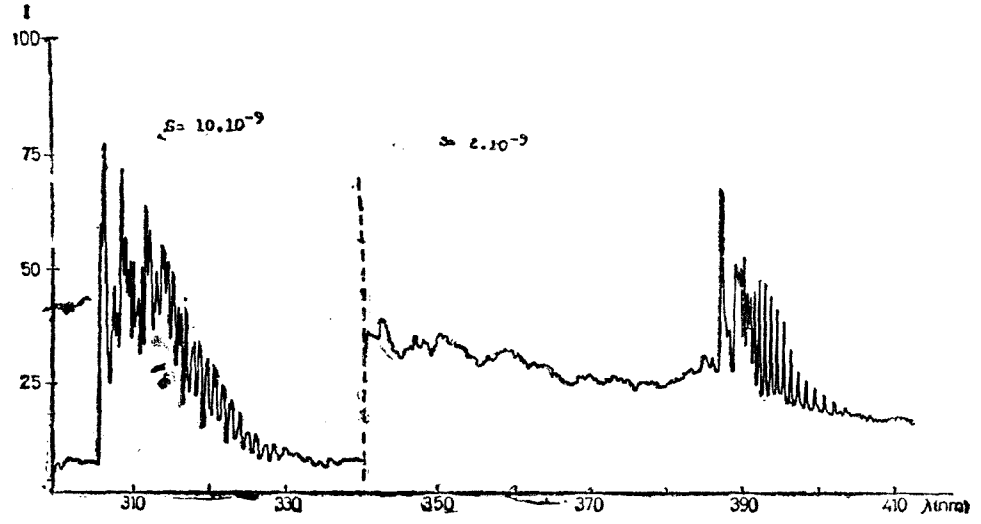

Fig. 2. The emission spectrum of the M—A flame in the spectral domain $\lambda = 300-410$ *nm*

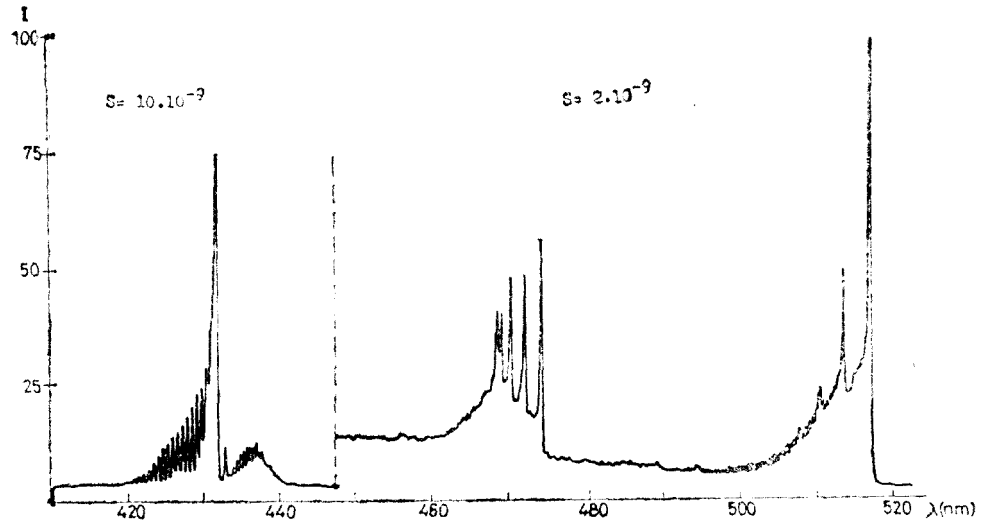

Fig. 3. The emission spectrum of the M—A flame in the spectral domain $\lambda = 410-520$ *nm*

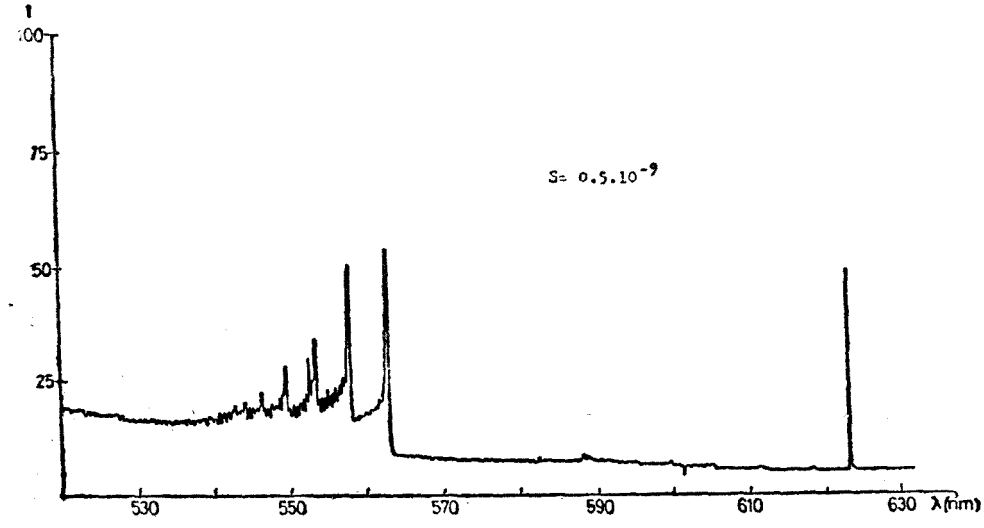

Fig. 4. The emission spectrum of the M—A flame in the spectral domain $\lambda = 520-630$ *nm*

From these spectra the wavelength of the spectral lines of the band heads have been determined. The emittent species were identified using spectral tables [6]. The results are summarized in Table 1.

In the next step the variation of the flame spectrum intensity versus the height over the burner head at 3 different methane-air ratios: 0.88; 1.00; 1.12, respectively, was determined. For this purpose the strongest band headlines corresponding to molecular radicals: for OH the line

Table 1

The band heads of the emittent species in the M—A flame

Wavelength (nm)	The emittent species	Wavelength (nm)	The emittent species
191.81	CO	416.78	CN
206.83	CO	431.20	CH
217.38	CO	437.14	C_2
237.82	C_2	467.86	C_2
248.63	C_2	468.48	C_2
258.90	C_2	469.76	C_2
260.90	OH	471.52	C_2
265.63	C_2	473.71	C_2
281.10	OH	509.77	C_2
285.50	C_2	512.93	C_2
294.50	OH	516.52	C_2
306.40	OH	547.03	C_2
308.90	OH	550.19	C_2
312.20	OH	554.07	C_2
318.50	OH	558.55	C_2
385.47	CN	563.55	C_2
387.14	CN	612.21	C_2
389.20	CH	619.12	C_2

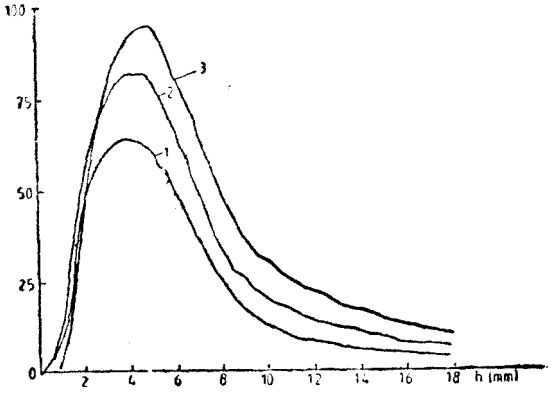

Fig. 5. The variation of the flame background at $\lambda = 306.4$ *nm* versus the height and the composition of the M—A flame, *1)* 0.88; *2)* 1.00; *3)* 1.12 $S = 20.10^{-9}$

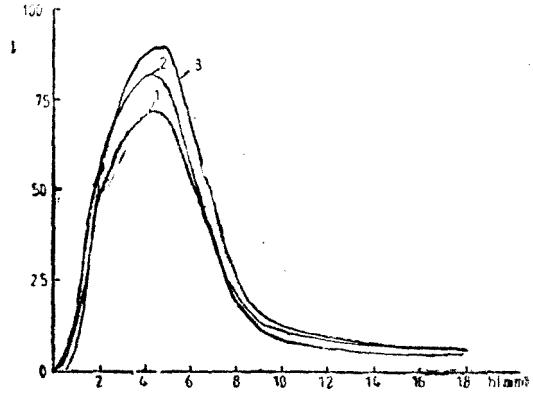

Fig. 6. The variation of the flame background at $\lambda = 385.5$ *nm* versus the height and the composition of the M—A flame, *1)* 0.88; *2)* 1.00; *3)* 1.12 $S = 2.10^{-9}$

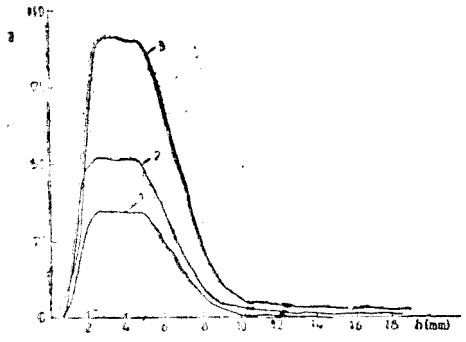

Fig. 7. The variation of the flame background at $\lambda = 431.2$ *nm* versus the height and the composition of the M—A flame, *1)* 0.88; *2)* 1.00; *3)* 1.12 $S = 10.10^{-9}$

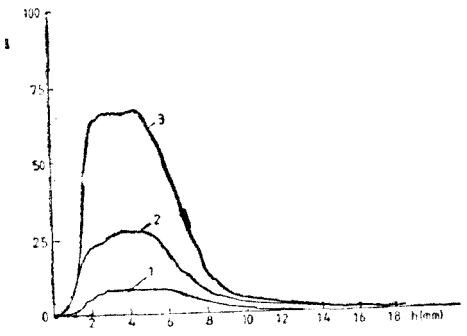

Fig. 8. The variation of the flame background at $\lambda = 516.5$ *nm* versus the height and the composition of the M—A flame, *1)* 0.88; *2)* 1.00; *3)* 1.12 $S = 2 \cdot 10^{-9}$

at $\lambda = 306.4$ *nm*; for CN the line at $\lambda = 385.5$ *nm*; for CH the line at $\lambda = 431.2$ *nm* and for C_2 the line at $\lambda = 516.5$ *nm* (see also Table 1.) were selected. The intensities of these lines were recorded between 0 and 18 *mm* over the burner head with a spatial resolution of 1 *mm*. The results are represented in Figures 5—8.

Results and discussion. From the emission spectra the presence in the M-A flame of the molecular radicals OH, CN, C_2, CH as well as of the stable molecules CO_2 and O_2 were identified. The spectra obtained are similar to the emission spectra of other hydrocarbon flames (C_2H_6, C_2H_4, C_2H_2, C_3H_5 etc.) with air. This confirmes that the same radicals are formed and similar burning reactions occur regardless of the hydrocarbon used [7]. The emission of the M-A flame is the strongest in the $\lambda = 300 - 400$*nm* and 510—520 *nm* regions respectively, decreasing towards the longer wavelenghts. The background increases with the methane-content of the gas mixture.

The background of the flame exhibits a variation with the height of the flame over the burner head too: First it increases sharply, reaching its maximum at 3—5 *mm* over the burner head, than decreases and about at 12 *mm* becomes insignificant, regardless of the composition of the gas mixture. Taking into account that the gas mixture is fed with a constant flow rate, the abscissas on Figures 5—8 represents in the same time the axes of time too. Considering this fact, from the shape of the curves results that the OH and CN radicals are formed relatively slow, through parallel reactions. Their maximum concentration is reached at 4.5—4.7 *mm* over the burner head. The lifetime of these radicals is relatively long and their concentration in different zones of the flame is only slightly influenced by the gas mixture composition.

The CH and C_2 radicals are formed faster than the OH and CN ones, their maximum concentration being observed at 2 *mm* and 3 *mm* respectively over the burner head. The presence of the plateau on the respective curves shows the attainement of a constant concentration of these radicals over 2—3 *mm* distance in the flame. The fact that the maximum concentration of

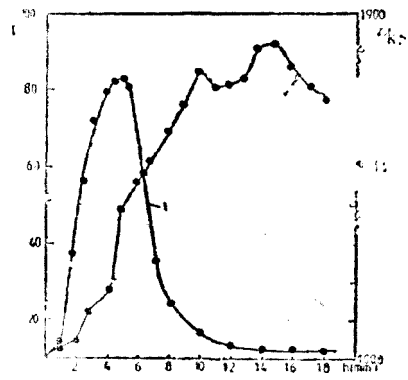

Fig. 9. The variation of the emission of the OH radicals (1) and the translational temperature (2) of the M—A flame versus the height

the CH radicals is attained earlier than that of the C_2 ones, shows that these radicals are formed by consecutive reactions. The sudden increase of the CH and C_2 radical concentration with the methane content of the gas mixture shows that the pyrolysis reactions predominate over the burning reactions. The lifetimes of these radicals are short due to high efficiency inelastic collisions with other particles.

If one compares the variation of the concentration of OH radicals as well as the translational temperature of the M-A flame versus the height (Fig. 9) it results that the translational temperature maximum appears much later than the emission maximum.

This denotes that the flame in the primary reaction zone is far from thermal equilibrium relative to different energetic states. The energy released by chemical reactions is stored most in vibrational and electronic states of the radicals and molecules. The thermal equilibrium between the different energetic states is reached only in the secondary reaction zone, in higher regions in the flame.

Conclusions. 1. The emission spectrum of the M—A flame consists of the molecular emission bands of the radicals OH, CN, CH and C_2 and of the stable molecules CO and O_2, respectively.

2. The spectrum is similar to those presented by other hydrocarbon flames with air.

3. The intensity of the emission spectrum increases with the methane content of the gas mixture. Its maximum value lies in the 3—6 *mm* region over the burner head. This region corresponds to the maximum concentration of radicals and to the optimal excitation conditions of different elements too.

4. The energy is released stepwise by chemical reactions in the primary reaction zone. This energy is stored most in the vibrational and electronic states of the radicals and molecules. The thermal equilibrium is reached only in the secondary reaction zone.

5. In order to maintain the excitation conditions constant in the flame, the composition of the gas mixture must be kept constant.

6. The most suitable spectral domain for analytical purposes lies in the domains of $\lambda = 200-300$ *nm*; 440—510 *nm* and 540—800 *nm*, respectively, where the background is relatively slow.

REFERENCES

1. I. Rubeska, Chem. Listy, **59**, 1119 (1965).
2. E. E. Pickett, S. R. Koirtyohann, Analyt. Chem., **41**, 28A (1969).
3. B. Thelin, Analyst, **112**, 62b (1987).
4. E. Cordoș, L. N. Kékedy, R. Hui, Brevet RSR, 67857/30.12.1977.
5. E. Cordoș, L. N. Kékedy, Studia, in press.
6. R. Mavrodineanu, H. Boiteux, *Flame spectroscopy*, Wiley, N.Y., 1965, p. 331.
7. G. A. Hornbeck, R. C. Hermann, J. Chem. Phys., **17**, 1344 (1949).

STUDIA UNIV. BABEŞ-BOLYAI, CHEMIA, XXXVII, 1—2, 1992

INTERCALATION COMPOUNDS. I. THEORETICAL ASPECTS

GEORGETA ŢARĂLUNGĂ*, L. ONICIU**, CS. BOLLA**, L. D. BOBOŞ**

Received: 15.12.1992

ABSTRACT. The electrochemical reaction of the lithium batteries is based on the intercalation phenomenon of the lithium ions in a host lattice of oxides or sulfides.

This paper presents some theoretical aspects concerning the intercalation of Li^+ as well as some structural characteristics of the resulting compounds, as Li_xMnO_2, Li_xCuO and Li_xTiS_2.

Introduction. In the lithium nonaqueous batteries there are used various cathodic depolarisants, such as oxides, calchogenides oxosalts etc. [1]. Their running is based on the intercalation phenomenon, which consists in the insertion of guest species between the layers of a crystalline compound lattice, without essential modifications of the host structure; the resulting products have been called intercalation compounds.

1. **Theoretical considerations about intercalation phenomenon.** The intercalation phenomenon takes place by diffusion of the metal ion, M^+, in a material lattice structure, which is proper for intercalation, and called host material ⟨H⟩. The intercalation reaction is given by:

$$xM^+ + xe^- + \langle H\rangle \rightleftarrows \langle M\ H\rangle, \tag{1}$$

where the coefficient x can vary continously from 0 to a maximum value x_{max} ($0 < x < x_{max}$). The degree of occupancy or the degree of intercalation, y, is defined by the relationship:

$$y = \frac{x}{x_{max}}. \tag{2}$$

In conformity with reaction (1), transport of material occurs through a double flux of charged species (M^+ and e^-) in the bulk of the host material whatever the concentration is. This fact has been demonstrated for Li_xMnO_2, Li_xNbSe compounds, which are characterized by the preferential diffusion paths [2].

The electrode potential variation at the equilibrium has experimentally been followed, finding out a value much deviated from the calculated one; also, the concentration of the lithium ions within the intercalation compounds has been found very different from the calculated value. These deviations occur because of some interactions which generate the structures with maximum distances between the nearest neighbours [3—5].

* *Babeş-Bolyai University, Laboratory of Electrochemistry, 3400 Cluj-Napoca, Romania*
** *Babeş-Bolyai University, Dept. of Physical Chemisry, 3400 Cluj-Napoca, Romania*

The influence of ion-ion interactions on intercalation kinetics has been investigated by Deroo et al. [6], who has improved Armand's theoretical model [2].

The chemical potential of an alkaline metal M^+ in a host structure is given by:

$$\mu_{M^+} = \mu^0_{M^+} + RT \ln [y/(1-y)] + ay, \tag{3}$$

where a is the mean interaction energy between nearest neighbour ions, y the intercalation degree, whose standard value is $y^0 = 0.5$, according to Yongfang [7].

The chemical potential of the ion M^+ in the electrolytic solution can be considered a constant if the concentration and the diffusion coefficient of M^+ are high.

Assuming that migration and convection fluxes are neglected, the overall flux is reduced to the diffusion component:

$$J = -C^0 D \, \partial y/\partial r, \tag{4}$$

where $D = D_0 [1 + ay(1-y)/RT]$ is the apparent diffusion coefficient and D^0 the diffusion coefficient in absence of ion-ion interactions.

Under these conditions, mass conservation is given by the relationship:

$$C^0 \frac{\partial y}{\partial t} = -\frac{1}{r^{d-1}} \frac{\partial}{\partial r} (r^{d-1} F), \tag{5}$$

where d is the dimension (uni, bi or tridimensional) of the diffusion space, C^0 is the maximum concentration of intercalated ion F-the Faraday and r is a space coordinate. Two possibilities were considered: the ions are not subjected to any interaction (a), and the interactions are involved (b).

(a) For this case the free energy variations for the ionic transfer from the electrolytic solution to the electrode are given by:

$$\Delta G_c = \Delta G^0_c + \beta z F \varepsilon \tag{6a}$$

and

$$\Delta G_a = \Delta G^0_a - (1-\beta) z F \varepsilon, \tag{6b}$$

where β is the cathodic transfer coefficient, $(1-\beta)$ the anodic transfer coefficient, z is the number of electrons changed, and ε the electrodic potential.

The kinetic constants in the two directions are expressed as:

$$k_c = k^0_c \exp\left[-\beta \frac{zF\varepsilon}{RT}\right] \tag{7a}$$

and

$$k_a = k^0_a \exp\left[(1-\beta) \frac{zF\varepsilon}{RT}\right], \tag{7b}$$

and the current density is given by:

$$i = zFk^0 C^0 \left\{ y \exp (1-\beta) \frac{zF\varepsilon}{RT} - (1-y) \exp\left[-\beta \frac{zF\varepsilon}{RT}\right] \right\}, \tag{8}$$

where $\eta_i = \varepsilon - \varepsilon^0 = -(\mu_{M^+} - \mu^0_{M^+})/F$ is the overpotential; the exchange current density is given by:

$$\log i^0 = 1/2\, zFk^0C^0. \tag{9}$$

(b) When ion-ion interactions are present, the free energy into the depolarisant is reduced by a value ay and if the interactions have the same effect on the surface and inside, it is expressed as:

$$\Delta G_c = \Delta G^0_c + \beta ay + \beta zF\varepsilon \tag{10a}$$

and

$$\Delta G_a = \Delta G^0_a - (1 - \beta)(zF\varepsilon - ay). \tag{10b}$$

The current density is became:

$$i = zFk^0C^0 \left\{ \exp\,(1 - \beta)\, \frac{(zF\eta_i + ay)}{RT} - (1 - y) \exp - \frac{(zF\eta_i + ay)}{RT} \right\}. \tag{11}$$

D e r o o et al. [6] has been concluded reasercheing ion-ion interaction in the homogeneous diffusion, the forces of repulsion favour grater spacing between ions and make ions to leave the intercalation material. In the case of semi-infinite diffusion, a great part of the repulsion forces favours the displacement of ions towards the bulk of the intercalated material; these interactions increase the coulombic efficiency of the galvanostatic discharge.

2. **Structure of the intercalation compounds.** At the time when the degree of intercalation is not exceeding a certain limit ($\sim 30\%$), the structure of the intercalation compound is not different from the host structure. However the intercalation generates a specific volumic modification for the last.

It has been found that, between MnO_2 crystallographic forms, only β — and — γ — MnO_2 modifications are favorable for the lithium insertion. These are coexisting as a mixture in the natural ore, which in considered as a disadvantage. For that reason it is preferable to use the electrolytic MnO_2 [8].

In the case of Li/MnO_2 cells, the active electromotive reaction is given by the insertion:

$$x\mathrm{Li}^+ + xe^- + \mathrm{MnO_2} \rightarrow \mathrm{Li}\,\mathrm{MnO_2};\ 0 < x < 1 \tag{12}$$

during them it takes place a partial reduction of the ions Mn^{4+}:

$$\mathrm{Mn}^{4+} + e^- \rightarrow \mathrm{Mn}^{3+}. \tag{13}$$

As the intercalation process advances ($y \geqslant 30\%$) by X-ray diffraction (*XRD*) has been found that Li_xMnO_2 alters the initial rutile-type [1×1] or ramsdellite-type [1×2] structure; it gives rise to the conditions for the coexistence of the ramsdellite-type with the rutile-type structure [8—11]. The difference between these structures is given by the distribution of manganese ions in the same hexagonally close-packed oxygen matrix.

Fig. 1 shows an idealized crystal structure of the resulted compound by the Li^+ insertion into rutile-type structure and its X-ray diagram for $x = 0.25$. The idealized structure has a tetragonal sublattice with the lattice constants

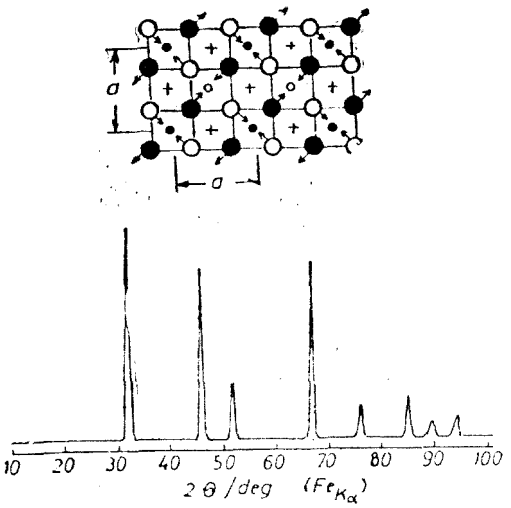

Fig. 1. The idealized rutile-type structure of the Li_xMnO_2 (x = 0,25)

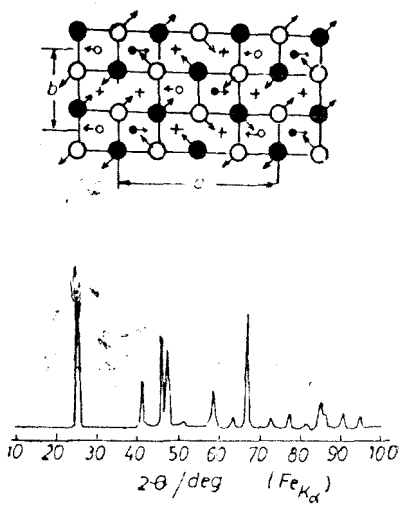

Fig. 2. The idealized remsdellite-type structure of the Li_xMnO_2 (x = 0,25)

$a = 5.0$ Å, $b = 5.0$ Å and $c = 2.85$ Å. The arrows indicate the possible Jahn-Teller distorsion of the $[Mn^{3+}O_6^{2-}]$ unit octahedron. The points noted with + indicate the possible octahedral sites in which lithium ions are located.

The idealized crystal structure of the resulted compound by the lithium intercalation into the ramsdellite-type structure and its X-ray diagram for $x = 0.25$ are illustrated in Fig. 2. This idealized structure has an orthorombic unit cell, which consists of two tetragonal sublattices with the reticular parameters: $a = 2 \times b = 9.9$ Å. The points noted with + represented the possible octahedral sites where the lithium ions may intercalate, and the arrows show the possible distorsion due to the repulsion and Jahn-Teller effect of Mn^{3+} ions.

The X-ray effected calculations indicate the existence of a little variations of the lattice constants, which permits to conclude that the significant changes of the intercalation compound structure do not arise in comparison with the host structure, where the lithium has been intercalated ($0 < x < 0.3$). It has been ensured a little expansion in the a-axis and an insignificant shrinkage in the c-axis as result of the lithium ion intercalation.

Another cathodic depolarisant material for nonaqueous lithium batteries is the copper oxide which has only two crystallographic structure: monoclinic and tetragonal lattice [12]. The monoclinic structure approaches TiO_2 rutile-type structure, which permits the lithium ions insertion with the formation of the intercalation compounds Li_xCuO [13].

The nonstoichiometric copper oxide has a relatively regular crystallographic lattice. The existent defects are favourable for the diffusion of lithium ions into the CuO crystallites.

The stoichiometric samples, thermally treated, maintain certain crystallographic deffects of a mosaic texture type, which are creating strains in the CuO crystallites, facilitating the diffusion of lithium ions [14].

The transition metal dichalcogenides have a layered structure. Thus, the disulfides are formed by two hexagonally close-packed sulphur layers between which reside the transition metal ions. These metal ions are found either in sites of octahedral symmetry or in ones of trigonal prismatic symmetry. The transition metals of the group IV B (Ti, Zr, Hf) are in octahedral symmetry, the group VI B (Cr, Mo, W) in the trigonal prismatic sites, but Nb and Ta of the group V B are found in both [15, 16].

The titanium disulfide has been the most studied. In Fig. 3 is shown the ordering of the Ti and S layers, as well as the octahedral symmetry sites. The S and Ti atoms are covalent bonded, but the sandwich-type building units are maintained together by van der Waals forces.

The compound is nonstoichiometric, the titanium or sulphur excess founding in the van der Waals layer. The titanium excess stabilizes the compound, but a subsequent intercalation becomes more difficult, and sulphur excess led to the moulding of the titanium trisulfide, which has been unable for reversible intercalation (Fig. 4).

The cell reaction, which results in the moulding of the intercalation compounds, is given by:

$$xLi^{+} + xe^{-} + MS_2 \rightarrow Li_xMS_2, \quad 0 < x < 1. \tag{14}$$

The diffusion of the lithium ions takes place only in the van der Waals layer, there being non-significant mobility perpendicular to these plase. Therefore, the diffusion is bidimensional and there is not diffusion through the sulphide layers [15].

The structure of the Li_xMS_2 intercalation compound is about the same with the crystalline structure of the host dichalcogenide. The structure of the intercalation compound Li_xTiS_2 ($x = 0.8$) is illustrated in Fig. 5.

The alkaly ions insertion into the crystallographic lattice of the dichalcogenides caused an increased distance between the hexagonally close-packed layers. By X-ray measurements, it has been observed an extension of the hexagonal lattice along the c-axis with about 10% [17].

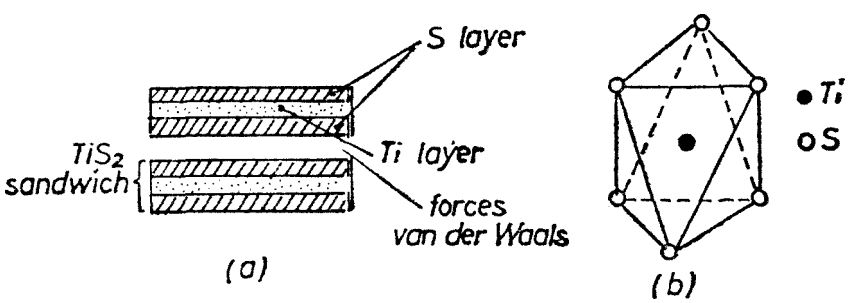

Fig. 3. The ordering layers in TiS_2 (a). The octahedral symmetry sites of the Ti Atoms (b).

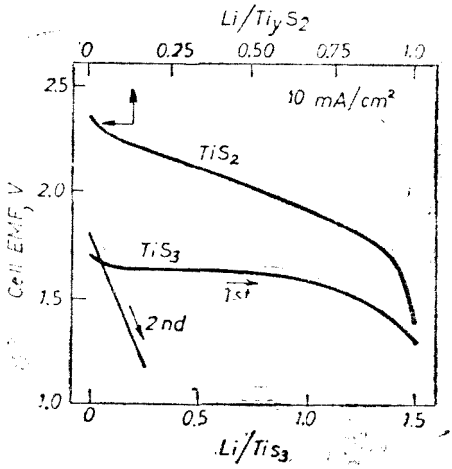

Fig. 4. Electrochemical characteristics of TiS_3.

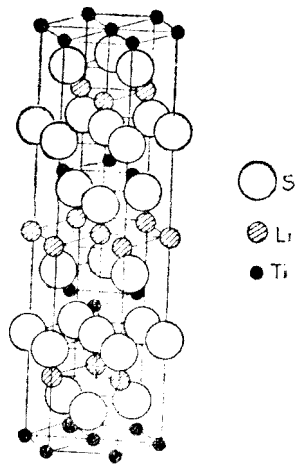

Fig. 5. Structure of $Li\,TiS_2$ compound ($x = 0.8$)

The a and c parameters of the some dichalcogenides as well as their intercalation compounds are given in Table 1.

The variation of the a lattice parameter shows the appearance of some crystalline lattice distorsions more pronounced for ZrS_2 and HfS_2 than for TiS_2. The different behaviour of the a parameter intercalated suggests a possible departure from close-packing of the anions, for the heavier elements. Thus, the little expand of the a parameter is expected because the electron density increases on the hexagonally close-packing. For the heavier elements of the group V B (Nb and Ta), if the transition metal resides the trigonal prismatic site, the a parameter is not changed, because niobium and tantal disulfides intercalate lithium very slowly ($x < 5\%$) even in the stoichiometric compound.

Table 1

X-ray parameters of the dichalcogenides and their intercalated compounds [15]

	MS_2			Li_xMS_2		
	a(Å)	c(Å)	c/a	a(Å)	c(Å)	c/a
TiS_2	3.407	1* × 5.696	1.672	3.455	1* × 6.195	1.793
ZrS_2	3.665	1* × 5.835	1.592	3.604	3* × 6.250	1.734
HfS_2	3.635	1* × 5.856	1.611	3.560	3* × 6.375	1.791
NbS_2	3.340	3* × 6.000	1.796	3.342	3* × 6.421	1.921
TaS_2	3.340	2* × 6.040	1.808	3.340	2* × 6.457	1.939
MoS_2	3.160	2* × 6.150	1.946	—	? × 6.400	—
WS_2	3.160	2* × 6.180	1.956	—	—	—

* number of the transitional metal layers of the unit cell.

The molybdenum disulfide is the most stable of these disulfides and the less favourable for the intercalation. However, at low lithium content ($x \ll 1$), Li_xMoS_2 is stable, but at higher values ($x \to 1$) is unstable, disproportionating in Li_2S and Mo.

Conclusion. The intercalation occurs by the diffusion phenomenon of same ions to the host crystalline lattice. If the diffusion takes place in the cathodic depolarisant of some galvanic cells, the intercalation is given by the cell reaction.

The crystalline structure of the intercalated compound is about the same with the host material, nonexisting an important variation of the unit crystalline cell parameters.

There are two essential factors which influence the intercalation. They are: the thermal treatment of the host material, and the size of the particles, which have an important role for the lithium ion intercalation.

In conclusion, the intercalation compounds can occur to the discharge process of the lithium batteries. The electrochemical performances as well as the features of these nonconventional systems are determined by the physical, chemical and structural properties of the active material, which takes part in the cell depolarisant.

BIBLIOGRAPHY

1. P. Lenfant, J. Power Sources **14**, 251 (1985).
2. M. Armand, Thesis, Grenoble (1978).
3. M. S. Whittingham, J. Electrochem. Soc., **123**, 315 (1976).
4. A. H. Thompson, J. Electrochem. Soc., **126**, 608 (1979).
5. T. Jacobsen, K. West and S. Atlung; Electrochem. Acta, **27** (8), 1007 (1982).
6. D. Deroo, D. Pedone and F. Dalarel, J. Appl. Electrochem., **20** (5), 835 (1990).
7. L. Yongfang and W. Hoaging, Electrochem. Acta, **34**, 157 (1989).
8. T. Ohzuku, H. Higeshimura and T. Hirai, Electrochem. Acta, **29**, 779 (1984).
9. T. Ohzuku and T. Hirai, *Progress in Batteries and Solar Cells*, **7**, 31 (1988).
10. T. Ohzuku, M. Kitagawa and T. Hirai, J. Electrochem. Soc., **136** (4), 3169 (1989).
11. T. Ohzuku, M. Kitagawa and T. Hirai, J. Electrochem. Soc., **137**, (1), 40 (1990).
12. S. Asbrimk and J. Berby, Acta Cryst., **326**, 6 (1970).
13. R. Bates and Y. Jumel, *Lithium Batteries* (ed. J. P. Gabano), Academic Press, London (1983).
14. P. Podhajecky, Z. Zabransky and P. Nowak, Electrochim. Acta, **35**, 245 (1990).
15. M. S. Whittingham, Prog. Solid. St. Chem., **12**, 41 (1978).
16. E. J. Frazer and S. Phang, J. Power Sources, **6**, 307 (1981).
17. M. S. Whittingham, J. Electrochem. Soc., **123**, 315 (1976).

STUDIA UNIV. BABEŞ-BOLYAI, CHEMIA, XXXVII, 1—2, 1992

CONSIDERATION ABOUT SETTLING AND DISCHARGING PROCESS IN SELF DISCHARGE CENTRIFUGAL SEPARATORS

RADU IATAN*, CĂLIN ANGHEL**, VIOLETA-DANIELA ANGHEL***

Received: 15.12.1992

ABSTRACT. Specific field and the basic method of operation of this type of centrifuges are well-known. The real way for accumulation of sediment, respectively solids discharging, is more difficult to be obtained, but it is very important for technological process. A short theoretical point of view is presented. The whole process is considered to reduce in two simultaneous phases, accumulation of sediment and solids settlement, and radius of cake surface, r_s, is given. Assumed as a basis, it is possible an automatic discharge control by an automatic cycle. Certainly, several experimental applications are required, to get useful informations.

SYMBOLS

$\Delta\rho$ — diferencial density
ω_T — angular velocity of bowl
r — curént radii for particle position
r_s — radii of sol$_i$d interface
φ — angle of slide
α — half included angle of disc
R_r — specific resistance to filtration of the cake
η — dinamic viscosity
x — volume rate
l — sediment layer thickness
Re — Reynold's number
R_T — radii of internal bowl
b — 1—s, index of compressibility
ρ — density of solid
π — universal constant
Co — initial solid concentration
C_f — final solid concentration

General aspects. Under the name of self discharge centrifugal separators are known all disc centrifuges [1, 2, 6] which have conical or biconical solid bowl and which are equiped around the periphery of the bowl by means of valves, by means of nozzles designed to open on a timed basis or posts opening on a timed cycled (commonly known as opening bowl centrifuges) etc., intended to discharge the solid phase.

Due to their construction, these separators may work in both manners, semi-continuous and continuous, depending on the technological requirements of the process. As exception, we mention nozzle discharge disc centrifuges with

* *Politechnical University Bucharest, Dept. of Technological equipment for process industries, Bucharest, Romania*
** *Babeş-Bolyai University, Dept. of industrial chemistry, 3400 Cluj-Napoca, Romania*
*** *„Farmec" S.A., 3400 Cluj Napoca, Romania*

continuous discharge of solid because their discharge dynamics is totally different ; for that case, discharge of solids is free, continuous or quasi-continuous.

As specific area of application, disc centrifuges are recommended to be used to clarify a liquid containing solid and to separate solids within a liquid (fine separation). As concrete exemples, there are as follows : recovery of precious elements within slurry, obtaining of B12, A, C vitamins and alcaloids, beer clarification etc. Although, continuous scroll discharge centrifuges and decantation apparatus working by extraction are characteristic for residual waters, but in the first stage of the purification process, for slurries which have lower concentration of solids, is very justified the use of self discharge centrifugal separators.

Theoretic presentation. Because solids discharge is conditioned first of all by technological requirements as recovery ratio, solids content etc., it is obviously required a specific automatic programming as far as solids discharge is concerned. The problem entailed merits special mention and that is the concordance between technological requirements confronted by sediment and physical means of solids to move within discharging area.

Consequently, the properties of the sediment — and that means solids quantity, ratio of solids to settlement, respectively, operation of the centrifugal separator — are conditioned by the dynamics of sedimentation.

It is well known that the dynamics of sedimentation has two different phases which take place simultaneously : accumulation of sediment, respectively, solids settlement. Both phases of the process are consequences of the high field of centrifugal forces created in the separator.

If for the accumulation it is possible to suppose relative stationary conditions, in a given technological situation, as far as the solids settlement phase is concerned, it is necessary to consider a centrifugal force of the solids sedimented strata which is increasing continuously, in accordance with the solids accumulation. This aspect is evaluated by the reference material [2, 4] as settling pressure :

$$\Delta p = p = \frac{\Delta \varrho \omega_1^2}{2} (r^2 - r_3^2) \tag{1}$$

The solids settlement phase is achieved mainly by decreasing residual moisture content of solids sedimented and by increasing dreid substance content of the sediment, both corresponding to a supplimentary evacuation of liquide phase as an effect of Δp settling pressure. The phenomenon is accepted only till the reach of a given settling factor, a, [4, 5] dependent on the solids sedimented compressibility factor, s, [2, 6], both with specific values for each type of slurry.

If solids sedimented settlement is analysed by assimilation with filtration through the precipitate stratum, in the opposite direction with the sense of the field of centrifugal forces, it is possible to considerate the following hypothese :

a) fluid particles dislocated by the solid particles, which continue accumulation will displace with a significant energetic consumption in the opposite direction of the field of centrifugal forces.

b) associated filtration is a filtration through the precipitate stratum with a constant rate of filtration, laminar flow conditions, $Re < 5 \ldots 40$, [6, 7].

c) the gradient of pressure which produces solids settlement is the same with that one which produces associated filtration.

These hypotheses make possible to evaluate the law of variation of cake thickness, that means to determine the current radius, r_s, depending upon the ratio of solids to settlement or upon the solids sedimented compressibility factor, both experimentally determinable. All these experiments are realised in such a way that sediment can be evacuated throughout discharge area.

The condition for the movement of the sediment deposited towards discharge areas is as follows:

$$\alpha \geqslant \text{arctg} \tag{2}$$

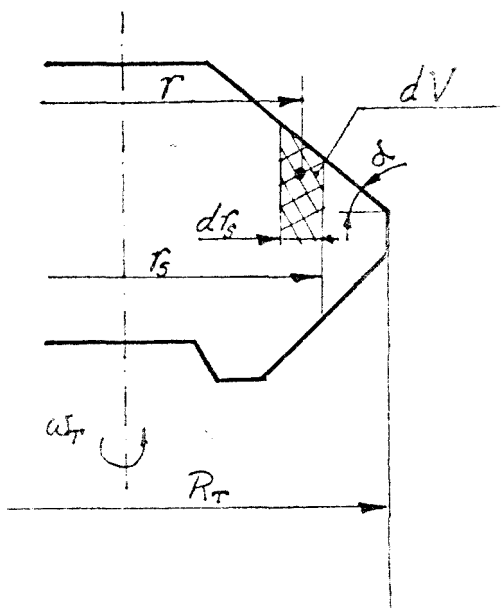

Fig. 1. Particle settling in a typical self discharge centrifugal separator

Considering sediment settlement as a result of the moving off the liquid — remanent humidity, and being governed by the differential equation of filtration through the deposed solids stratum [6]:

$$\frac{dl}{dt} = \frac{(\Delta p)^{1-s}}{K_L \cdot L} \tag{3}$$

and for compressible sediment, where

$K_L = R_r \cdot \eta \cdot /x$, experimentally determinable and expressing the moving layer thickness, as:

$$l = R_T - r_s \tag{4}$$

Equation (3) takes the form:

$$(\Delta p)^b = -\frac{dr_s}{dt} K_L (R_T - r_s) \tag{5}$$

In conformity with hypothesis c), Equations (1) and (5) permit to obtain the expression of the law of variation of cake thickness and that means to calculate r_s as radius of solids sedimentation layer.

Equation (3) becomes:

$$(\Delta p)^b = -\frac{dr_s}{dt} K_T (R_L - r_s) \tag{5}$$

where:

$$b = 1 - s$$

In conformity with hypothesis c), Equations (1) and (6) are equal. That situation appears when the law of variation for radius of solids sedimentation, r_s, is succeded.

Because it is not intended to obtain a law of an absolute variation for the layer thickness, practice cannot verify it; it is more important to evaluate a limite situation, reached for the maximum rank of settlement, when the solid sedimented becomes practically incompressible, Equation (6) becomes:

$$\Delta p = -\frac{\mathrm{d}r_s}{\mathrm{d}t} \cdot K_L(R_T - r_s), \text{ because } b \simeq 1.$$

The approximation is verified by practice, for a wide range of technological situations.

Usually, the cake compressibility factor, s, has values between 0,1 ... ... 0.2 [2].

From Equation (1) and (5) we have:

$$\frac{\Delta\rho\omega_T^2}{2}(R_T^2 - r_s^2) = -\frac{\mathrm{d}r_s}{\mathrm{d}t} K_L(R_T - r_s) \tag{6}$$

if:

$$r = \frac{r_s}{R_T},$$

Equation (6) becomes:

$$\frac{\Delta\rho\omega_T^2 R_T}{2K_L}(1 - r^2) = -\frac{\mathrm{d}r}{\mathrm{d}t}(1 - r), \tag{7}$$

where, r is a variable depending on sediment accumulation.

Separating variables and interpreting, we obtain, from Equation (7), as follows:

$$r_s = R_T\left[cc^{-\frac{\Delta\rho\omega_T^2 R_T}{2K_L}t} - 1\right]$$

For initial conditions, $t = 0$, $r \simeq 1$, the expression of the law of variation of sediment accumulation, in limit situation, becomes:

$$r_s = R_T\left(2c^{-\frac{\Delta\rho\omega_T^2 R_T}{2K_L}t} - 1\right) \tag{8}$$

Considering, in the same time, that the dynamics of sediment accumulation is simultaneously achieved with the solids settlement process, when elementary mass accumulation and elementary volume accumulation are:

$$\mathrm{d}m = \rho_s \frac{\mathrm{d}V}{1 + \varepsilon}$$

$$\mathrm{d}V = 2\pi(R_T - r_s)r_s \mathrm{d}r_s \operatorname{tg}\alpha \tag{9}$$

In conformity with Eq. (5):

$$r_s = R_T e^{-k_s \int_0^t q(t)dt}, \tag{10}$$

where: $q(t)$ = unit flow capacity,

$$k = \frac{D}{2R_T}; \; D = -D_1 \frac{\Delta \rho \omega^2 r a}{g}; \; D_1 = \frac{1}{2\pi \rho \operatorname{tg} \alpha}$$

Evaluation of r_s with $q(t) \neq$ const., (for a big variation of porosity in the sediment stratum) in conformity with Eq. 5 is recommended:

$$r_s = R_T e^{-\sqrt{K \int_0^t q(t:dt}}, \tag{11}$$

where:

$$\beta = 1 + \eta, \; K = \frac{a_k}{4\pi \rho R_T \operatorname{tg} \alpha}; \; a_k = \frac{2\left(\ln \frac{R_T}{r_s}\right)}{g}$$

Evaluation of r_s with $q(t) =$ const, is as follows:

$$r_s = R_T e^{-\sqrt[\beta]{Kqt}} \tag{12}$$

or,

$$r_s = R_T e^{-Kqt} \tag{13}$$

As far as the unit flow capacity is concerned, for the yield capacity of the centrifuge $Q(t)$, the next equation is obtained:

$$q(t) = Q(t)[c_0 - c_f] \tag{14}$$

Concluding, if the requests concerning the efficiency and quality of the self-discharge centrifugal separators are respected, it is obviously necessary to use accurate methods and devices to evaluate and control the solids sedimented within the bowl of centrifuges.

Conclusions. In the conditions of industrial separation, in many cases, the solids concentration on the feed slurry varies between wide limits. The commands to discharge solids sedimented, based on a timed cycle pre-established, are not any more efficient because they lead to solid phase losses, decrease of productivity etc.

It is necessary a very accurate analysis of the situation using the considerations presented before.

For the recovery of solids, following a very good rate of recovery at a minimal number of discharges, it is necessary to control through sensor system, a value of the sediment stratum, $R_s \leqslant r_s$, according to Eq. (8).

The limit value of the Eq. (8) means incompressible sediment which practically does not move through orifices, but this value is a certain limit value comming from the choice.

To establish the real discharge condition, R_s, experimental trails are recommended.

If the advanced sensors permit to verify continuously the sediment, it is possible to use curent values, doubled by continuous analyse of solids' concentration within the clarified effluent values given by Eq. (9) ... (13) to establish discharge programming.

Based on such theoretical considerations, practice imposed the following versions of self discharge centrifugal separators:

— Discharge by parametric pre-established commands as: sediment level, sediment quantity etc., using expressions in the form of Eq. (8);
— Discharge by mixed commands — parametric and temporizing commands, pre-establishing the duration of separation cycle using expressions in the form of Eq. (1);
— Discharge by other adapting commands, with closed loop, slurry feeding-sediment discharge, corrected by optical control of solids concentration within the clarified liquid.

REFERENCES

1. Hemfort, H.; Kohlstette, W., „Zentrifugalseparatoren und Dekanter für die Biotehnologie", Westfalia Separator, 1984.
2. Derek, B. Purchas; Richard J. Wakeman, „Solid-Liquid separation", Upläander Press LTD, 1986, 278–290.
3. * * * Klär-Separator, Westfalia Separator technische daten, 1985.
4. Elenboghen, M. M., Batîrev, R. F., Him.i.neft.maş. 3, 1979, 19–21.
5. Batirev, R. J., Elenboghen, M. M., Him.i.neft. maş. 4, 1978, 3–5.
6. Jinescu, Gh., Procese hidrodinamice şi utilaje specifice în industria chimică, E.D.P., Buc., 1983, p. 373–404.
7. Reuter, H., Chem. Ing. Techn., 39, 9/10; 1967, 5–6.

IN MEMORIAM

100 de ani de la naşterea profesorului Ioan Tănăsescu

PROFESORUL IOAN TĂNĂSESCU

Anul 1992 marchează 100 de ani de la naşterea profesorului şi omului de ştiinţă Ioan Tănăsescu, cel care a dat strălucire Facultăţii de Chimie din Cluj ca şef al catedrei de chimie organică între anii 1931—1959.

Serii de studenţi poartă în memorie şi în suflet imaginea Omului Profesorului, Cercetătorului de mare anvergură, numit simplu, cu respect şi afecţiune „Magistrul".

Profesorul Ioan Tănăsescu s-a născut la 23 februarie 1892 la Bucureşti, unde a urmat atît liceul cît şi universitatea ca student al Facultăţii de Chimie-Fizică, avînd profesori iluştri printre care : C. Istrate, A. Ostrogovich, D. Rădulescu şi alţii. După terminarea facultăţii şi a şcolii militare este angajat ca şi chimist în cadrul laboratorului de chimie al armatei, în perioada campaniei din 1916—1918. În 1919, anul naşterii României Mari, înfiinţîndu-se Universitatea Daciei Superioare din Cluj, profesor A. Ostrogovich şi prof. D. Rădulescu răspund invitaţiei de onoare de a pune bazele învăţămîntului chimic românesc. Tînărul doctorand I. Tănăsescu, îi însoţeşte fiind numit asistent la catedra de chimie-fizică şi chimie organică condusă de prof. D. Rădulescu.

Asistentul I. Tănăsescu susţine cu deplin succes teza de doctorat (conducător prof. D. Rădulescu), fiind primul doctor în chimie a noii universităţi clujene, titlu ce-i confirma excelenta pregătire teoretică şi practică şi îi deschide porţile carierei universitare (şef lucrări, profesor agregat, profesor titular în 1931). Numit şef de catedră, va conferi acesteia, prin activitatea didactică şi ştiinţifică un prestigiu şi o individualitate bine conturate şi recunoscute.

Alături de activitatea de la catedră s-a implicat şi în conducerea unor colective de lucru atît în cadrul Institutului de Chimie a Filialei din Cluj a Academiei cît şi al Institutului de Cercetări Chimico-Farmaceutice. Locul pe care acest eminent om de ştiinţă îl ocupă în rîndul celor ce sînt preocupaţi de domeniul chimiei îl confirmă şi faptul că în 1948 a fost ales membru corespondent, iar în 1957 membru titular al Academiei, fiind de asemeni membru al societăţilor de chimie din Franţa şi Germania.

Prin stingerea din viaţă în 1959 a Profesorului Ioan Tănăsescu ştiinţele chimice şi învăţămîntul chimic din Cluj şi din ţară au suferit o grea pierdere.

Profesorul I. Tănăsescu acorda prelegerii o deosebită atenţie sub felurite aspecte. În primul rînd al conţinutului — an de an erau inserate după o riguroasă selecţie noutăţile ce îmbogăţeau capitolele clasice cărora li se adăugau altele noi impuse mai ales prin perspectivele ce le deschideau aprofundării cunoaşterii. Răsfoind caietele în care îşi nota cu consecvenţă trimiterile din revistele de centralizare, se remarcă semnalarea nu numai a lucrărilor direct legate de cercetările pe care le efectua el şi a celor care aduceau ceva principial nou în chimia organică sau chiar în domenii conexe.

Dotat cu o putere de stăpînire de sine rar întîlnită prof. I. Tănăsescu era în măsură să ţină prelegeri mereu egale în cel mai bun sens al cuvîntului. Dispoziţia de moment nu se trăda în nici un fel ca şi cînd în faţa auditoriului orice alte preocupări care grevează starea sufletească (decepţii, bucurii) dispăreau. Cursurile aveau o deosebită claritate. Ori de cîte ori apărea posibilitatea, se urmărea firul logic al faptelor experimentale care pas cu pas impuneau atribuirea unei anumite structuri pentru compuşi cu molecule mai complexe sau o anumită explicaţie a unor comportări. Nu rare erau ocaziile în care se atrăgea atenţia asupra problemelor ce îşi aşteaptă rezolvarea. Prin aceasta, fără să-şi dea seama, studentul se familiariza cu tehnica cercetării.

Prin expunerea calmă în care accentele se puneau nuanţat, fără stridenţe, folosind un limbaj ales şi adecvat, cursurile prof. I. Tănăsescu au rămas un model pentru cei care au avut şansa de a-l avea dascăl. Importanţa acordată lucrărilor practice o ilustrează între altele eforturile făcute spre a crea studentului posibilitatea de a lua contact cu metodele de lucru moderne.

E semnificativă, din acest punct de vedere, introducerea în programul lucrărilor a microanalizei într-o perioadă în care această metodă, la alte facultăţi de profil nu numai de la noi, abia începea să fie folosită în cercetare. În această ordine de idei e de menţionat că prof. I. Tănăsescu este autorul primei cărţi de lucrări practice de chimie organică tipărită în ţara noastră.

La examene, prof. I. Tănăsescu era exigent şi deosebit de corect avînd răbdarea să asculte pe fiecare student. Prin felul întrebărilor urmărea să vadă în ce măsură cel audiat poate opera cu noţiunile de bază şi valorifica cunoştinţele. Căuta să convingă pe cel care nu era suficient pregătit, de lacunele pe care le are şi care se cer completate.

În îndrumarea activităţii de cercetare a doctoranzilor acorda o mare pondere libertăţii de acţiune. În discuţiile purtate privind strategia atacării problemelor nu impunea categoric punctul său de vedere chiar dacă intuiţia şi ascendenţa sub multe aspecte ale prof. Tănăsescu erau argumente de prim plan pentru o anumită cale de urmat. Prefera ca doctorandul să analizeze diferitele alternative şi să se convingă singur, experimental, de cea care e mai eficientă.

Profesorul I. Tănăsescu a avut o foarte bogată activitate ştiinţifică ilustrată prin cele peste 100 lucrări publicate, dintre care majoritatea (60) au apărut în reviste de specialitate de prestigiu din străinătate (Bulletin de la Societe Chimique de France, Berichte der deutschen Chemischen Gesellschaft (Chemische Berichte), Journal für praktische Chemie).

Activitatea de cercetare, care în jurul anului 1935 a fost cea mai fructuoasă se resimte, datorită celor 5 ani în care facultatea, ca urmare a dictatului de la Viena, a fost obligată să se refugieze la Timişoara de unde a revenit la Cluj abia după eliberarea Ardealului de Nord. Greutăţile inerente unei reinstalări şi cele datorate urmărilor războiului au făcut, ca abia după 1950, treptat, activitatea de investigare să revină la ritmul iniţial.

Chiar şi o analiză mai puţin aprofundată a contribuţiilor aduse prin cercetările efectuate, scoate în evidenţă cîteva trăsături definitorii pentru omul de ştiinţă I. Tănăsescu.

În primul rînd interesul pentru problemele de actualitate sau de perspectivă. Chiar lucrarea de doctorat, condusă de prof. D. Rădulescu se înscrie într-un domeniu abia apărut, acel al chiralităţii în clasa spiranilor. Rezumîndu-se doar la încă un exemplu, sînt de menţionat cercetările din clasa steroidelor, clasă de compuşi pentru care se întrevedeau deja implicaţiile majore în biologie.

Reţine apoi atenţia curajul cu care s-au atacat probleme complexe a căror rezolvare cerea un volum mare de muncă şi ridicau dificultăţi la interpretare Să nu uităm că la acea vreme laboratorul era tributar aproape exclusiv metodelor chimice extrem de laborioase şi implicit cronofage.

Pot fi amintite în acest context condensările o-nitrobenzaldehidelor cu compuşii aromatici, reacţii ce pot lua cursuri diferite: închiderea ciclului acridinic formarea de fenilantranili, trifenilametani, benzofenone, direcţia preferată fiind impusă de factori structurali (natura substituenţilor grefaţi pe nucleele de bază) sau condiţiile de lucru (mediu, temperatură, etc.) ceea ce duce la preponderenţa unuia sau altuia dintre componenţii amestecului complex de reacţie. În aceeaşi ordine de idei, revenind la steroide, ţinînd seama de importanţa pe care conformaţia o are pentru înţelegerea comportării lor şi implicit în alegerea modului de a ataca molecula, apar evidente dificultăţi pe care le ridică abordarea unei asemenea probleme într-o perioadă cînd structura acestei clase de compuşi nu era cunoscută pînă la detalii conformaţionale. Nu mai puţin complexe (era de prevăzut) s-au dovedit reacţiile fotochimice la compuşii în care este prezent scheletul o-nitrobenzaldehidic, în special acetalii de acest tip.

Mulţi din cei 37 colaboratori care au avut norocul să fie îndrumaţi în cercetare de profesorul I. Tănăsescu şi-au putut dă seama de îndeminarea de

experimentator şi uşurinţa cu care, chiar din primele date experimentale la care se ajungea intuia esenţa procesului urmărit. Principalele domenii pe care prof. I. Tănăsescu le-a abordat au fost chimia heterociclurilor, fotochimia derivaţilor o-nitrobenzaldehidelor şi chimia steroizilor.

În clasa heterociclurilor s-au adus contribuţii deosebit de valoroase în clasa acridinelor, antranililor, tiazolochinolinelor. Dintre rezultatele la care s-a ajuns în această direcţie e de remarcat o nouă sinteză a acridonelor, rămasă în literatură sub denumirea de reacţia Tănăsescu—Lehmsted, metodă brevetată de consorţiul german I. G. Farben-Industrie în 1930.

Unul din cele mai importante rezultate înregistrate la investigarea comportărilor fotochimice ale acetalilor o-nitrobenzaldehidei cu compuşii polihidroxilici este cel care a dus la constatarea că acetalii galactozei, manozei şi glucozei sub acţiunea luminii se transformă în unul şi acelaşi produs derivînd de la galactoza racemică. Prin aceasta s-a demonstrat posibilitatea unor izomerizări fotochimice încă nesemnalate în clasa glucidelor cu ecouri foarte interesante în biogeneza lor.

În sfera steroizilor, cercetările au fost focalizate în special spre urmărirea acţiunii amestecului nitrant asupra acizilor biliari cu formarea esterilor nitrici şi între altele posibilitatea de valorificare a lor în sinteză. Pe baza acestor rezultate s-a elaborat o metodă originală de preparare a acetatu ui de dezoxicorticosteronă (hormon steroid). Aşa cum reiese din această succintă prezentare pot fi remarcate contribuţiile foarte valoroase ale cercetărilor iniţiate şi conduse de prof. I. Tănăsescu care au îmbogăţit cunoştinţele în domeniul chimiei organice atît sub aspect teoretic cît şi aplicativ.

În ceea ce priveşte primul aspect, ar fi de scos în evidenţă încercările de a înscrie într-un context cît mai general, interpretarea fenomenelor observate, aşa cum o ilustrează poate cel mai convingător şi titlul uneia dintre lucrări „Explicarea mecanismului izomerizărilor şi a reacţiilor spontane în chimia organică cu ajutorul teoriei polarităţii valenţelor".

Referitor la cel de-al doilea aspect, cel aplicativ, ar mai fi de adăugat la cele deja amintite, contribuţiile aduse la prepararea unor medicamente: sulfatiazol, PAS, atebrină, plasmochină. Nu în ultimul rînd se cere menţionat ecoul pe care l-au avut cercetările efectuate de profesorul I. Tănăsescu în lumea chimiştilor aşa cum rezultă şi din discuţiile purtate cu specialişti de prim rang ca A. Kliegel, F. Arndt, H. Gilemann, K. Lehmstedt şi alţii, reflectate de conţinutul unora din lucrările publicate de cei de mai sus amintiţi cît şi de corespondenţa purtată.

Profesorul I. Tănăsescu a fost şi un om de cultură interesat în mod deosebit de literatură. Competenţa în aprecierea valorilor culturale o ilustrează între altele şi invitaţia acceptată de a face parte din comitetul de lectură a Teatrului Naţional din Cluj. Admiraţia pentru natură l-a făcut un mare iubitor al drumeţiilor, fiind unul dintre membrii activi ai „Turing Clubului".

Cultul pentru adevăr, pentru dreptate, pentru demnitate au făcut din profesorul I. Tănăsescu un model al dîrzeniei, un simbol al rezistenţei, al dăinuirii valorilor morale într-o perioadă, cea mai întunecată a istoriei noastre, cînd monstruoasa ideologie comunistă impusă cu forţa poporului român, se străduia să distrugă tot ce era autentic: tradiţie, cultură, demnitate umană şi naţională. A avut de suferit din partea mai marilor acelor zile de tristă amintire, dintre care mulţi, după ce au pus umărul la instaurarea şi consolidarea comunismului în ţară, au părăsit-o şi beneficiază azi de pensii în dolari, mărci sau shekeli. Prof. Tănăsescu asumîndu-şi toate riscurile, nu a cedat în faţa presiunilor şi a şantajului, a rămas aceeaşi distinsă personalitate stimată şi admirată de marea majoritate a celor din jurul său, care credeau în acest simbol al speranţei şi demnităţii, sperau, în supravieţuirea adevăratelor valori morale şi spirituale ale naţiunii.

Această succintă prezentare a personalităţii şi realizărilor profesorului I. Tănăsescu este departe de a reflecta dimensiunile operei sale de educator, cercetător şi creator. Este doar un pios omagiu adus Magistrului lor de către cei care l-au cunoscut, preţuit şi respectat, este un mesaj de suflet transmis tinerelor generaţii datoare să cunoască şi să urmeze pilda iluştrilor înaintaşi.

REDACŢIA „STUDIA"

CRONICA

THE 42nd MEETING OF INTERNATIONAL SOCIETY OF ELECTROCHEMISTRY

Montreux, Switzerland, August 25—30, 1991

Montreux and Vevey, resorts located on Lake of Geneva, have aptly earned the nickname of „Pearl of the Swiss Riviera": 16 kilometers of sheltered bays bordered by palm trees and tropical flowers. Surrounded by vineyrad, they rank amongst one of the most sunny areas of Switzerland, and are protected from the cold winds by the Rochers de Naye (2042 m) stretching up behind Montreux. During, spring, the fields above Montreux-Vevey are covered with milions of fragrant narcisses. Not far, the Chillon castle symbolizes thee presence of the savoyards in this area; the castle was the princely residence of Pierre Comte de Savoie (1203—1268). Among the famous people attracted by this place were J. J. Rousseau and Byron.

The main theme of the 42nd Meeting was APPLIED ELECTROCHEMISTRY: PROCESSES AND PRINCIPLES, with the following simposia:

1. Fuel Cells for stationary Power Generation: Electrochemical Engineering Aspects (31 posters);

TIMETABLE

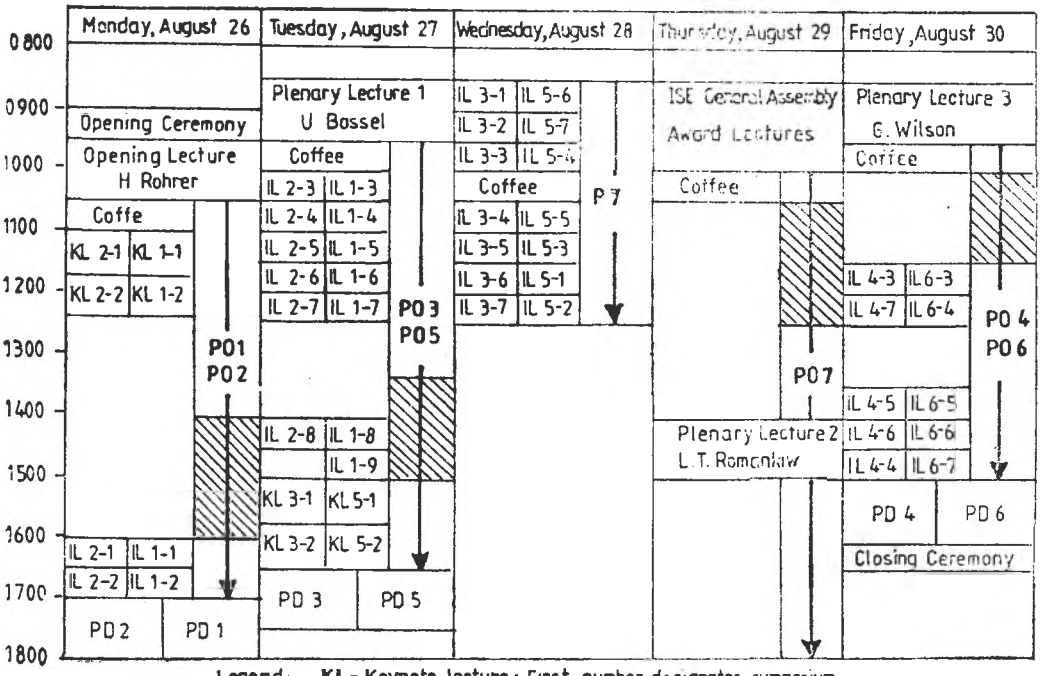

Legend: **KL** - Keynote lecture: First number designates symposium
IL - Invited lecture: First number designates symposium
PO - Poster Sessions: Number designates symposium
PD - Poster discussion: Number designates symposium
Hatched areas Authors were present at posters

2. Electrodeposition and Dissolution in Electronics (64 posters);
3. Electrochemical Synthesis of Thin Film Materials (61 posters);
4. Mechanism of Inhibition in Corrosion and Electroplating (38 postres);
5. Electrochemistry of Water Treatment and Recycling (29 posters);
6. Electrochemical Sensors for Medical Applications (28 posters);
7. General Session (201 posters).

The Meeting has totalized 6 plenary lectures, including the opening lecture and the 2 award lectures, 12 Keynote lectures, 45 invited lectures and 459 posters (See Time table).

The plenary lectures:

1. Perspectives of Nanometer Scale Science and Technology, H. ROHRER, Nobel Prize Winner 1986.
2. Fuel Cells for Stationary Power Generation: An Engineer's View, U. G. BOSSEL.
3. Electrochemical Technology in Electronics: Past Achievements and Future Challenges, L. T. ROMANKIW.
4. The Role of Bioelectrochemistry in Medicine: An Electrochemist's View, G. WILSON.
5. The Study of Surface Reactions with Atomic Scale Resolution, D. M. KOLB, Pergamon-Electrochimica Acta m dalist, 1990.
6. Electrochemical Studies of Some Biologically Active Molecules, J. M. RODRIGUEZ-MELLADO, Tajima-Prize winner 1990.

There were 539 participants, the most numerous from Germany, 88 persons (16,3%), from Switzerland 73 (13,5%), Japan 65 (12%), France 55 (10,2%), USA 38 (7%) etc. Roumania was represented by 4 persons: 3 from the University of Cluj-Napoca (Prof. L. Oniciu, Assistant Prof. I. C. Popescu and Assistant Prof. ing. S. Agachi) and 1 from the Technical University of Bucarest (lecturer ing. M. Ungureanu).

The posters from our University (Faculty of Chemistry and Industrial Chemistry) were:

— Classification Procedure for Selectivity Control in Acrylonitrile Electroreduction (L. Oniciu, D. A. Löwy and D. Dumitrescu).
— Linear Sweep Voltametry in the System $MnSO_4/(NH_4)_2SO_4/H_2SeO_3$ in the Presence of Some Additives (Zn^{2+}, $H_2C_2O_4$) (L. Oniciu, I. C. Popescu and P. Ilea).
— Application Software Concerning the Control of De Nora Brine Electrolysis (L. Oniciu, S. Agachi, A. Imre-Lucaci and I. Socol).

During the Meeting they were some very attractive social events, starting with the welcome reception, and continuing with the reception (Vin d'honneur) at the Congress Center, offered by the City of Montreux and the Canton of Vaud, steam boat tour on the Lake Geneva, excursion to the Berner Oberland and ending with the banquet at the Casino of Montreux.

All meetings were held at the Congress Center, in Montreux. Among the 22 sponsors can be mentioned Asea Brown Boveri, Ciba-Geigy, Crédit Suisse, Nestlé, Sandoz, Swisair, Sulzer-Innotech.

LIVIU ONICIU

THE XI-th ANALYTICAL CHEMISTRY NATIONAL CONFERENCE,
September 24—25, 1992, Cluj-Napoca, Romania

The XI-th Analytical Chemistry National Conference was organized by Faculty of Chemistry (Cluj-Napoca) under the direct guidance of Romanian Analytical Chemistry Society (SCAR). Romanian specialists and well-known, remarcable scientists from abroad participated at this Conference.

The scientific program covered all fundamental aspects, new developments and applications in the filed of Analytical Chemistry.

This scientific meeting was consisted of plenar conferences, of papers presented within four sections: Separation Methods, Spectrometric Methods, Electrometric Methods and Various Methods; and of poster presentation.

The following plenar conferences were presented:

* "Analytical Chemistry in Romania" by G. E. Baiulescu and G. L. Radu from University of Bucharest, Romania;
* "Industrial Problems Solved by Combinated Techniques" by Jeanette G. Grasselli from Ohio University, U.S.A.;
* "Mechanisms for Working Ion-Selective Electrodes" by E. Pungor from Technical University of Budapest, Hungary

* "Instrumental Chemistry-Strategy for New Methods" by Y. Gohshi from University of Tokyo, Japan.
* "Technological Innovations by the co-operations University-Industry" by G. R. Brown, University of Claveland, U.S.A.
* "Progresses in Analytical Chemistry" by L. Kékedy from University of Cluj-Napoca, Romania.

A lot of plenar conference was presented also for each section:

* "Trace analysis of metals by HPLC methods", V. A. Ilie and G. E. Baiulescu, ICECHIM-Bucharest and University of Bucharest.
* "Progresses in TLC", S. Gocan, University of Cluj-Napoca.
* „Correlation between structure of analytical systems and mathematical structures which reflect them", I. Al. Crişan, University of Cluj-Napoca.
* "Ion-sensitive membrane-electrodes with PVC support", E. Hoţârtean, V. Cosma, A. Coroian, Institute of Chemistry, Cluj-Napoca.
* "Electroanalytical study of some electrodic surfaces", Al. Duca et al., Polytechnical Institute of Iaşi.
* "Active transport mechanisms through membranes, with macrociclic transportors", C. Luca, Polytechnic Institute of Bucharest.
* "Quality assurance of analytical measurements", I. Rică, Siderurgica S. A. Hunedoara.

It were presented also a total number of 134 papers and 60 posters. Themes of these works were very diverse and covered a field of major interest in Analytical Chemistry.

The XII-th Conference of Analytical Chemistry in Romania will take place between September 22—24, 1994 at the "Ovidius" University of Constanţa.

SIMION GOCAN

RECENZII

Mircea Diudea, Michaela Pitea, Mioara Butar, **Fenotiazine şi medicamente structural înrudite,** Ed. Dacia Cluj, 1992, p. 250.

The well-known publishing house "Dacia" from Cluj, had issued in 1992 the book having the above mentioned title *("Phenothiazines and structurally related drugs")* It is included in the collection "Biblioteca Farmacistului") and consists of 250 pp., 58 tables, 179 eqs, 22 schemes, and 13 figs.

The phenothiazine derivatives — sulfur containing heterotricycles — have imposed themselves in modern therapy because of their psychotropic properties, able of influencing some psychical states, and especially human behaviour.

On the other side, progress in the chemistry of heterocycles has lead to new types of compounds, structurally related to them such as: azaphenothiazines, homothioxanthenes, thioxanthones, thianthrenes, dibenzothiepines, dibenzothiazepines, which have proved to be especially active from biological point of view.

The book, organised in 10 chapters and one appendix, approaches a series of problems concerning the chemistry and pharmacology of these psychotropic drugs,out of each the phenothiazines are the most important. Because in the last years the progress in instrumental and computing tehniques has brought a decisive contribution to the enhancement of our knowledges on these heterocycles. *the first five chapters* deal with their electronic structure and their kinetic response when reacting with nucleophiles. These aspects are essential in understanding the SAR (Structure Activity Relationship) and OSAR (Quantitative Structure Activity Relationship) studies, the reaction mechanisms, the pharmacokinetics of these compounds, all these topics being developed in the following chapters.

Chapter 6 shows the spectrum of biological activities, the last results of research in this area included: antihistaminic antiparkinson, anticholinergic, antibacterial, antiproliferative. A classification of these drugs, based on chemical and pharmacological criteria, is proposed.

The problem of relationship between chemical structure and biological activity, both from SAR and OSAR points of view, is developed in *chapters 7* and *8*, by stressing the structural and steric factors responsible for a given pharmacological profile. The various possible conformations for such a structure have been suggested to be the cause of the polyvalent action of these pharmaceuticals. The OSAR studies attempt a quantitative approach of the steric and electronic contributions of selected fragments in these molecules.

An important wieght was given to the study of mechanisms of biological action, stressing the molecular interaction of drugs with dopaminergic receptors and their antagonism with camoduline. Pharmacokinetics of metabolites supplement these biological studies.

The *last chapter*, "Topological description of the receptor", illustrates the authors' original contribution to the OSAR studies. By analysing substructures both qualitatively and quantitatively, attempts were made in describing the pharmacophore probably responsible for the antipsychotic activity of these drugs.

An appendix lists the computer program used for the topological description of molecules therein discussed.

The list of refereces (exceding 1200 entries) is only selectively, chronologically presented, according to well known methods of computerized data storage.

Because of the complexity of considered topics, the book can be viewed as a monography in the field, a singular one in our country and apart of the books with the same issued in the foreigh literature. It is useful for specialists involved in drug research: chemists, biologists, physicians as well as for students.

SORIN MAGER

Hellmut York, Werner Funk, Walter Fischer, Hans Wimmer ; **Thin Layer Chromatography, Reagents and Detection Methods, Physical and Chemical Detection Methods: Fundamentale, Reagents I,** VCH Verlagsgesellschaft mbH, D-6940 Weinhein, 1990, 464 pag.

În cromatografia pe strat subţire şi în general, în cromatografia plană, metodele

de detecţie au un rol primordial, dar cu toate acestea ele nu au fost tratate în mod special pînă acum. De obicei, aceste metode erau prezentate în cărţile de specialitate la exemple practice de separare sau, în cel mai fericit caz, într-un capitol separat. Volumele elaborate de specialiştii York, Funk, Fischer, Wimmer, şi anume: "Physical and Chemical Detection Methods", "Radiometric Detection Methods" şi "Biochemical and Biological Detection Methods" vor umple acest gol în literatura de specialitate. Aceste date vor fi de mare folos analiştilor care lucrează în domeniul cromatografiei plane, astfel că ei vor putea optimiza în mod separat procesul de separare de cel de detecţie.

Revenind la volumul "Physical and Chemical Detection Methods: Fundamentals, Reagents", acest volum cuprinde două părţi, şi anume: "Metode de detecţie" şi "Reactivi în ordine alfabetică". Metodele de detecţie sînt grupate în metode de detecţie fizică şi metode de detecţie chimică, astfel că permit experimentatorului alegerea metodelor optime scopului propus.

Alături de aceste metode, autorii prezintă un capitol separat cu probleme de documentaţie şi sugestii pentru experţii în cromatografie.

În partea a doua a cărţii, sînt prezentaţi o serie de reactivi utilizaţi în detecţia cromatografică. Descrierea lor, modul de preparare a soluţiilor, modul de utilizare, precum şi reacţia care are loc între reactiv şi substanţa de detectat reprezintă un sprijin real pentru cel care efectuează o separare cromatografică, indiferent dacă este chimist, farmacist, biolog sau medic.

Cititorul care lecturează această carte, primeşte informaţiile necesare pentru separarea şi identificarea unor clase de substanţe prin cromatografia pe strat subţire. Pentru o documentaţie mai profundă se pot utiliza indicaţiile bibliografice care sînt în număr destul de mare în această carte.

CONSTANTIN MĂRUŢOIU

Tiparul ex. la Imprimeria „Ardealul"
Cluj-Napoca Comanda nr. 242

În cel de al XXXVII-lea an (1992) *Studia Universitatis Babeş-Bolyai* apare în următoarele serii:

matematică (trimestrial)
fizică (semestrial)
chimie (semestrial)
geologie (semestrial)
geografie (semestrial)
biologie (semestrial)
filosofie (semestrial)
sociologie-politologie (semestrial)
psihologie-pedagogie (semestrial)
ştiinţe economice (semestrial)
ştiinţe juridice (semestrial)
istorie (semestrial)
filologie (trimestrial)
theologie ortodoxă (semestrial)

In the XXXVII-th year of its publication (1992) *Studia Universitatis Babeş-Bolyai* is issued in the following series:

mathematics (quarterly)
physics (semesterily)
chemistry (semesterily)
geology (semesterily)
geography (semesterily)
biology (semesterily)
philosophy (semesterily)
sociology-politology (semesterily)
psychology-pedagogy (semesterily)
economic sciences (semesterily)
juridical sciences (semesterily)
history (semesterily)
philology (quarterly)
orthodox theology (semesterily)

Dans sa XXXVII-e année (1992) *Studia Universitatis Babeş-Bolyai* paraît dans les séries suivantes:

mathématiques (trimestriallement)
physique (semestriellement)
chimie (semestriellement)
géologie (semestriellement)
géographie (semestriellement)
biologie (semestriellement)
philosophie (semestriellement)
sociologie-politologie (semestriellement)
psychologie-pédagogie (semestriellement)
sciences économiques (semestriellement)
sciences juridiques (semestriellement)
histoire (semestriellement)
philologie (trimestriellement)
théologie orthodoxe (semestriellement)